Supporting Information

Fluorogenic Platinum(IV) Complexes as Potential Predictors for the Design of Hypoxia-Activated Platinum(IV) Prodrugs

Jevon W. Marsh,[a‡] Lina Hacker, [b,‡] Shitong Huang,[a] Marie H. C. Boulet, [a] Jhanelle R. G. White[c], Louise A. W. Martin,[b] Megan A. Yeomans,[a] Hai-Hao Han,[d] Ismael Diez-Perez,[c] Rebecca A. Musgrave,[c] Ester M. Hammond [b]* and Adam C. Sedgwick[a,c]*

[a]Chemistry Research Laboratory, University of Oxford, Mansfield Road, OX1 3TA, United Kingdom

[b]Department of Oncology, University of Oxford, Old Road Campus Research Building, Oxford, OX3 7DQ, United Kingdom

[c]Department of Chemistry, King's College London, 7 Trinity Street, London, SE1 1DB, United Kingdom

Emails: ester.hammond@oncology.ox.ac.uk and adam.sedgwick@kcl.ac.uk

Table of Contents

1. General Information and Methods

All chemicals and reagents were purchased commercially and were of analytical grade. Fluorescence and absorbance spectra were collected on a PerkinElmer LS55 Luminescence spectrometer and Jasco V-770 spectrophotometer, respectively, using quartz cuvettes (1 cm path length). Column chromatography was performed under a positive pressure of N_2 using Merck® silica gel 60. All eluent ratios are reported as volume percentages. NMR spectra were recorded on Bruker AVIII 400, Bruker AVII 500 (with cryoprobe) and Bruker AVIII 500 spectrometers, and chemical shifts are reported as δ values in ppm. HPLC analyses was carried out using a Thermo Scientific Vanquish HPLC system with an Ascentils C-18 column [15 cm x 4.6 mm, 5 µm]; HPLC conditions: injection volume: 40 µL, flow rate: 1.5 mL/min, 25 °C, 0–35 min [2:98 MeCN:H_2O (both with 0.1% acetic acid), 5 min hold → 100% MeCN with 0.1% acetic acid for 20 min, 2 min hold → 2:98 MeCN:H_2O (both with 0.1% acetic acid), 2 min → 2:98 MeCN:H_2O (both with 0.1% acetic acid), 6 min hold]. High Resolution Mass Spectrometry (HRMS) was performed using Waters Micromass LCT and Bruker microTOF spectrometers. All complexes investigated in the solution studies were dissolved in DMSO to afford 5 mM stock solutions, except for CisNap, which was freshly prepared before each study in DMF. Each stock solution was then diluted in milli-Q water to afford 50 µM working solutions for HPLC analysis. Pt(IV)(OH)(OAc) reagents, Cis(OH)(OAc), Oxali(OH)(OAc) and Carbo(OH)(OAc) (complexes **1**–**3**, respectively; see Scheme S1) were synthesised according to literature procedures.[1,2] Nap-NH_2 was synthesised according to previous published procedures.[3,4]

1.1 Electrochemistry

Electrochemical experiments were carried out using an Autolab IMP potentiostat (Metrohm, Netherlands) equipped with a three-electrode configuration comprised of (i) a 3 mm glassy carbon working electrode, (ii) a platinum wire counter electrode, and (iii) a Basi Ag/AgCl (3 M KCl) reference electrode. The 3 mm glassy carbon working electrode was polished with 1 µm alumina slurry and sonicated in Milli-Q water (18.2 MΩ, Millipore) prior to being immediately transferred to a 1 mM electrolyte solution of the compound studied in PBS buffer (pH 7.4) with DMF (10%). All electrolyte solutions were deaerated with N_2 prior to each run; all measurements were obtained at room temperature under N_2.

1.2 Cell Experiments

1.2.1 Cell Culture

A549 cells were cultured in DMEM medium supplemented with 10% FBS at 37°C, 5% CO_2 in a humidified incubator. All cell lines were routinely mycoplasma tested using a HEK-Blue™ detection kit (Invivogen) and found to be negative. Chemical reduction experiments were performed using Sodium Ascorbate (Sigma Aldrich).

1.2.2 Hypoxia exposure

Hypoxia treatments at <0.1% O_2 were carried out in a Bactron II Chamber (Shel Laboratory) and treatments at 2% O_2 were carried out in a M35 variable atmosphere workstation (Don Whitley Scientific). Oxygen concentrations were periodically validated using anaerobic oxygen indicator strips (ThermoFisher) and an OxyLite probe (Oxford Optronix).

1.2.3 Flow Cytometry

Cells were seeded onto 6 cm^2 glass dishes, treated with 10 µM of probe and exposed to hypoxia as required. Cells were scraped in 1 mL of 1x PBS into a 1.5 mL tube and fixed inside the hypoxia chamber with 4% PFA (w/v paraformaldehyde in PBS) for 10 minutes. Samples were washed three times with 1x PBS. Samples were measured on a CytoFLEX (Beckman Coulter), and data analysed using FlowJo software. Filter sets used for **CarboNap** were FITC (excitation 488 nm / emission 525/40 nm) and for **CarboRes** PC5.5 (excitation 561 nm / emission 690/50 nm).

1.2.4 Fluorescent Microscopy

Cells were seeded onto autoclaved cover slips (Menzel-Glaser) before treatment and hypoxia exposure. Cells were fixed inside the hypoxia chamber in 4% PFA for 10 minutes. Cells were mounted onto microscopy slides (Menzel Glaser) with ProLong™ Gold Antifade Mountant with DAPI to visualise the nucleus (Invitrogen™). Cells were imaged with an LSM780 confocal microscope (Carl Zeiss Microscopy Ltd) at 63x magnification. Excitation and emission wavelengths used were: DAPI 370/470 nm, **CarboRes** 571/584 nm and **CarboNap** 491/516 nm.

1.2.5 Colony Survival Assay

Cells were seeded at low density in 6-well plates and incubated for 4 h at 37 °C to adhere. The compounds were added (10 μM) and incubated at the indicated oxygen concentrations for 16 hours. Cells were returned to normoxic conditions and left to form colonies for 10 days. The media was changed on day 3. Colonies were stained with 2% crystal violet (diluted in 50% methanol and 20% ethanol) and counted manually. Plating efficiency was calculated by dividing the number of colonies by the number of cells seeded. Surviving fraction was determined by dividing plating efficiency for treatment by the plating efficiency for the respective control.

1.2.6.Statistical Analysis

Statistical analysis was performed by using GraphPad Prism 10 software (GraphPad Software Inc.). The one-way ANOVA test was used to evaluate the statistical difference in fluorescence compared to the normoxic control in the flow cytometry analysis. The two-way ANOVA test was used to evaluate the statistical difference in cell viability between hypoxic and normoxic conditions at different compound concentrations in the colony assay analysis. Unless otherwise stated, all data represent the mean ± standard deviation (SD) from three independent experiments.

2. Synthetic Schemes

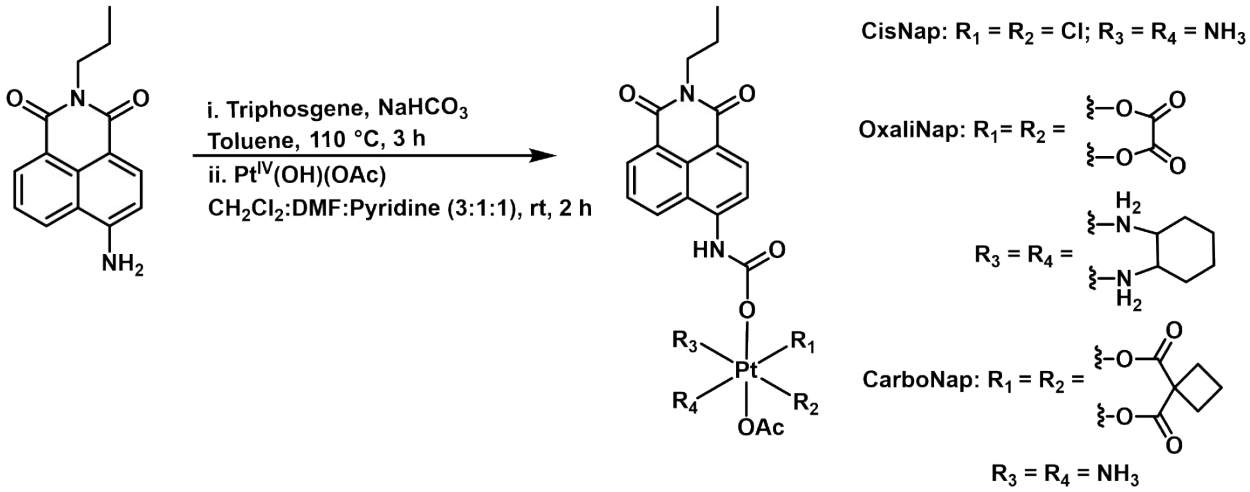

Scheme S1. General synthetic scheme for **CisNap** (top), **OxaliNap** (middle) and **CarboNap** (bottom).

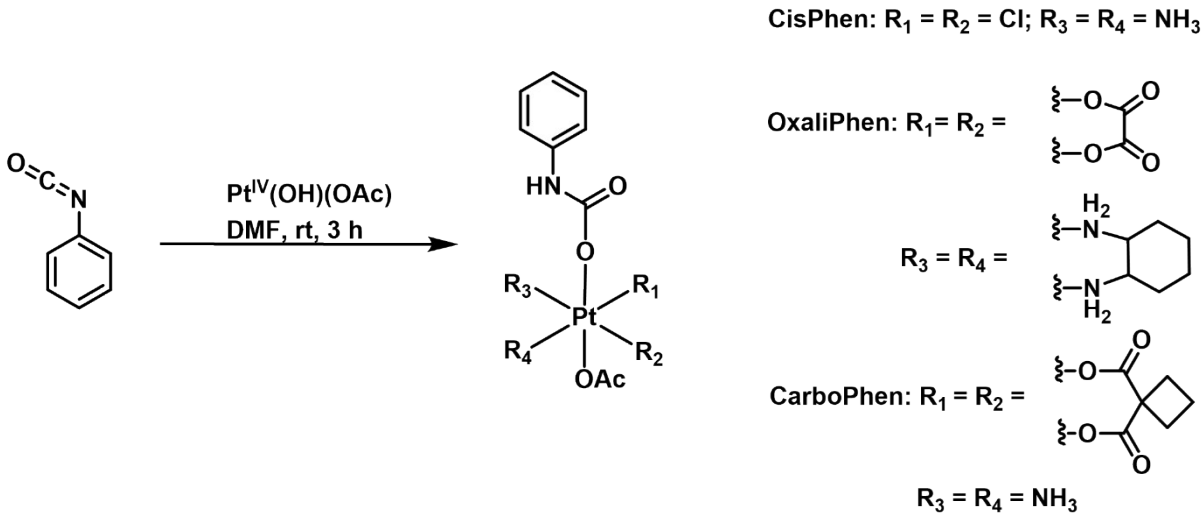

Scheme S2. General synthetic scheme for **CisPhen** (top), **OxaliPhen** (middle) and **CarboPhen** (bottom).

CarboBisOAc

Scheme S3. Synthesis of **CarboBisOAc**.

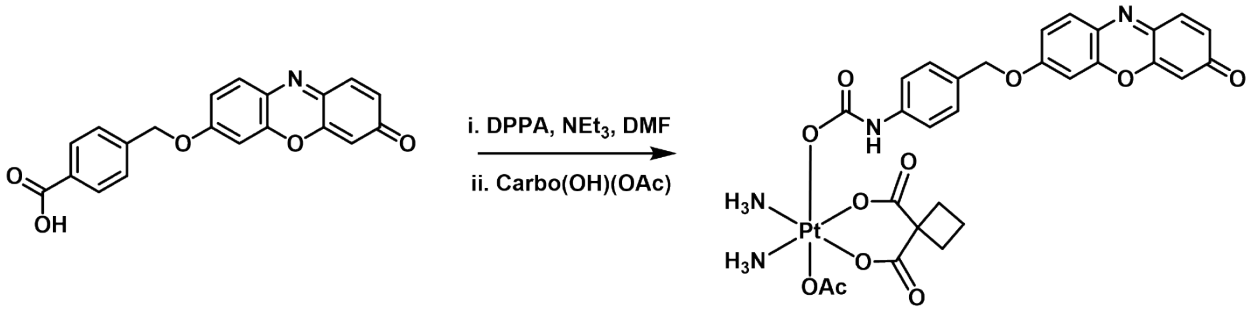

Scheme S4. Synthesis of **CarboRes**.

3. Synthetic Procedures

General synthetic procedure for Pt(IV)-Naphthalimide complexes

CisNap, **OxaliNap** and **CarboNap** were synthesised by modifying our previously reported procedure.[3] 6-amino-2-propyl-1*H*-benzo[*de*]isoquinoline-1,3(2*H*)-dione (Nap-NH_2) (80 mg, 0.315 mmol) was suspended in toluene (6 mL) and to this stirring suspension, $NaHCO_3$ (79.4 mg, 0.945 mmol, 3 eq.) and triphosgene (5467 mg, 1.57 mmol, 5 eq.) were added. The reaction mixture was then heated to 110 °C for 3 h to obtain a dark yellow solution. Toluene was removed under reduced pressure and the obtained solid residue was suspended in CH_2Cl_2 and added dropwise to a stirring suspension of the corresponding Pt(IV)–OH reagent (**1** for **CisNap**, **2** for **OxaliNap** and **3** for **CarboNap**, 1 eq.) in a CH_2Cl_2/DMF/pyridine (3:1:1) mixture, protected from light with aluminium foil and stirred at room temperature for 2 h. Once deemed complete by TLC analysis, the reaction mixture was immediately purified by column chromatography on silica gel [100% hexane → 100% EtOAc → 100% DCM → 10% MeOH in DCM] to obtain the corresponding yellow solids. Each solid was then rinsed with minimal amounts of cold methanol, centrifuged, decanted and placed under high vacuum to obtain the desired products. All complexes were characterised by ^{1}H NMR, ^{13}C NMR, ^{195}Pt NMR and HRMS, and their purity checked by HPLC prior to toxicity studies.

[$Pt(NH_3)_2Cl_2(OOCNHC_{15}H_{12}NO_2)(OAc)$], CisNap

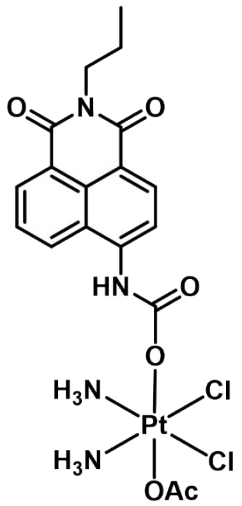

Yellow solid. Yield (28.3 mg, 14 %). ^{1}H NMR (400 MHz, DMF-d_7) δ (ppm): 10.39 (br s, 1H), 9.10 (d, *J* = 8.5 Hz, 1H), 8.58 (d, *J* = 7.0 Hz, 1H), 8.52 – 8.37 (m, 2H), 7.88 (dd, *J* = 8.5, 7.3 Hz, 1H), 7.11 (br, 6H), 4.08 (t, *J* = 7.5 Hz, 2H), 1.95 (s, 3H), 1.72 (q, *J* = 7.5 Hz, 2H), 0.96 (t, *J* = 7.5 Hz, 3H). ^{13}C NMR (400 MHz, DMSO-d_6) δ (ppm): 178.3, 163.6, 163.1, 160.1, 142.9, 131.7, 130.7, 129.9, 128.4, 125.7, 123.5, 123.4, 122.0, 118.1, 115.3, 22.8, 20.9, 11.4. ^{195}Pt NMR (107 MHz, DMSO-d_6) δ (ppm): 1256. HRMS: m/s calculated for $C_{18}H_{23}Cl_2N_4O_6Pt$, $[M+H]^+$: 656.0637, found 656.0642.

[Pt(DACH)(ox)(OOCNHC$_{15}$H$_{12}$NO$_2$)(OAc)], OxaliNap

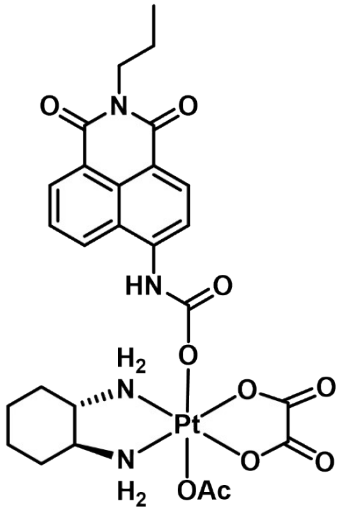

Yellow solid. Yield (40 mg, 24%). ^{1}H NMR (400 MHz, DMSO-d_6) δ (ppm): 9.71 (s, 1H), 8.64 (d, *J* = 8.5 Hz, 1H), 8.50 (dd, *J* = 7.3, 1.0 Hz, 1H), 8.41 (d, *J* = 8.3 Hz, 1H), 8.51 – 8.26 (br, 4H), 8.10 (d, *J* = 8.4 Hz, 1H), 7.89 – 7.78 (m, 1H), 3.99 (dd, *J* = 8.7, 6.2 Hz, 2H), 2.87 (d, *J* = 11.4 Hz, 1H), 2.62 (d, *J* = 10.8 Hz, 1H), 2.15 (d, *J* = 12.0 Hz, 2H), 1.99 (s, 3H), 1.64 (q, *J* = 7.5 Hz, 2H), 1.53 (d, *J* = 9.5 Hz, 4H), 1.18 (s, 2H), 0.91 (t, *J* = 7.4 Hz, 3H). The obtained analytical data was consistent with our previous literature report.[3]

[Pt(NH_3)$_2$(CBDCA)(OOCNHC$_{15}$H$_{12}$NO$_2$)(OAc)], CarboNap

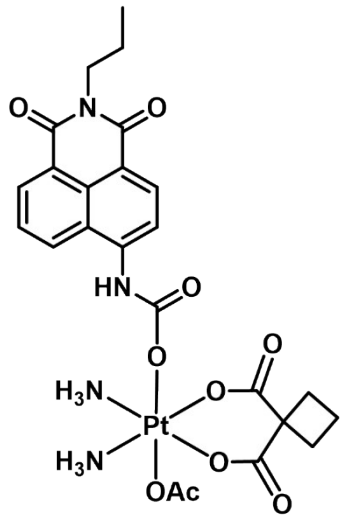

Yellow Solid. (29 mg, 13%). ^{1}H NMR (400 MHz, DMSO-d_6) δ (ppm): 9.75 (s, 1H), 8.72 (d, *J* = 8.5 Hz, 1H), 8.48 (d, *J* = 7.2 Hz, 1H), 8.40 (d, *J* = 8.3 Hz, 1H), 8.14 (d, *J* = 8.4 Hz, 1H), 7.77 (t, *J* = 7.9 Hz, 1H), 6.52 (br, 6H), 3.99 (t, *J* = 7.5 Hz, 2H), 2.62 (t, *J* = 8.0 Hz, 2H), 1.94 (s, 3H), 1.90 – 1.79 (m, 2H), 1.64 (q, *J* = 7.4 Hz, 2H), 0.91 (t, *J* = 7.4 Hz, 3H). ^{13}C NMR (400 MHz, DMSO-d_6) δ (ppm): 177.5, 176.2, 163.6, 163.1, 159.5, 142.7, 131.7, 130.8, 129.7, 128.4, 125.8, 123.4, 122.0, 117.8, 115.4, 55.5, 41.0, 33.3, 29.0, 22.4, 20.9, 15.7, 11.4. ^{195}Pt NMR (107 MHz, DMSO-d_6) δ (ppm): 1972. HRMS: m/z calculated for $C_{24}H_{29}N_4O_{10}Pt$, $[M+H]^+$: 728.1526, found 728.1528.

Synthesis of Pt(IV)-Phen complexes

CisPhen, **OxaliPhen** and **CarboPhen** were synthesised following the same procedure as reported in literature.[2] Pt(IV)(OH)(OAc) (**1** for **CisPhen**, **2** for **OxaliPhen** and **3** for **CarboPhen** and phenylisocyanate (3 eq.) were dissolved in DMF (3 mL) and the reaction was protected from light and stirred at room temperature for 3 h. Once complete, the reaction mixture was immediately purified by column chromatography on silica gel [100% hexane → 100% EtOAc → 100% DCM → 10% MeOH in DCM] to obtain the corresponding solids. All complexes were characterised by ^{1}H NMR, ^{13}C NMR, ^{195}Pt NMR and HRMS, and their purity checked by HPLC prior to toxicity studies.

[Pt(NH$_3$)$_2$Cl$_2$(OOCNHC$_6$H$_5$)(OAc)], CisPhen

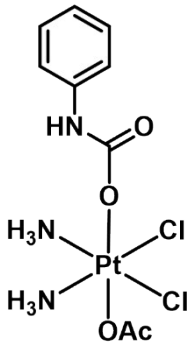

Yellow solid. Yield (37 mg, 29%). ^{1}H NMR (400 MHz, DMSO-d_6) δ (ppm): 9.04 (s, 1H), 7.50 – 7.42 (m, 2H), 7.29 – 7.10 (m, 2H), 6.95 – 6.80 (m, 1H), 1.94 (s, 3H). ^{13}C NMR (101 MHz, DMSO-d_6) δ (ppm): 178.31, 140.73, 128.22, 120.92, 118.01, 22.82. ^{195}Pt NMR (107 MHz, DMSO-d_6) δ (ppm): 1257. HRMS: m/z calculated for $C_9H_{16}Cl_2N_3O_4Pt$, $[M+H]^+$, 495.0160 found 495.0152.

[Pt(DACH)(ox)(OOCNHC$_6$H$_5$)(OAc)], OxaliPhen

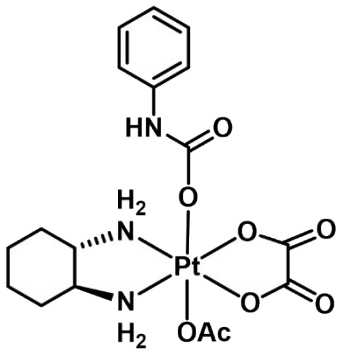

Yellow Solid. Yield (44 mg, 24%) .^{1}H NMR (400 MHz, DMSO-d_6) δ 9.22 – 8.21 (m, 4H), 7.40 (d, *J* = 7.8 Hz, 2H), 7.20 (t, *J* = 7.7 Hz, 2H), 6.91 (t, *J* = 7.3 Hz, 1H), 2.73 (s, 1H), 2.60 (d, *J* = 8.2 Hz, 1H), 2.15 (d, *J* = 12.3 Hz, 2H), 1.97 (s, 3H), 1.66 – 1.23 (m, 4H), 1.16 (d, *J* = 11.0 Hz, 2H).^{13}C NMR (101 MHz, DMSO-d_6) δ 178.25, 163.44, 163.38, 161.11, 139.97, 128.42, 121.67, 118.39, 61.08, 60.97, 30.93, 23.54, 22.87. ^{195}Pt NMR (107 MHz, DMSO-d_6) δ (ppm): 1624 HRMS: m/s calculated for $C_{17}H_{24}Cl_2N_3O_8Pt$, $[M+H]^+$: 593.1206, found 593.1221.

[Pt(NH_3)$_2$(CBDCA)(OOCNHC$_6$H$_5$)(OAc)],CarboPhen

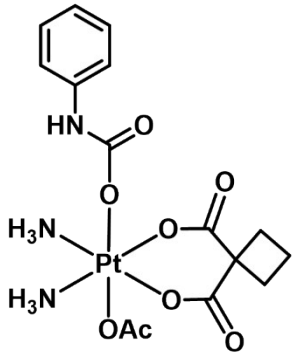

Yellow Solid. Yield (25 mg, 28%). ^{1}H NMR (400 MHz, DMSO-d_6) δ (ppm): 8.99 (s, 1H), 7.41 (d, *J* = 8.1 Hz, 2H), 7.17 (t, *J* = 7.8 Hz, 2H), 6.86 (t, *J* = 7.3 Hz, 1H), 6.53 (br, 6H), 2.57 (t, *J* = 8.0 Hz, 2H), 2.50 – 2.41 (m, 2H), 1.92 (s, 3H), 1.82 (t, *J* = 8.0 Hz, 2H). ^{13}C NMR (101 MHz, DMSO) δ 177.54, 176.15, 160.11, 140.58, 128.29, 121.14, 118.08, 55.39, 32.76, 29.56, 22.47, 15.74. ^{195}Pt NMR (107 MHz, DMSO-d_6) δ (ppm): 1968. HRMS: m/s calculated for $C_{15}H_{22}N_3O_8Pt$, $[M+H]^+$: 567.1049, found 567.1046.

[Pt(NH$_3$)$_2$(CBDCA)(OAc)$_2$], CarboBisOAc

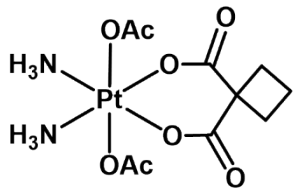

CarboBisOAc was synthesised according to a modified literature procedure.[5] Briefly, Carbo(OH)(OAc) was suspended in a 1:2 mixture of Acetic Anhydride:DMF and stirred overnight at room temperature. The next day the suspension was centrifuged, the yellow supernatant collected and added to cold diethyl ether and vigorously stirred to obtain a colourless precipitate. The solid was decanted, dissolved in minimal DMF and purified by column chromatography on silica gel [100% Hexane → 100% CH_2Cl_2 → 15% MeOH/85% CH_2Cl_2] to obtain a colourless solid (30 mg, 25%). ^{1}H NMR (400 MHz, DMSO-d_6) δ (ppm): 6.36 (br m, 6 H), 2.50 (under solvent peak, 4 H), 1.89 (s, 6 H), 1.81 (t, 2 H). The obtained analytical data is consistent with the literature report.[5]

[Pt(NH$_3$)$_2$(CBDCA)(OOCNHC$_{19}$H$_{12}$NO$_3$)(OAc)], CarboRes

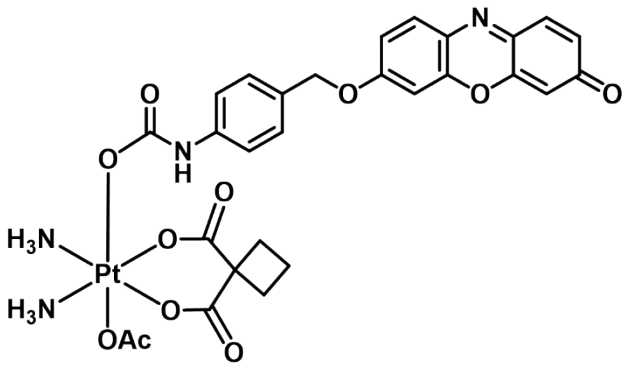

CarboRes was synthesised according to a modified literature procedure.[3] 4-(((3-oxo-3*H*-phenoxazin-7-yl)oxy)methyl)benzoic acid (0.040 g, 0.107 mmol, 3.0 equiv.) was suspended in dimethylformamide (3 mL). Triethylamine (Et_3N, 22 µL, 0.107 mmol, 3.0 equiv.) and diphenyl phosphoryl azide (DPPA, 34 µL, 0.107 mmol, 3.0 equiv.) were added and the reaction mixture was stirred for 30 minutes at room temperature followed by heating at 70 °C for 3 hours. The reaction mixture was cooled to room temperature. Carbo(OH)(OAc) (0.016 g, 0.036 mmol, 1.0 equiv.) was added and the reaction was stirred at 100 °C. Upon completion, the crude mixture was purified via column chromatography (100% Hexane to 100% EtOAc to CH_2Cl_2/MeOH 9:1). The recovered solid was triturated with EtOAc and MeOH to afford the title compound as a dark red solid (0.012 g, 0.015 mmol, 42%). ^{1}H NMR (400 MHz, DMSO-d_6) δ: 9.11 (s, NH), 7.78 (d, *J* = 8.9 Hz, 1H), 7.54 (d, *J* = 9.5 Hz, 1H), 7.46 (d, *J* = 8.2 Hz, 2H), 7.31 (d, *J* = 8.9 Hz, 2H), 7.18 (d, *J* = 2.6 Hz, 1H), 7.11 (dd, *J* = 2.6, 8.9 Hz, 1H), 6.80 (dd, *J* = 2.0, 9.5 Hz, 1H), 6.52 (m, NH_3), 6.27 (d, *J* = 3.0 Hz, 1H), 5.15 (s, 2H), 2.57 (t, *J* = 7.0 Hz, 2H), 2.46 (m, 2H), 1.92 (s, 3H), 1.82 (t, *J* = 7.6 Hz, 2H) ppm. ^{13}C NMR (176 MHz, DMSO-d_6) δ: 185.3, 177.5, 176.1, 162.5, 160.0, 149.7, 145.2, 145.1, 140.7, 134.9, 133.7, 131.1, 128.7, 128.3, 127.9, 117.9, 114.4, 105.6, 101.1, 70.4, 55.4, 32.8, 29.5, 22.4, 15.7 ppm. ^{195}Pt NMR (107 MHz, DMSO-d_6): 1970 ppm. HRMS (*m/z*) calcd. for $C_{28}H_{28}N_4O_{11}Pt$ $[M+Na]^+$ 814.1295, found 814.1302.

4. Additional Analyses

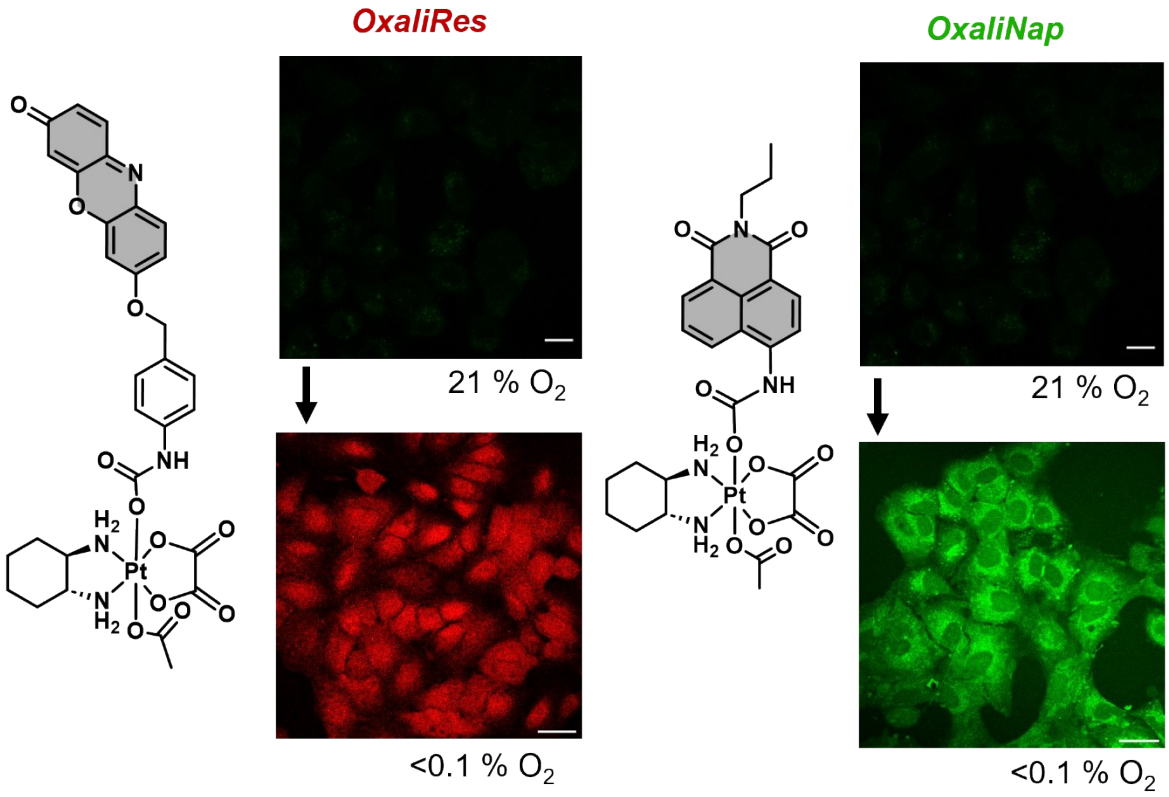

Figure S1. Chemical structures and fluorescent images of the hypoxia-dependent fluorescence response in cancer cells with our previously reported fluorogenic Pt(IV) complexes **OxaliRes** (left) and **OxaliNap** (right).

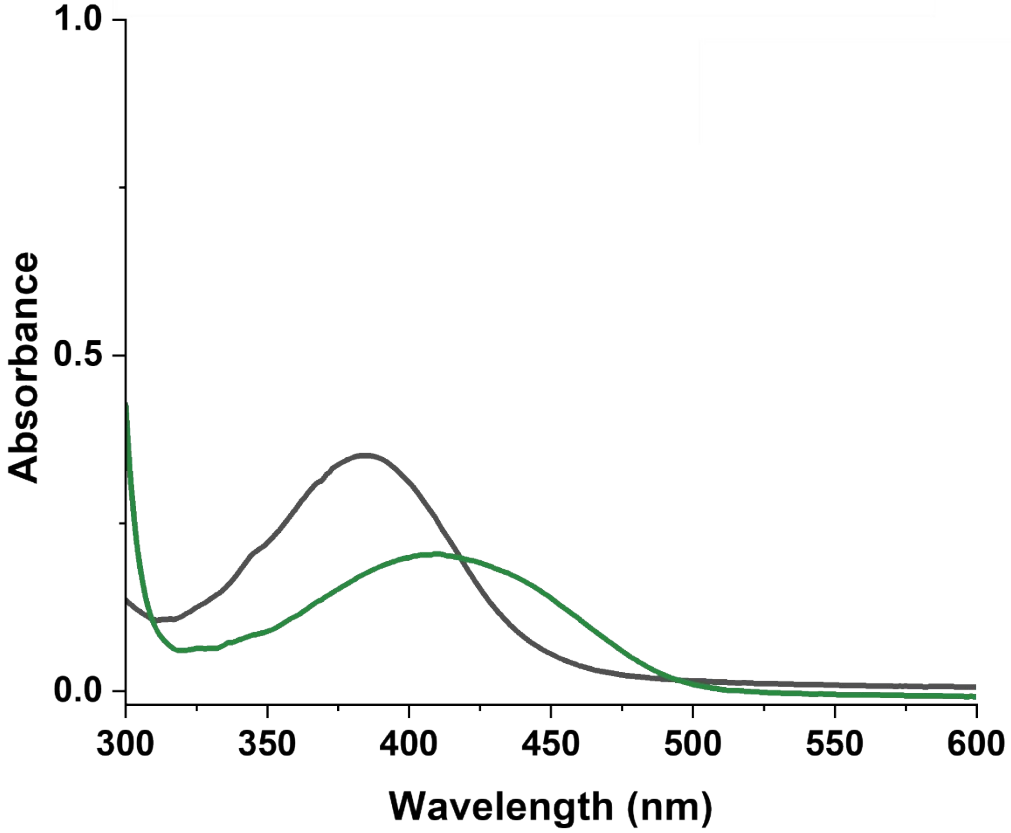

Figure S2. Absorbance spectra of **CisNap** (25 µM) before (**black**) and after (**green**) 1 h incubation with NaAsc (50 mM) in PBS (pH 7.4).

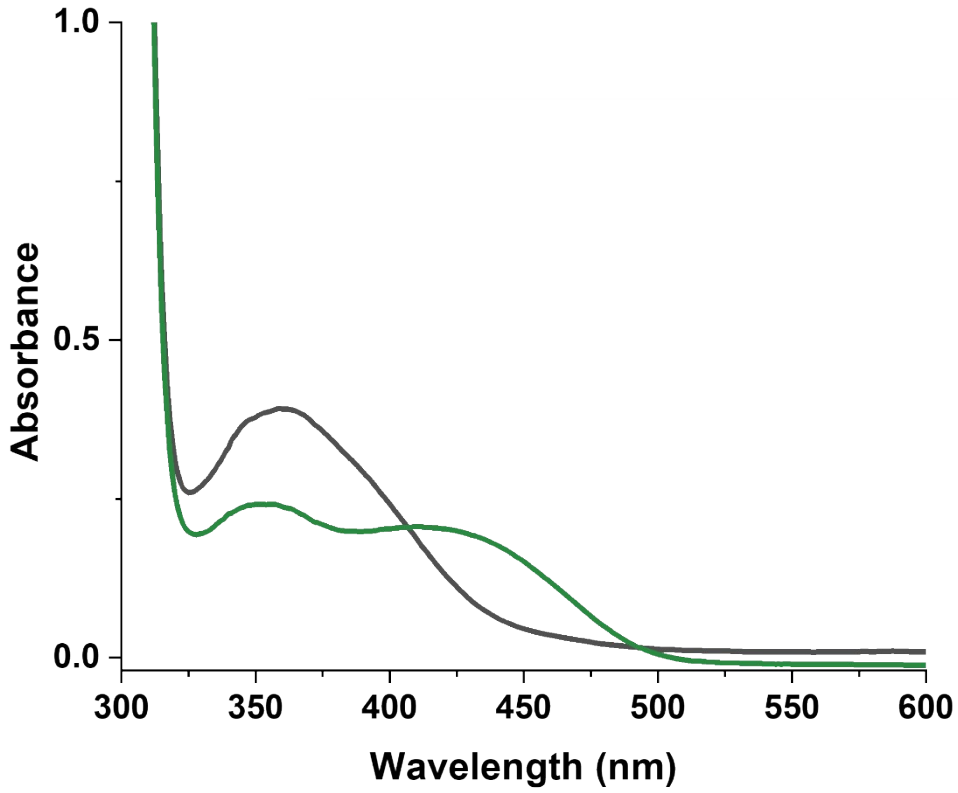

Figure S3. Absorbance spectra of **OxaliNap** (25 μM) before (**black**) and after (**green**) 1 h incubation with NaAsc (50 mM) in PBS (pH 7.4).

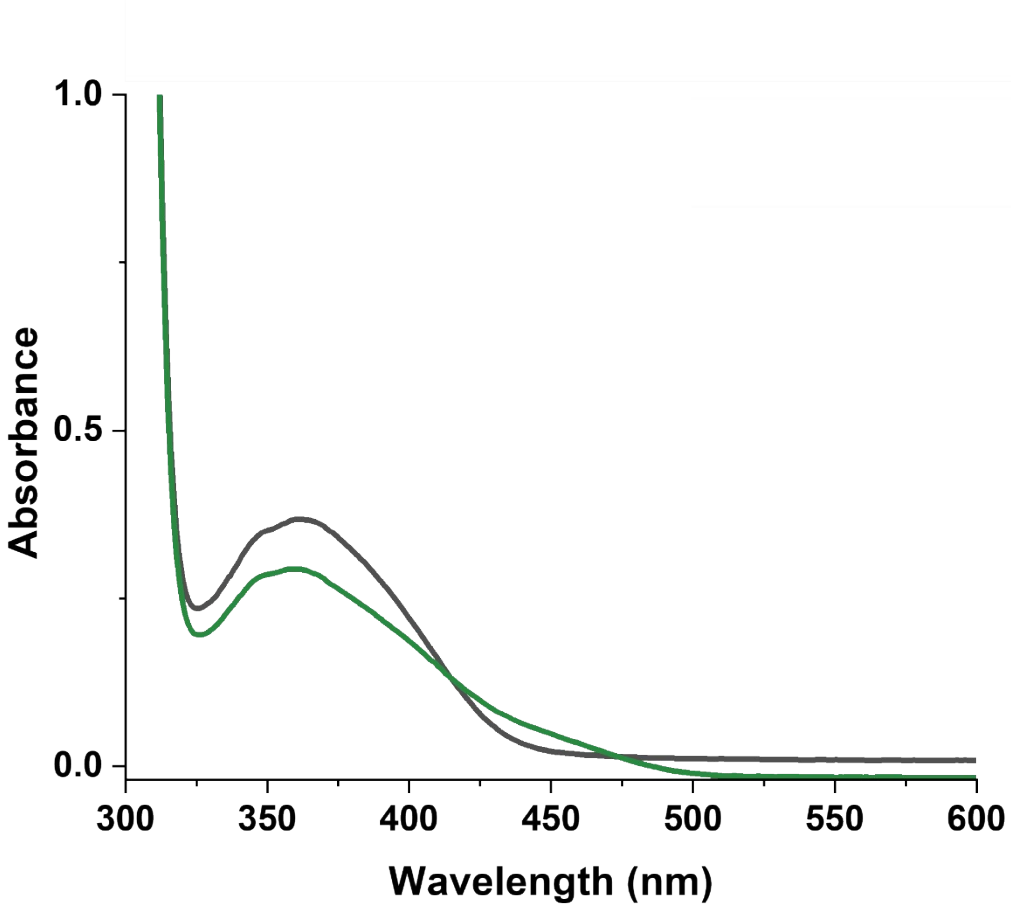

Figure S4. Absorbance spectra of **CarboNap** (25 µM) before (**black**) and after (**green**) 1 h incubation with NaAsc (50 mM) in PBS (pH 7.4).

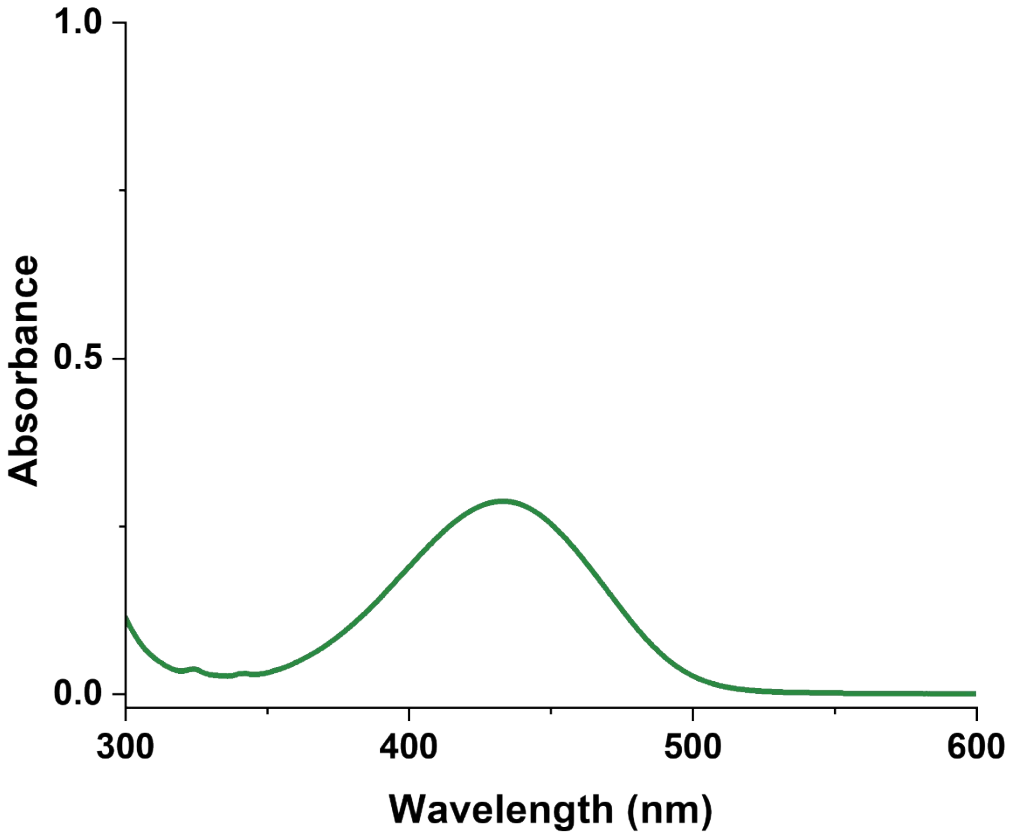

Figure S5. Absorbance spectra of **Nap-NH_2** (12.5 µM) in PBS (pH 7.4).

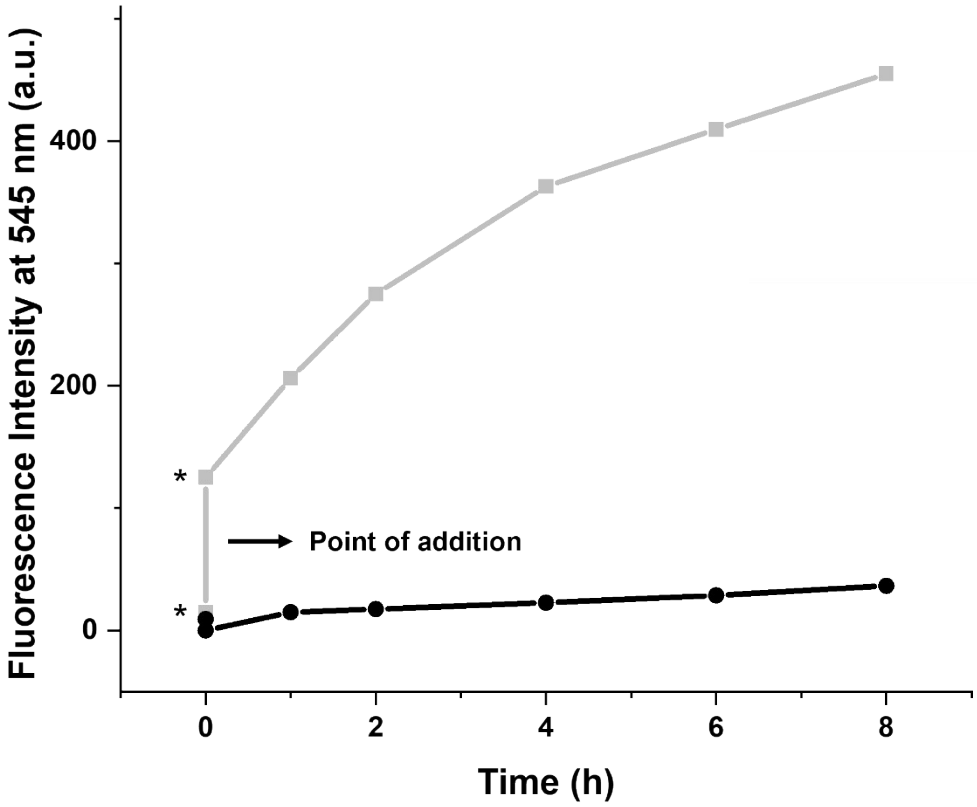

Figure S6. Changes in fluorescence emission intensity at 545 nm of **CisNap** (5 μM) at different time points (0,* 1, 2, 4, 6, 8 h) with (**grey**) and without (**black**) NaAsc (1 mM). All measurements were performed in PBS Buffer (pH = 7.4), λ_{ex} = 430 nm (slit widths: 10 nm and 3.5 nm). *Before and after addition of NaAsc showing the instantaneous response of **CisNap** to NaAsc.

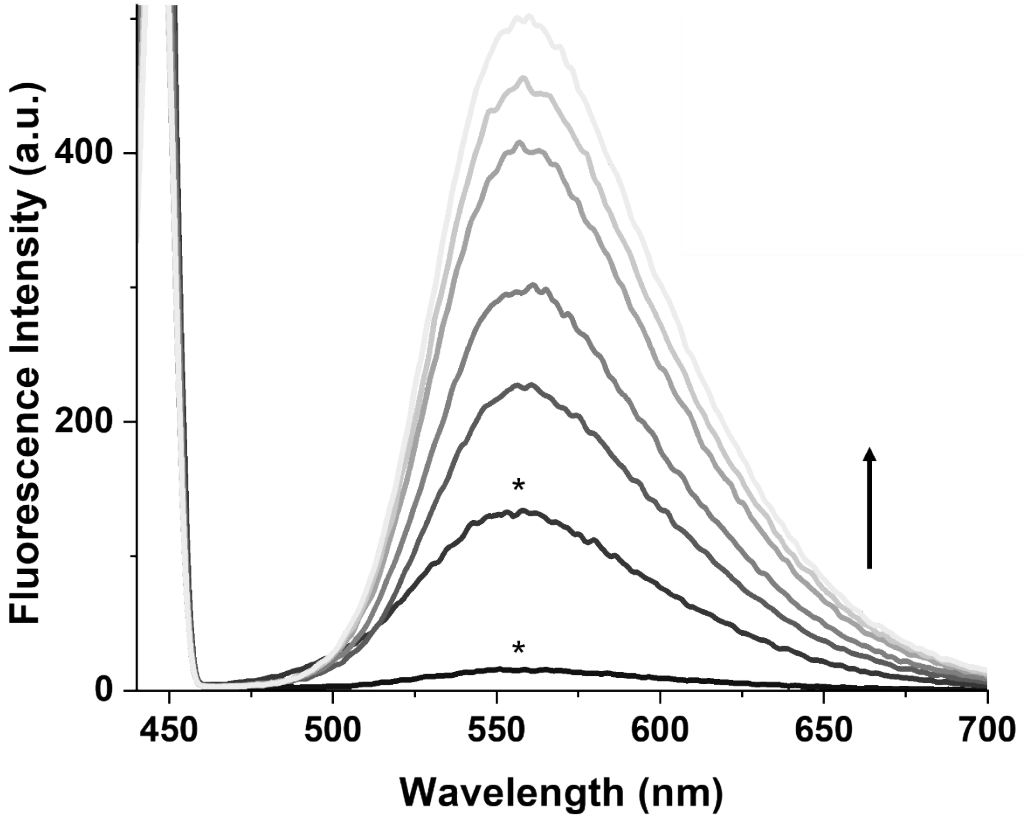

Figure S7. Fluorescence spectra of **CisNap** (5 μM) incubated with NaAsc (1 mM) at different time points (0*, 1, 2, 4, 6, 8 h). All measurements were performed in PBS Buffer (pH = 7.4). λ_{ex} = 430 nm, slit widths: 10 nm and 3.5 nm. *Before and after addition of NaAsc showing the instantaneous response of **CisNap** to NaAsc.

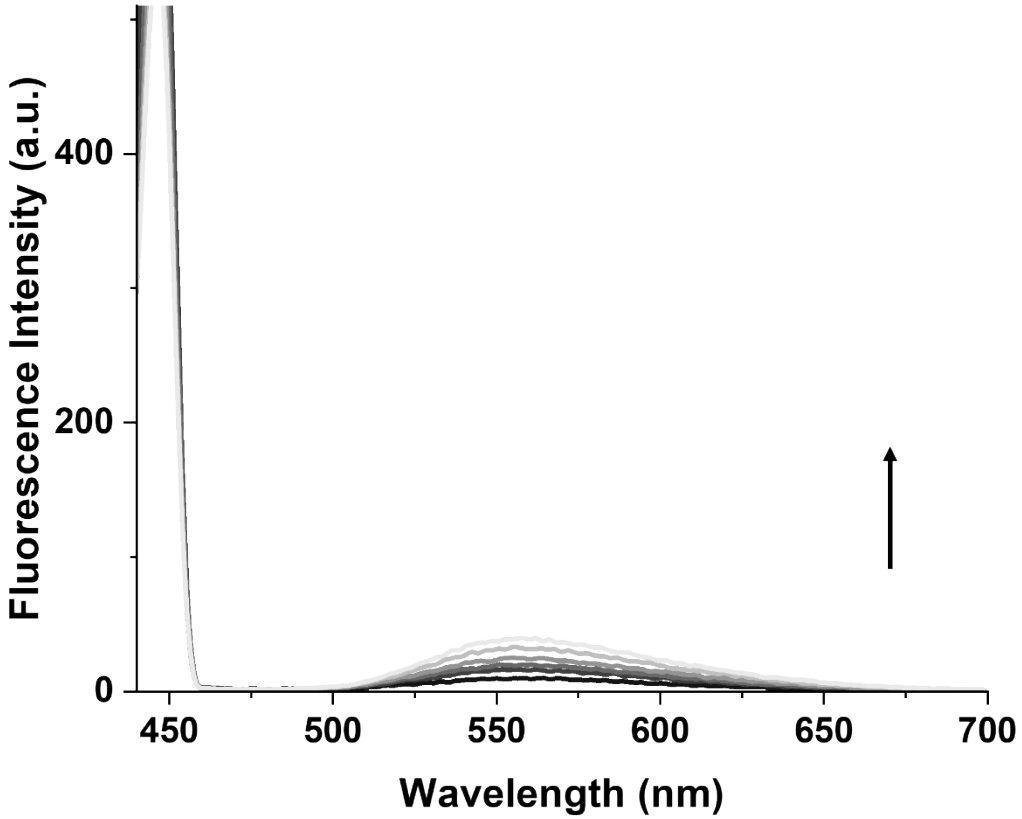

Figure S8. Fluorescence spectra of **CisNap** (5 µM) at different time points (0, 1, 2, 4, 6, 8 h). All measurements were performed in PBS Buffer (pH = 7.4). λ_{ex} = 430 nm, slit widths: 10 nm and 3.5 nm.

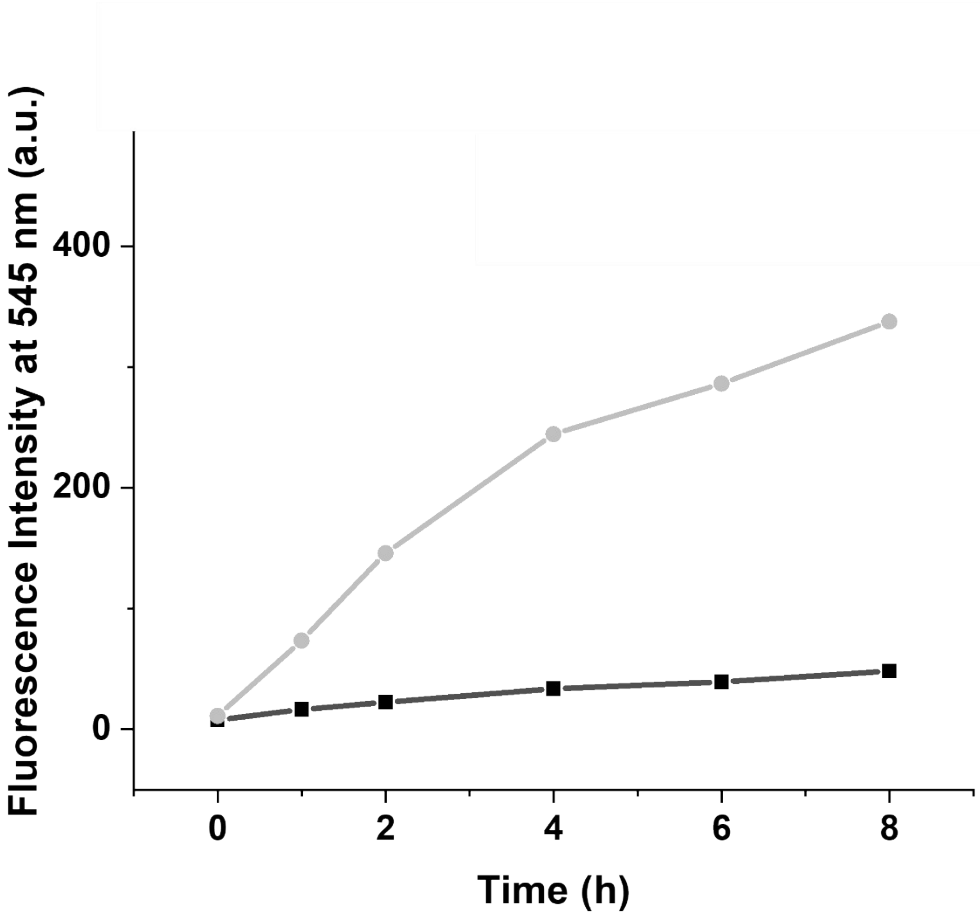

Figure S9. Changes in fluorescence emission intensity of **OxaliNap** (5 μM) at 545 nm at different time points (0, 1, 2, 4, 6, 8 h) with (**grey**) and without (**black**) NaAsc (10 mM). All measurements were performed in PBS Buffer (pH = 7.4), λ_{ex} = 430 nm, slit widths: 10 nm and 3.5 nm.

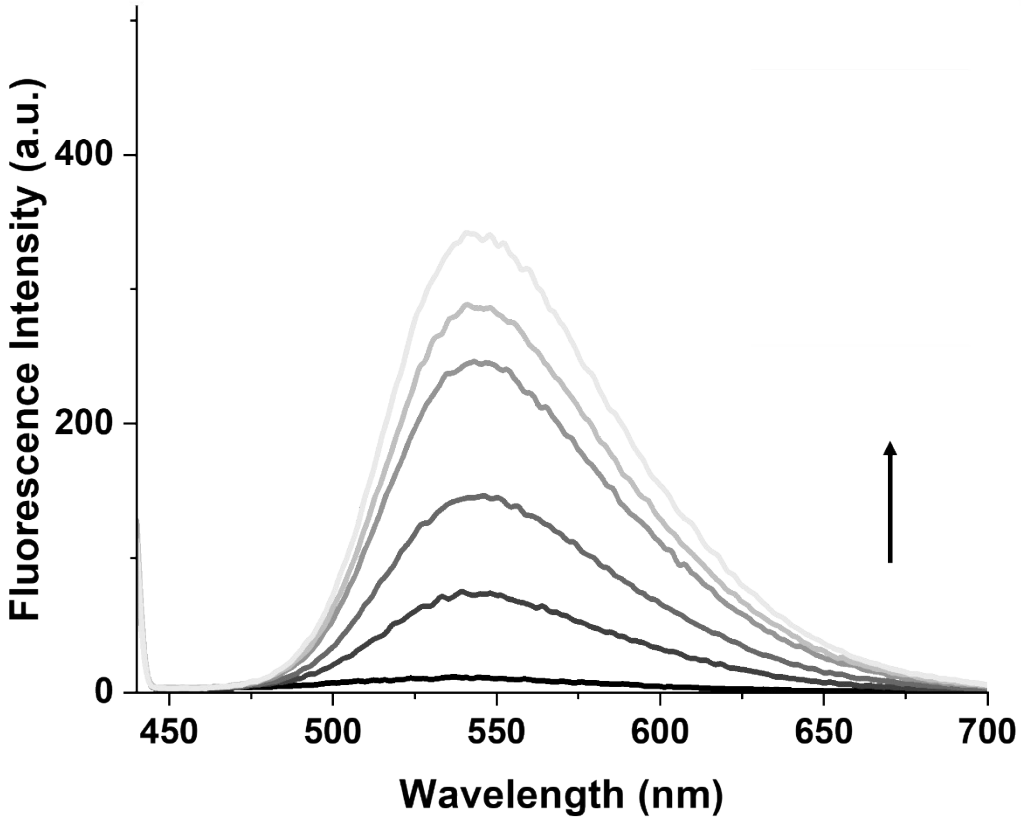

Figure S10. Fluorescence spectra of **OxaliNap** (5 µM) incubated with NaAsc (10 mM) at different time points (0, 1, 2, 4, 6, 8 h). All measurements were performed in PBS Buffer (pH = 7.4). λ_{ex} = 430 nm, slit widths: ex = 10 nm, em = 3.5 nm.

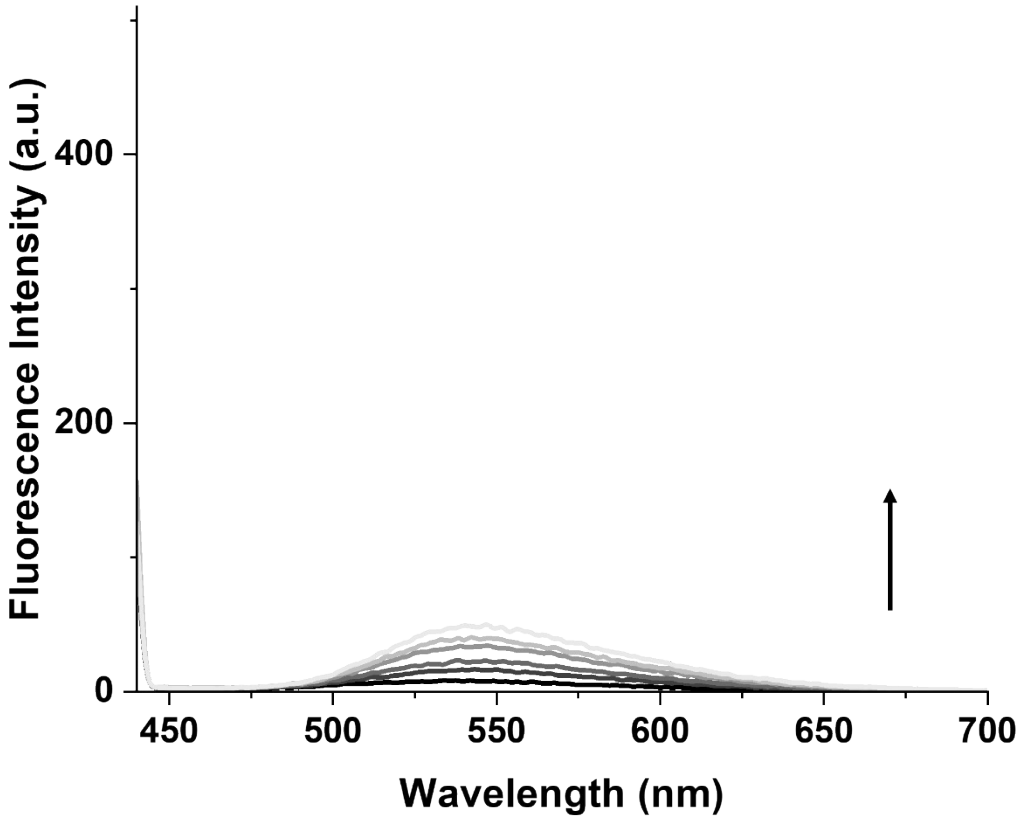

Figure S11. Fluorescence spectra of **OxaliNap** (5 µM) at different time points (0, 1, 2, 4, 6, 8 h). All measurements were performed in PBS Buffer (pH = 7.4). λ_{ex} = 430 nm, slit widths: 10 nm and 3.5 nm.

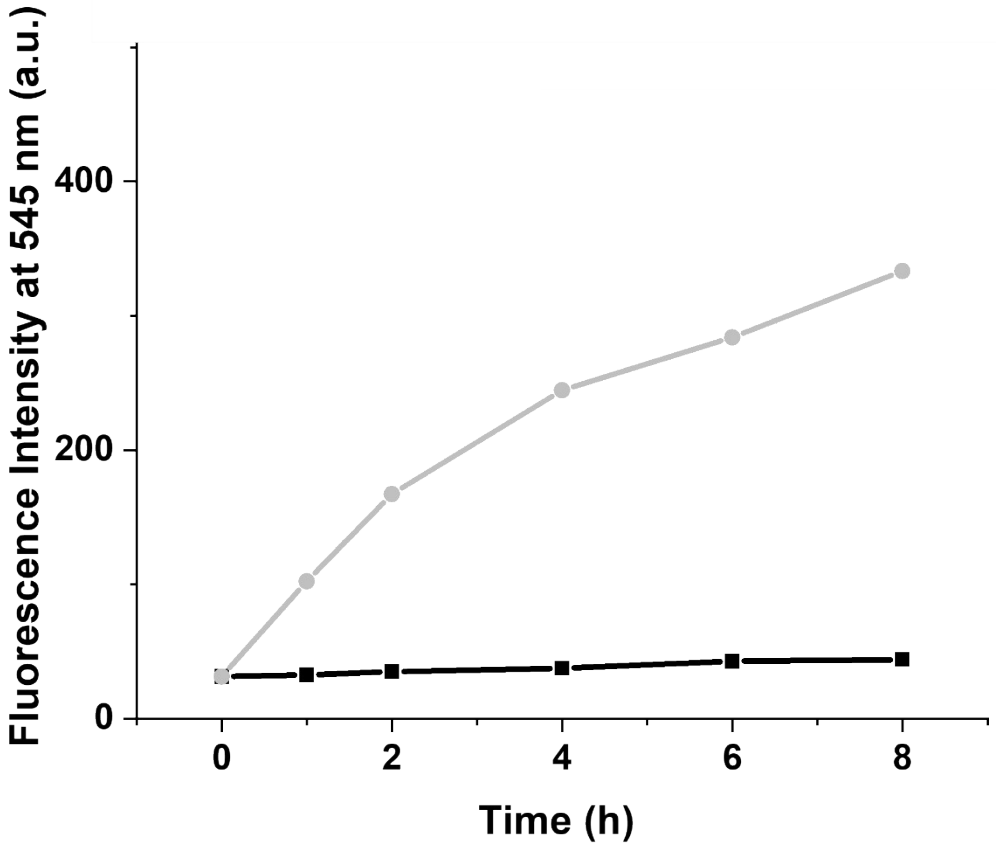

Figure S12. Changes in fluorescence emission intensity of **CarboNap** (5 µM) at different time points (0, 1, 2, 4, 6, 8 h) with (**grey**) and without (**black**) NaAsc (10 mM). All measurements were performed in PBS Buffer (pH = 7.4). λ_{ex} = 430 nm, slit widths: 10 nm and 3.5 nm.

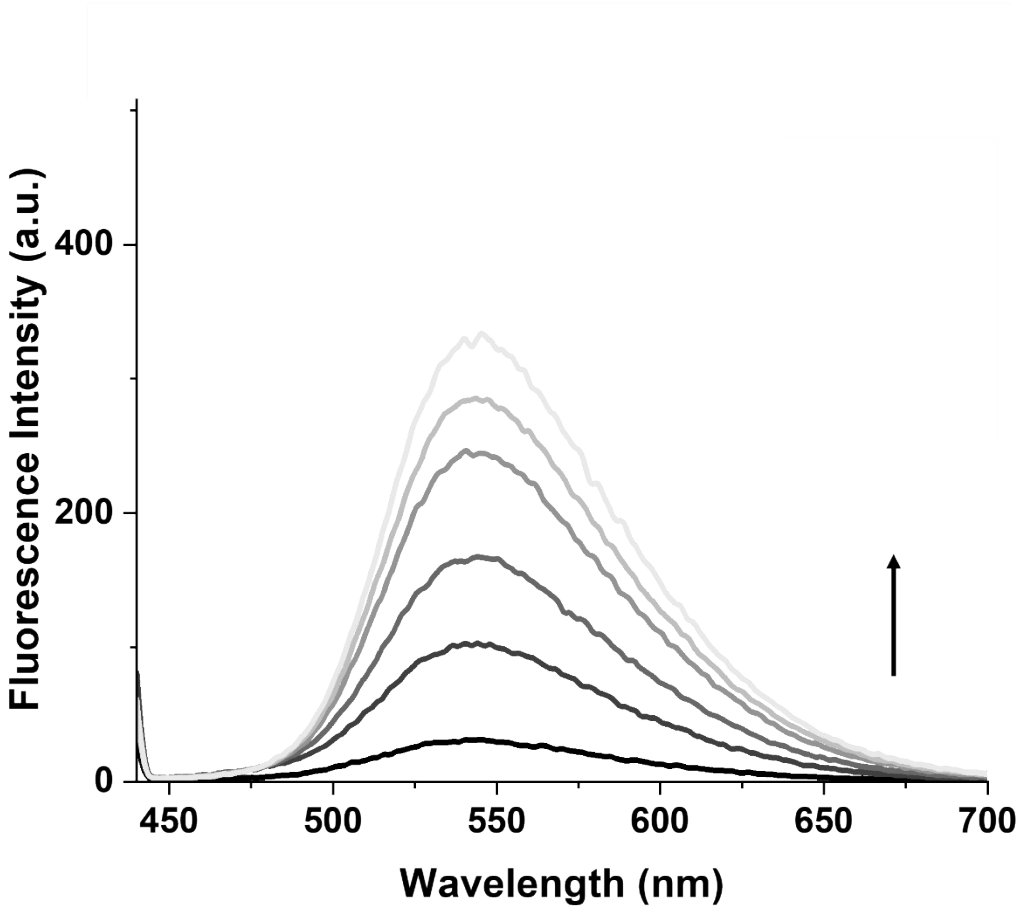

Figure S13. Fluorescence spectra of **CarboNap** (5 μM) incubated with NaAsc (10 mM) at different time points (0, 1, 2, 4, 6, 8 h). All measurements were performed in PBS Buffer (pH = 7.4). λ_{ex} = 430 nm, slit widths: ex = 10 nm, em = 3.5 nm.

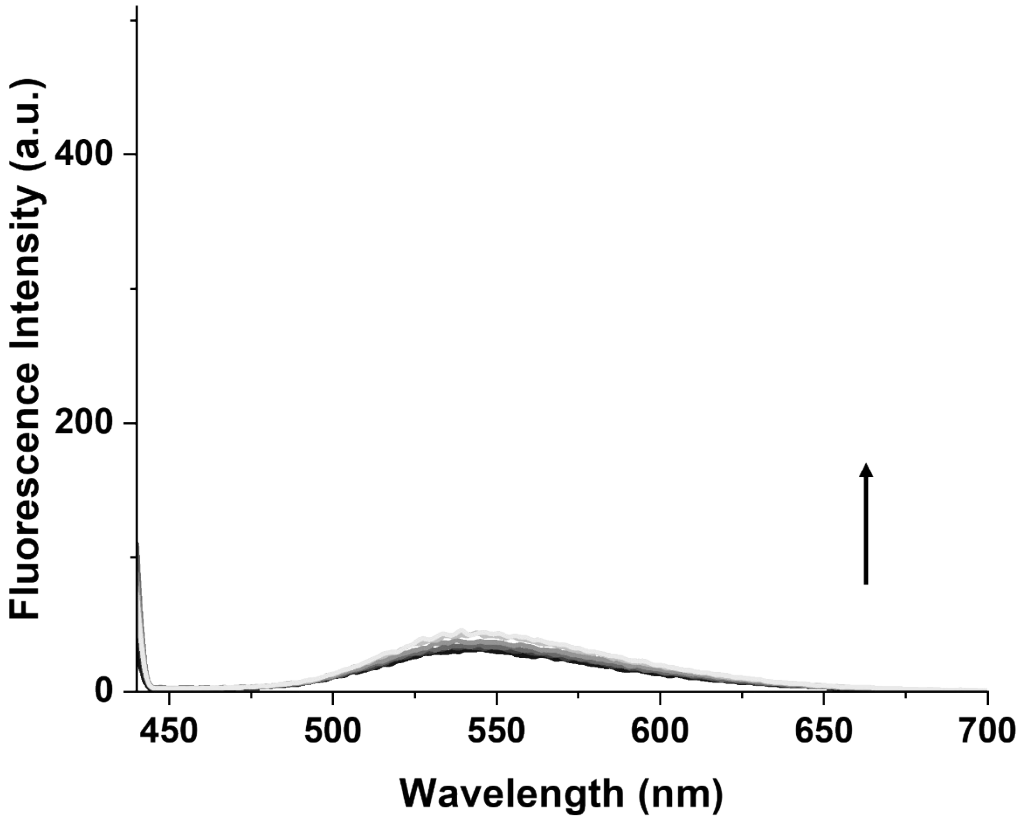

Figure S14. Fluorescence spectra of **CarboNap** (5 μM) at different time points (0, 1, 2, 4, 6, 8 h). All measurements were performed in PBS Buffer (pH = 7.4). λ_{ex} = 430 nm, slit widths: 10 nm and 3.5 nm.

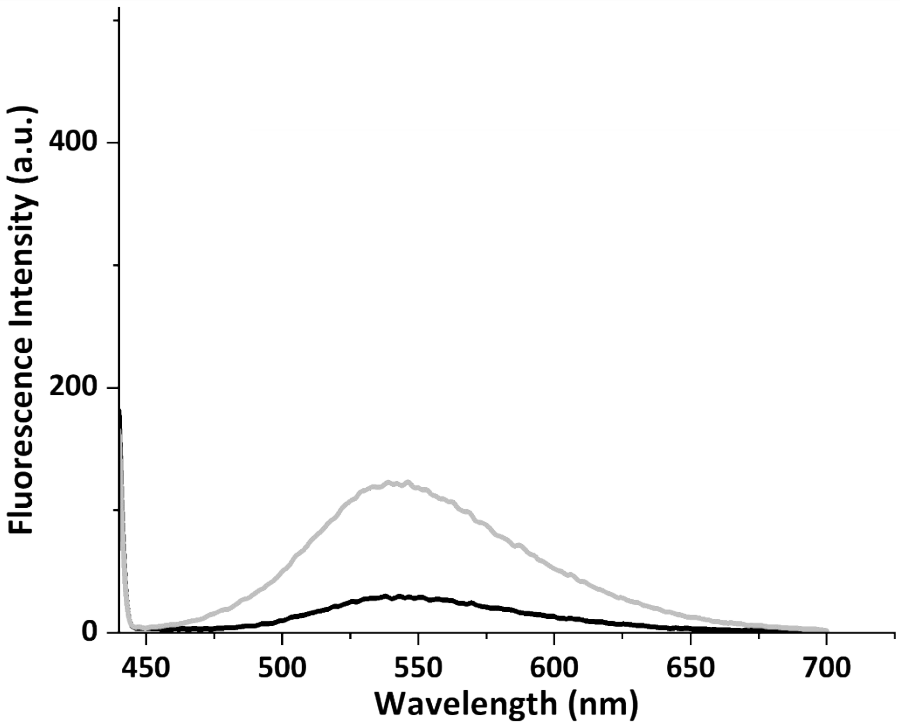

Figure S15. Fluorescence spectra of the instantaneous response of **CisNap** to NaAsc (250 μM) in PBS Buffer (pH = 7.4), λ_{ex} = 430 nm, slit widths: 10 nm and 3.5 nm.

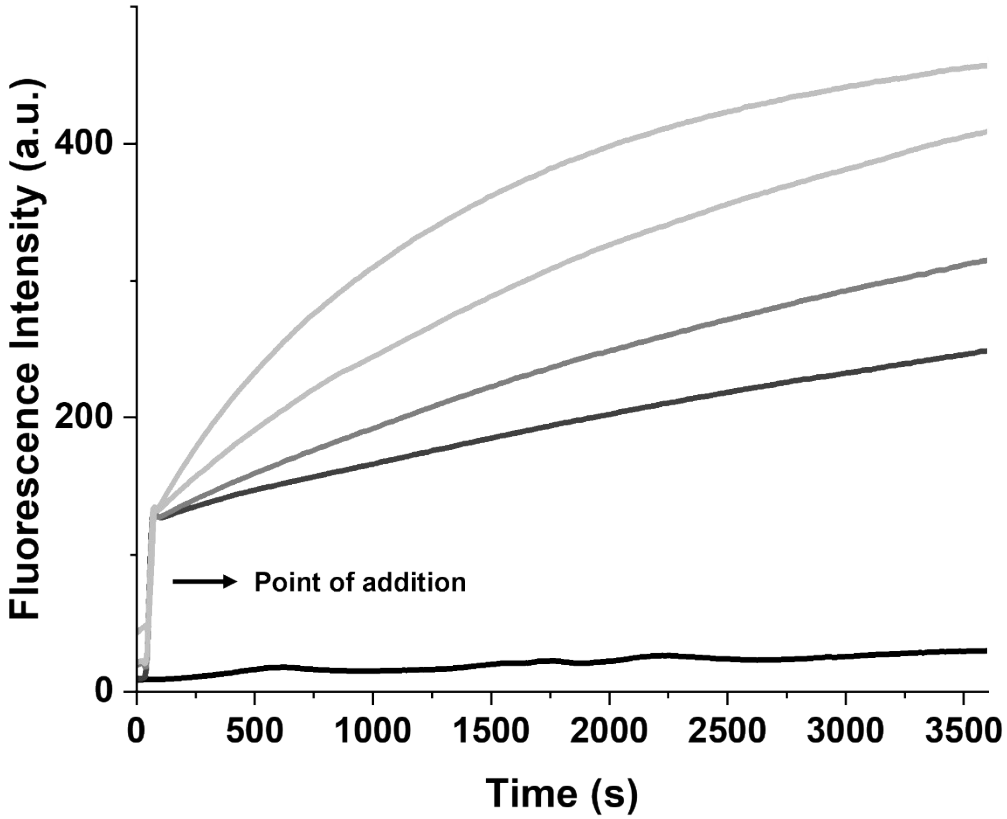

Figure S16. Changes in fluorescence emission intensity of **CisNap** (5 µM) incubated with different concentrations of NaAsc (0 mM, 2 mM, 4 mM, 8 mM, 15 mM) for 1 h. All measurements were performed in PBS Buffer (pH = 7.4), λ_{ex} = 430 nm, slit widths: 10 nm and 3.5 nm.

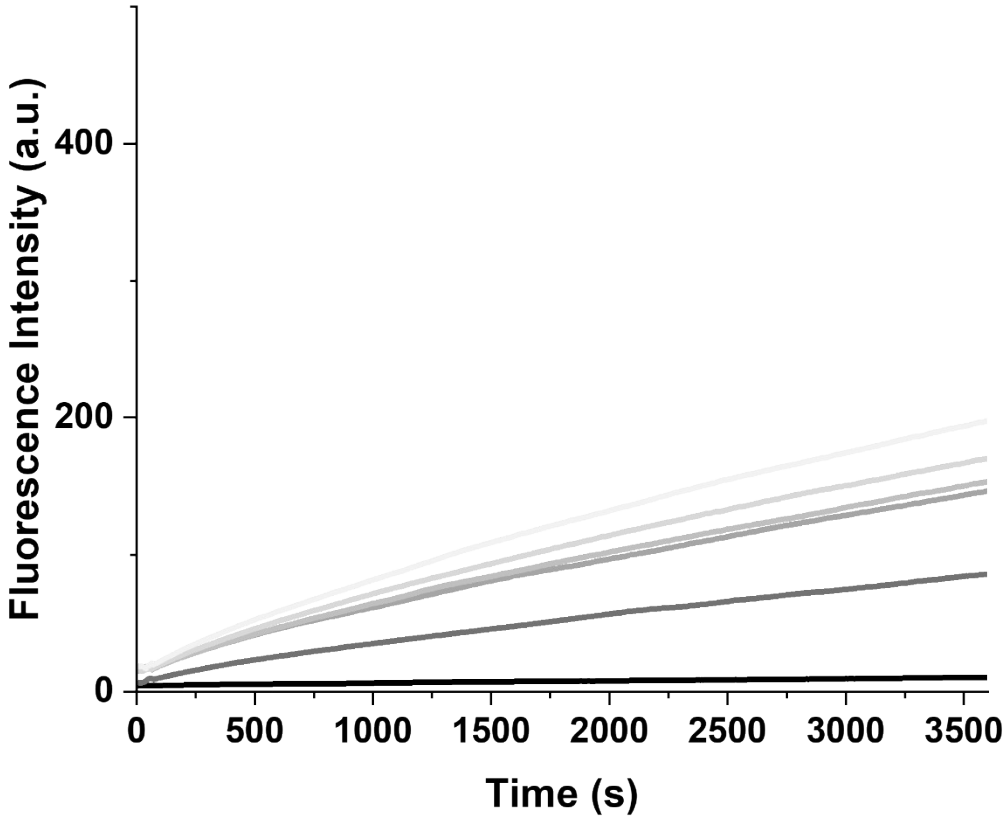

Figure S17. Changes in fluorescence emission intensity of **OxaliNap** (5 µM) at 545 nm incubated with different concentrations of NaAsc (0 mM, 10 mM, 20 mM, 30 mM, 40 mM, 50 mM) for 1 h. All measurements were performed in PBS Buffer (pH = 7.40), λ_{ex} = 430 nm, slit widths: ex = 10 nm and em = 3.5 nm.

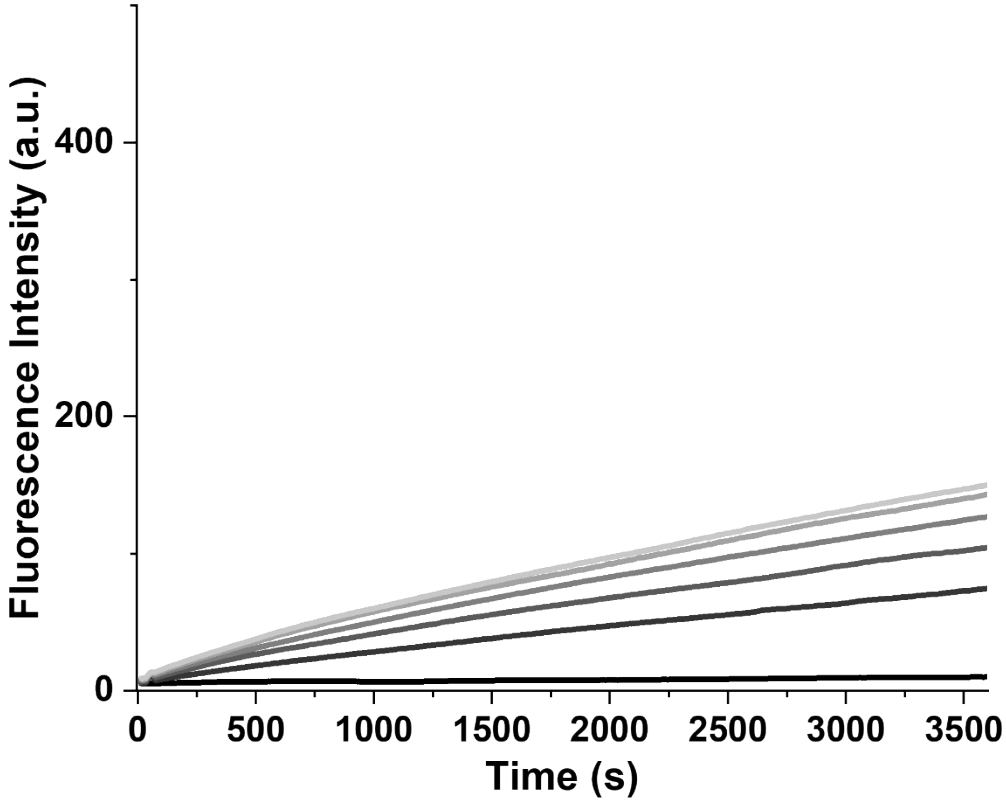

Figure S18. Changes in fluorescence emission intensity of **CarboNap** (5 μM) at 545 nm incubated with different concentrations of NaAsc (0 mM, 10 mM, 20 mM, 30 mM, 40 mM, 50 mM) for 1 h. All measurements were performed in PBS Buffer (pH = 7.40), λ_{ex} = 430 nm, slit widths: ex = 10 nm and em = 3.5 nm.

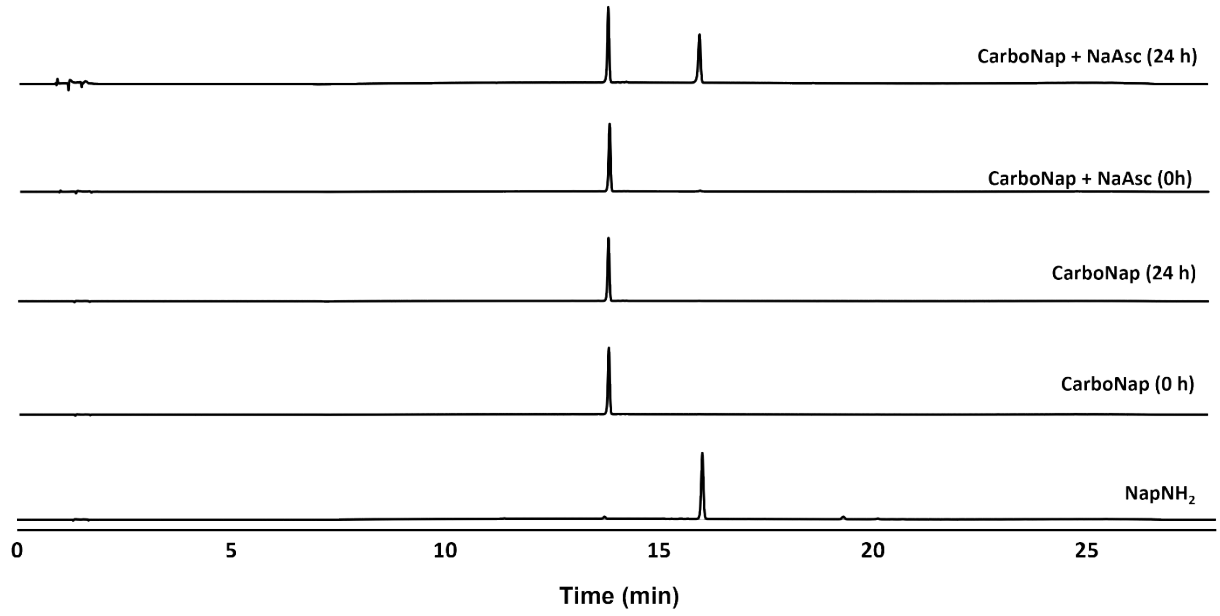

Figure S19. HPLC chromatograms of **CarboNap** (50 µM) incubated with and without NaAsc (50 mM) in deionised H_2O for 24 h (absorption at 380 nm).

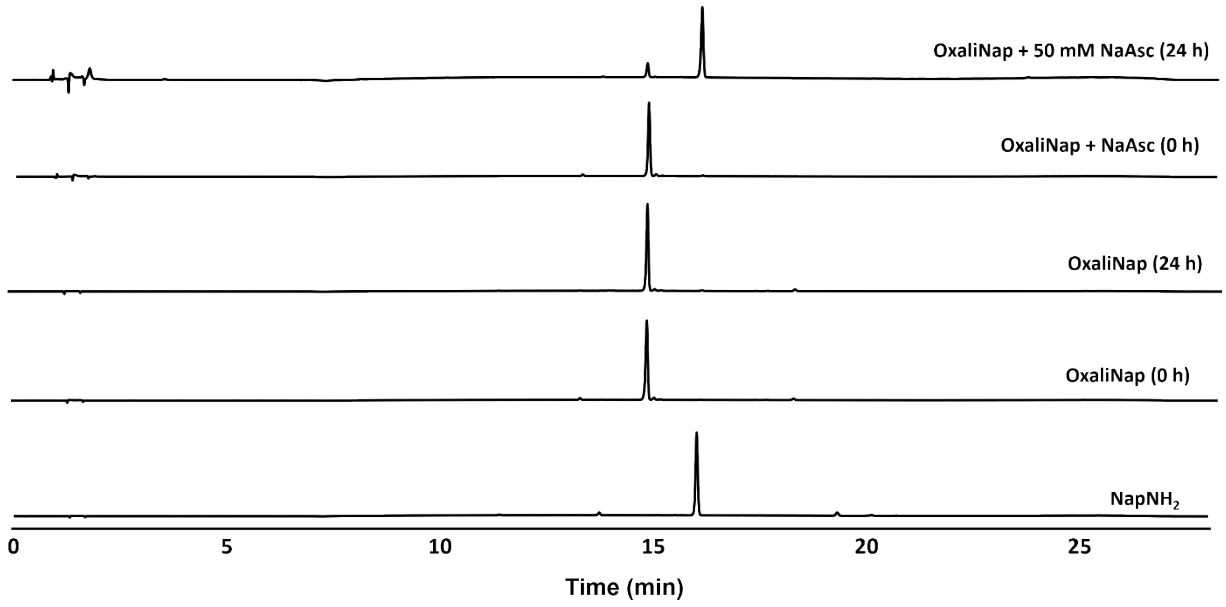

Figure S20. HPLC chromatograms of **OxaliNap** (50 µM) incubated with and without NaAsc (50 mM) in deionised H_2O for 24 h (absorption at 380 nm).

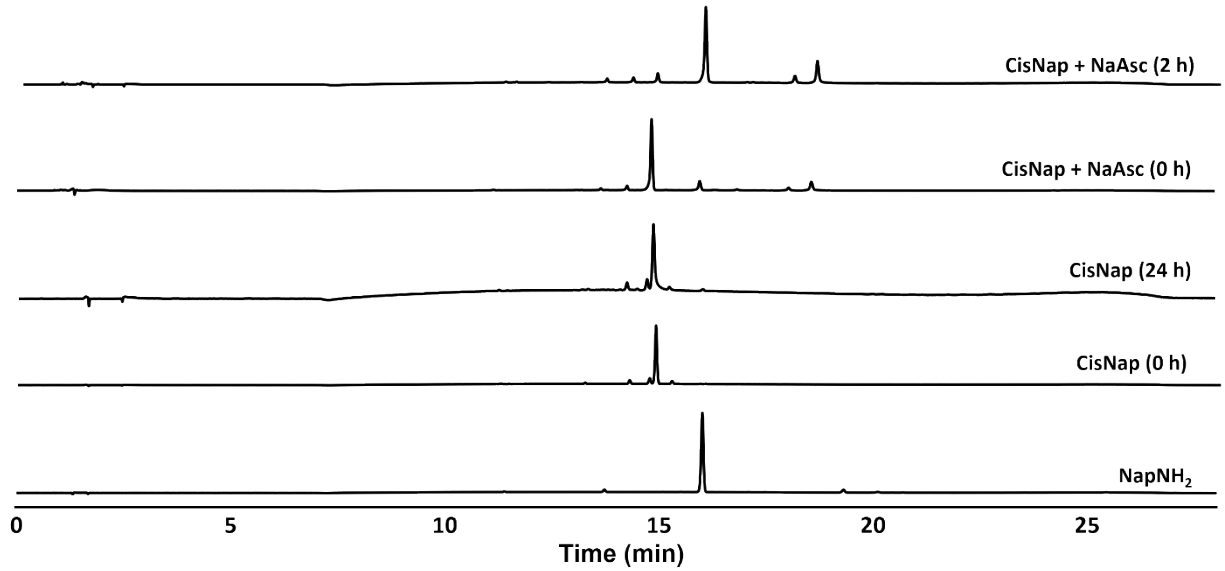

Figure S21. HPLC chromatograms of **CisNap** (50 µM) incubated with and without NaAsc (10 mM) in deionised H_2O for 24 h (absorption at 380 nm).

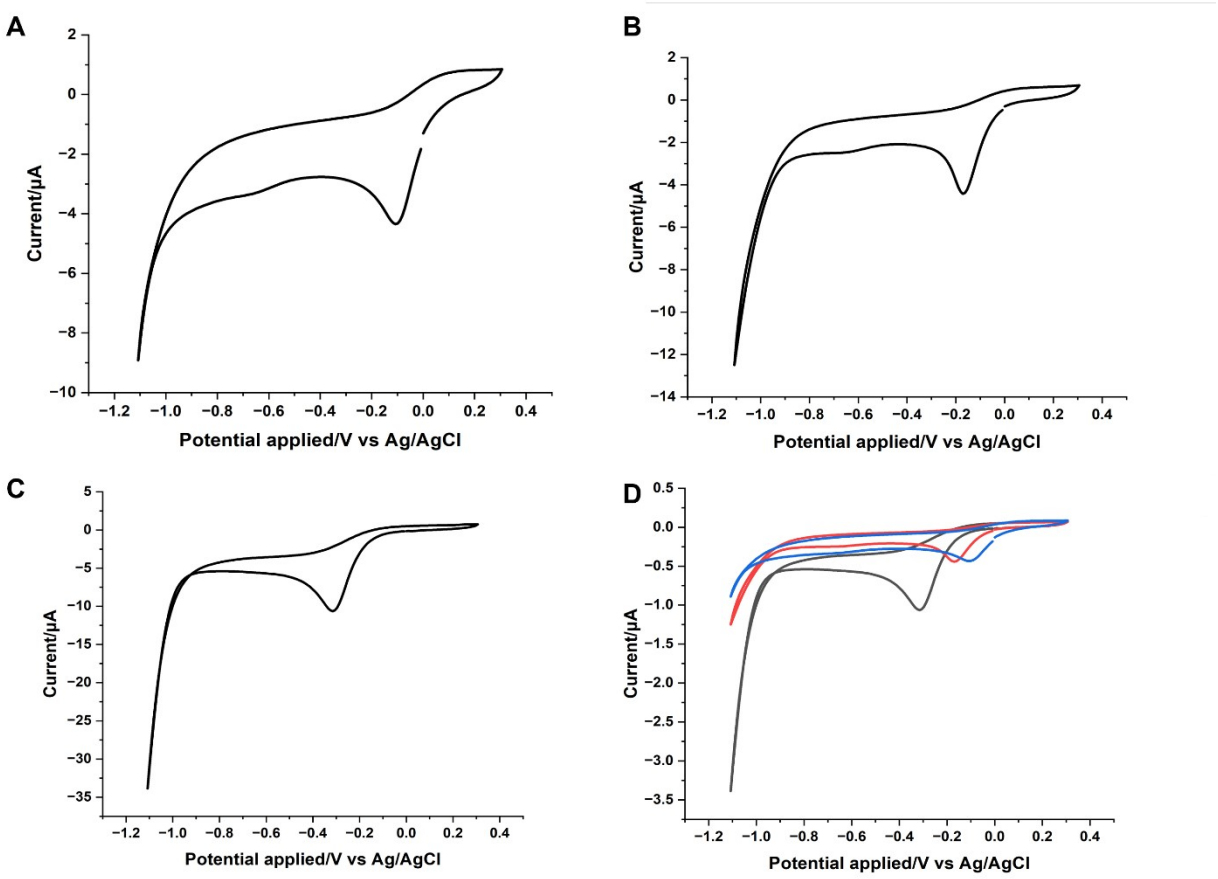

Figure S22. Cyclic Voltammogram of a 3 mm glassy carbon electrode immersed in 1 mM solution of **CisNap** (**A**), **OxaliNap** (**B**), **CarboNap** (**C**), and an overlay comparison of **CarboNap** (**black**), **OxaliNap** (**red**) and **CisNap** (**blue**) (**D**) in PBS buffer (pH 7.4, with 30% DMF for **CisNap***; 10% DMF for **OxaliNap** and **CarboNap**) at a scan rate of 0.1 V/s. *A greater percentage of DMF was required for **CisNap** due to solubility issues.

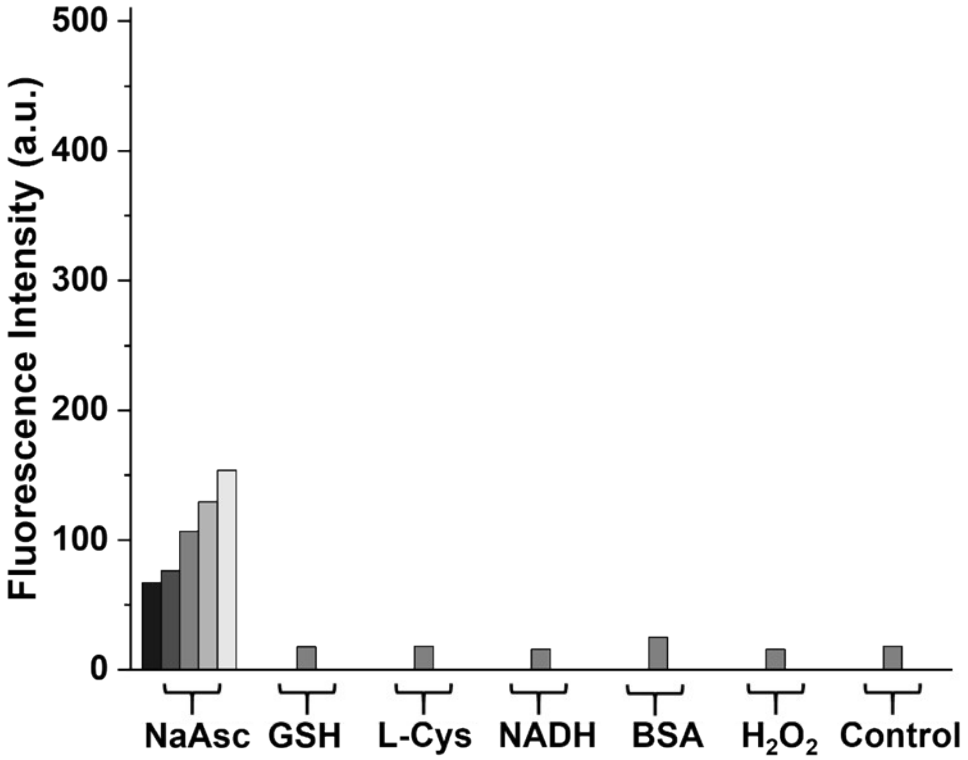

Figure S23. Changes in fluorescence emission intensity of **CarboNap** (5 μM) after a 1 h incubation with various analytes: NaAsc (5 mM, 10 mM, 20 mM, 30 mM, 40 mM); NADH (0.5 mM); GSH (4 mM); L-Cysteine (100 μM); BSA (1 equiv.) and H_2O_2 (100 μM). All measurements were performed in PBS Buffer (pH = 7.4), λ_{ex} = 430 nm, slit widths: 10 nm and 3.5 nm.

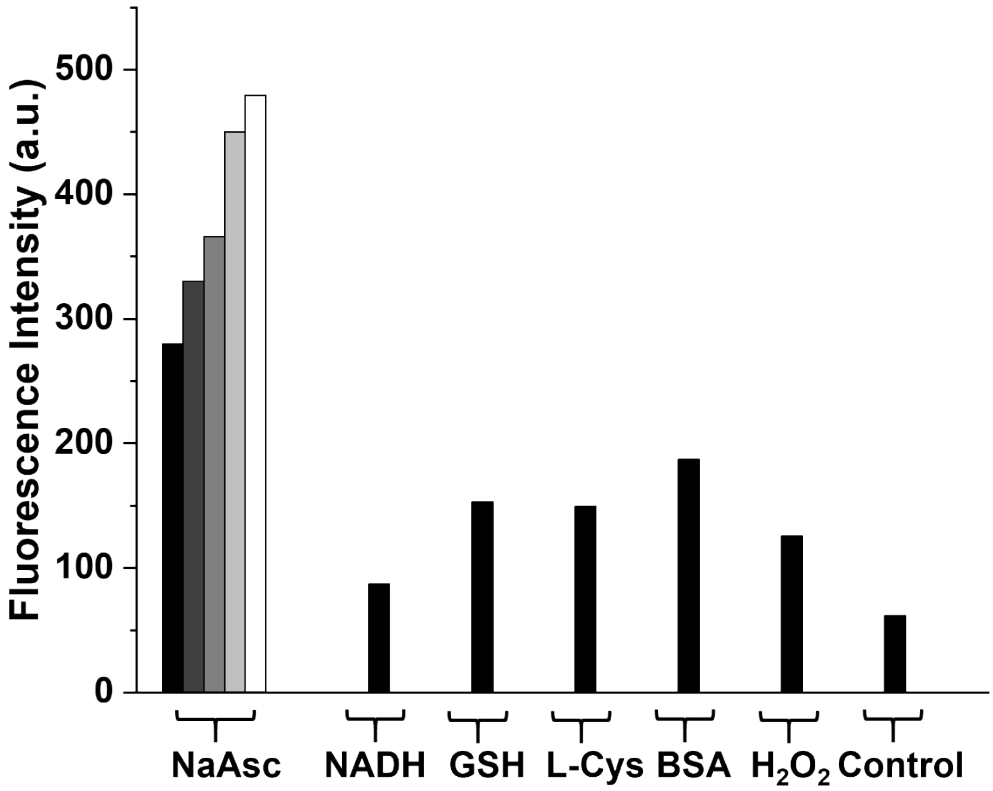

Figure S24. Changes in fluorescence emission intensity of **CisNap** (5 μM) after a 1 h incubation with various analytes: NaAsc (0.5 mM, 1 mM, 2 mM, 4 mM, 8 mM); NADH (0.5 mM); GSH (4 mM); L-Cysteine (100 μM); BSA (1 equiv.) and H_2O_2 (100 μM). All measurements were performed in PBS Buffer (pH = 7.4), λ_{ex} = 430 nm, slit widths: 10 nm and 3.5 nm.

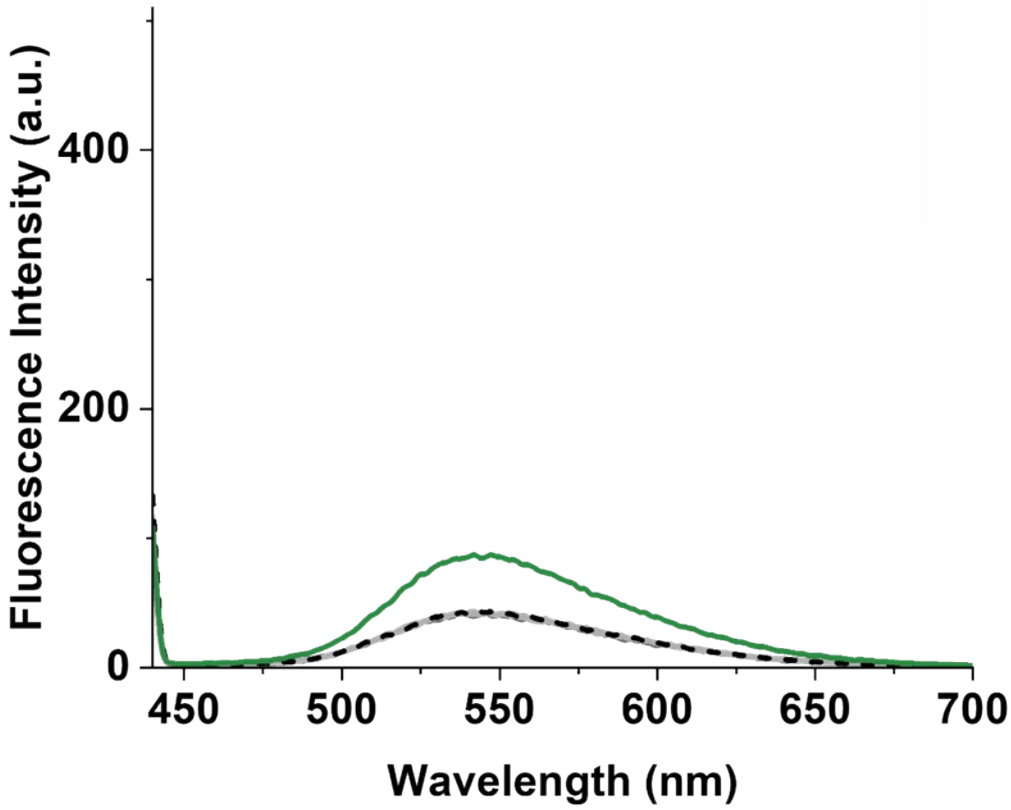

Figure S25. Fluorescence spectra of **OxaliNap** (5 µM) before (black dotted line) and after a 1 h incubation with GSH (2 mM, 4 mM, 6 mM, 8 mM, grey) and NaAsc (10 mM, green). All measurements were performed in PBS Buffer (pH = 7.4), λ_{ex} = 430 nm, slit widths: 10 nm and 3.5 nm.

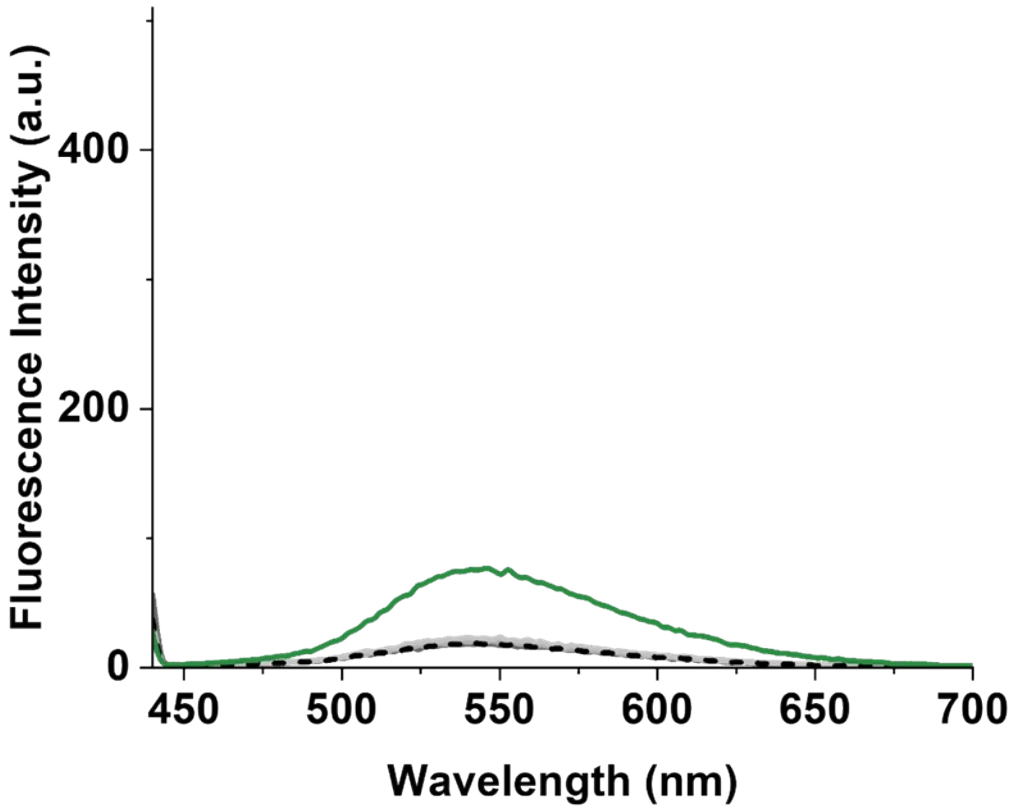

Figure S26. Fluorescence spectra of **CarboNap** (5 µM) before (black dotted line) and after a 1 h incubation with GSH (2 mM, 4 mM, 6 mM, 8 mM, grey) and NaAsc (10 mM, green). All measurements were performed in PBS Buffer (pH = 7.4), λ_{ex} = 430 nm, slit widths: 10 nm and 3.5 nm.

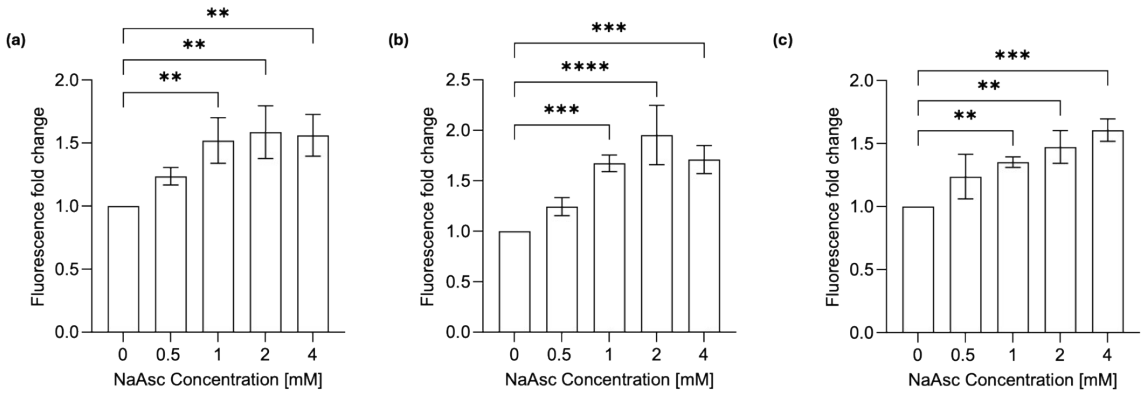

Figure S27. Flow cytometry analysis of A549 cells treated with (a) **CisNap**, (b) **OxaliNap**, and (c), **CarboNap** (all 10 µM) with the indicated concentrations of NaAsc. Fluorescence fold change of the geometric mean intensity is displayed. Error bars represent SD. Significance compared to probe alone condition. ** $p < 0.01$, and *** $p < 0.001$. n = 3.

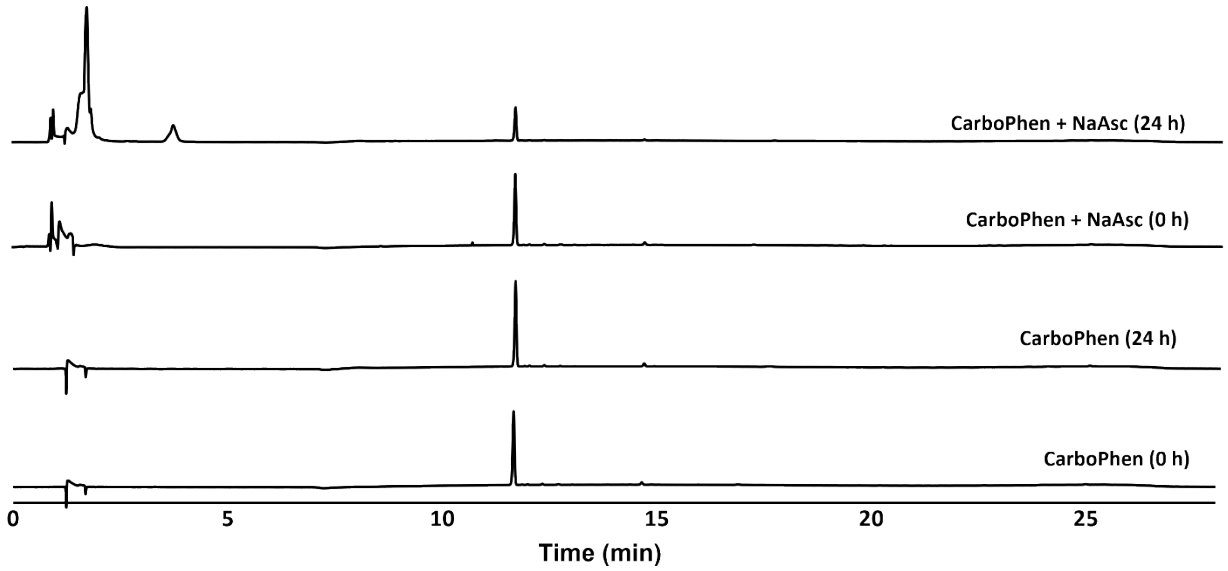

Figure S28. HPLC chromatograms of **CarboPhen** (150 µM) incubated with and without NaAsc (150 mM) in deionised H_2O for 24 h (absorption at 380 nm).

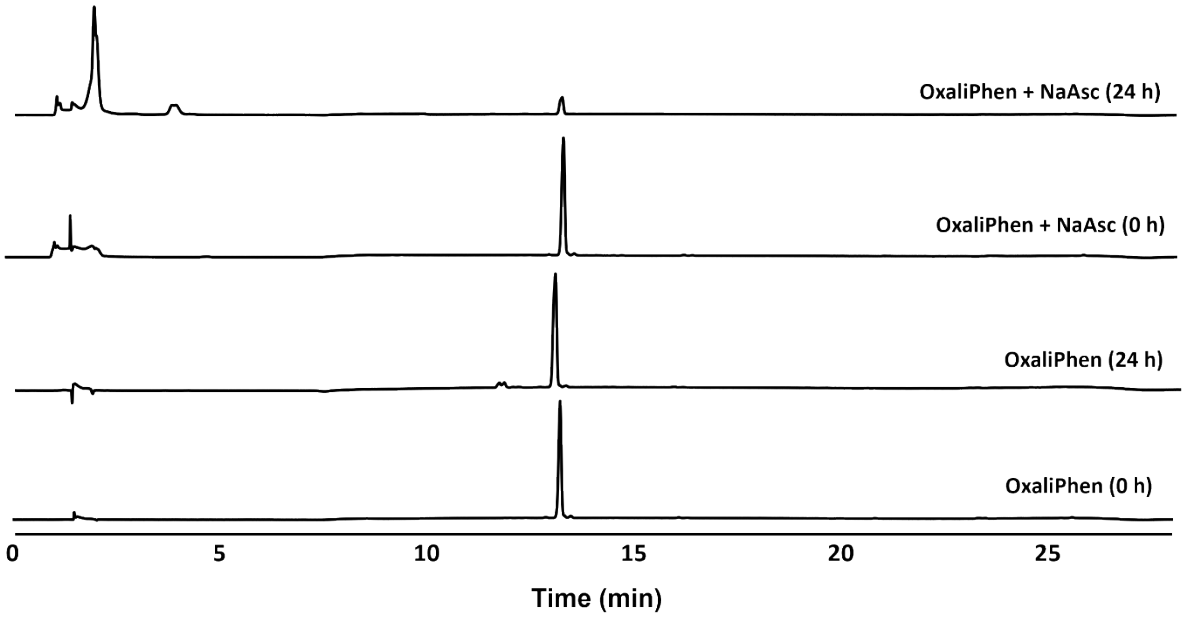

Figure S29. HPLC chromatogram of **OxaliPhen** (150 µM) incubated with and without NaAsc (150 mM) in deionised H_2O for 24 h (absorption at 380 nm).

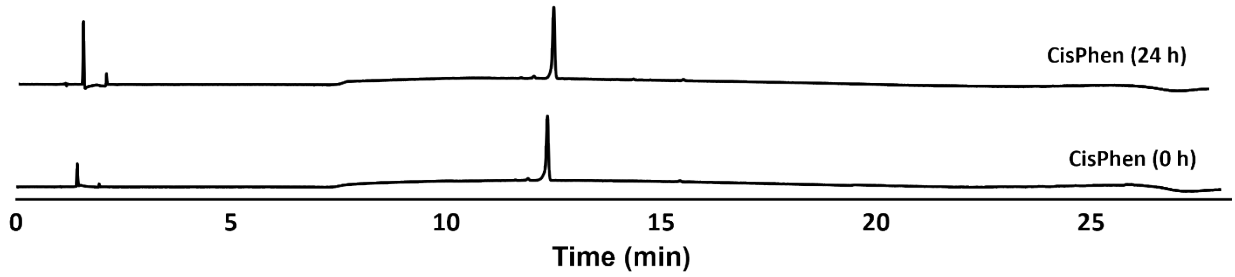

Figure S30. HPLC chromatogram of **CisPhen** (150 µM) over 24 h in a NaCl solution (5 mM, absorption at 380 nm).

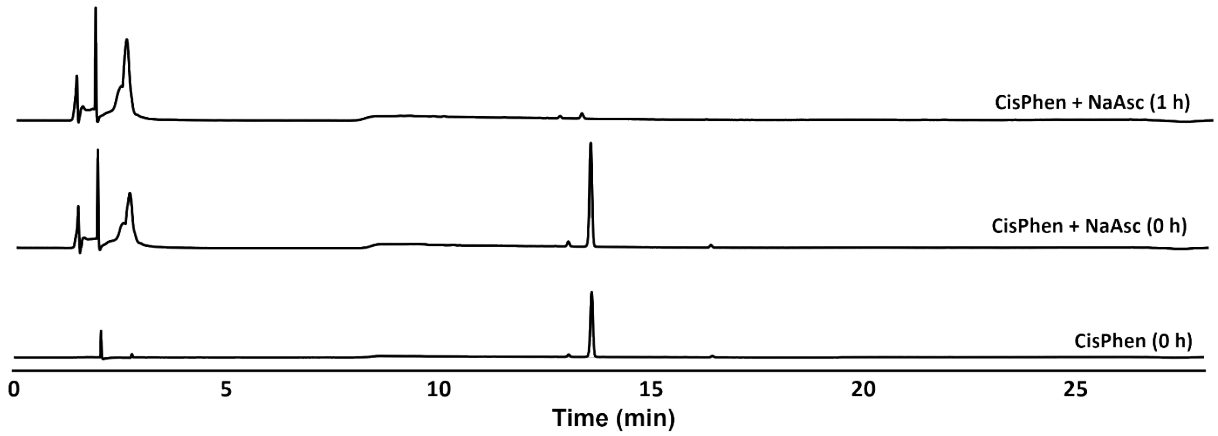

Figure S31. HPLC chromatogram of **CisPhen** (150 µM) incubated with NaAsc (150 mM) for 1 h in deionised H_2O (absorption at 380 nm).

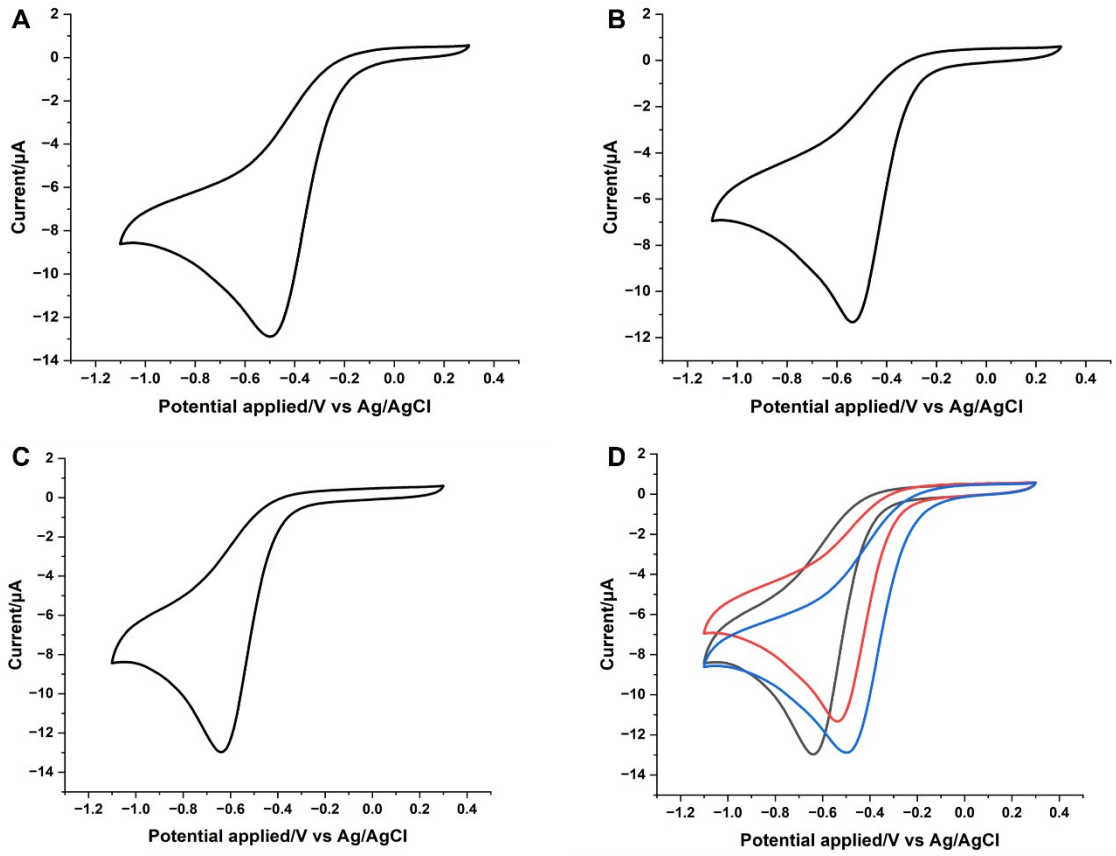

Figure S32. Cyclic Voltammogram of a 3 mm glassy carbon electrode immersed in 1 mM solution of **CisPhen** (**A**), **OxaliPhen** (**B**), **CarboPhen** (**C**), and an overlay comparison of **CarboPhen** (**black**), **OxaliPhen** (**red**) and **CisPhen** (**blue**) (**D**) in PBS buffer (pH 7.4, with 10% DMF) at a scan rate of 0.1 V/s.

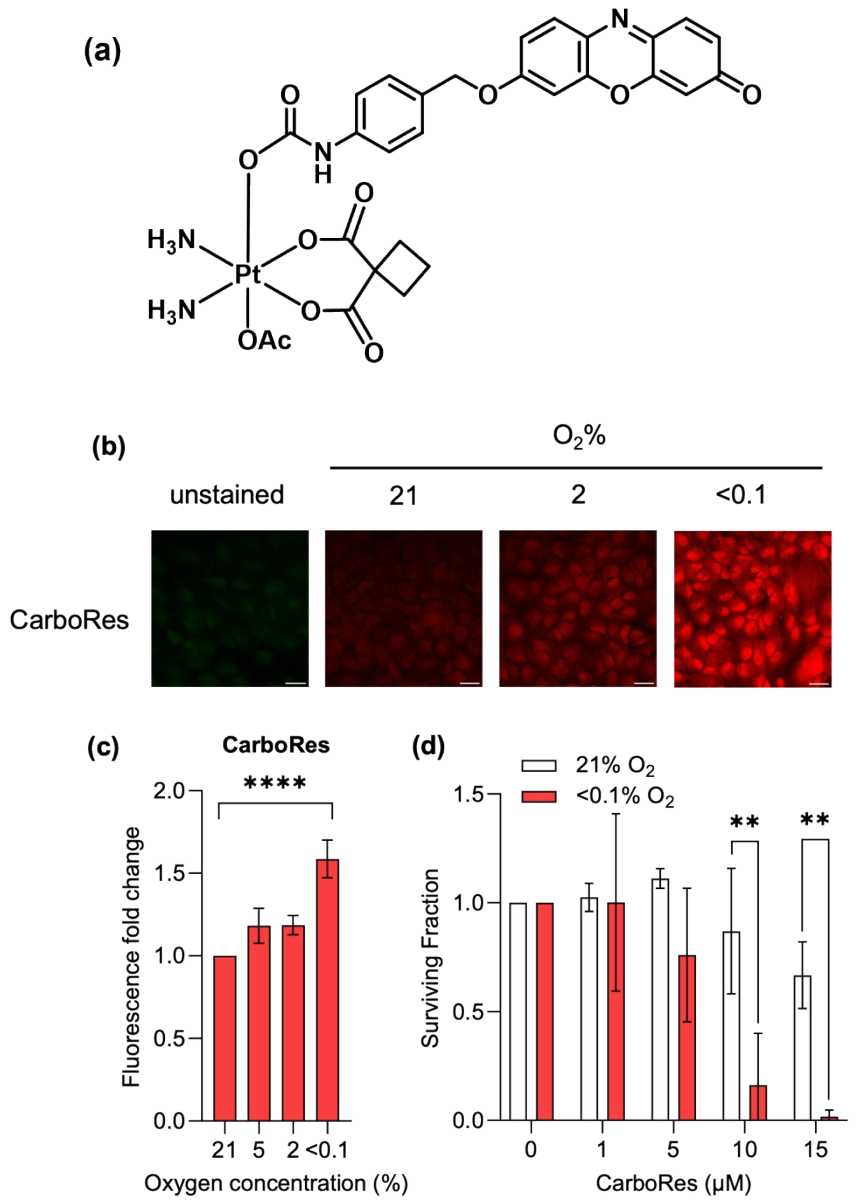

Figure S33. (a) Chemical structure of **CarboRes**. (b) Representative fluorescence images of A549 cells treated with **CarboRes** (10 μM) for 16 hours in the oxygen conditions indicated. Scale bar represents 12 μM. (c) Flow cytometry of A549 cells treated with **CarboRes** (10 μM) for 16 hours in the oxygen conditions indicated. Fluorescence fold change of the geometric mean intensity is displayed. (d) Cell viability results measured by clonogenic assay. Error bars represent SD. Significance compared to normoxic control. *p< 0.05, **p< 0.01 and *** p < 0.001. n=3.

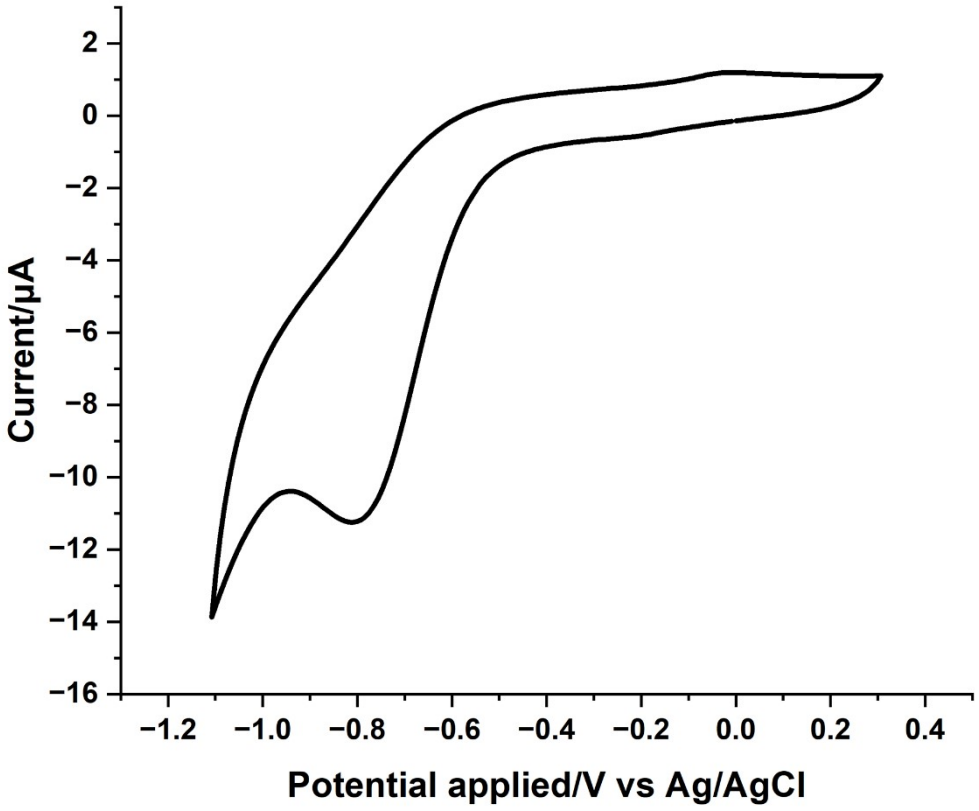

Figure S34. Cyclic Voltammogram of a 3 mm glassy carbon electrode immersed in 1 mM solution of **CarboBisOAc** in PBS buffer (pH 7.4, with 10% DMF) at a scan rate of 0.1 V/s.

5. NMR and HRMS Spectra

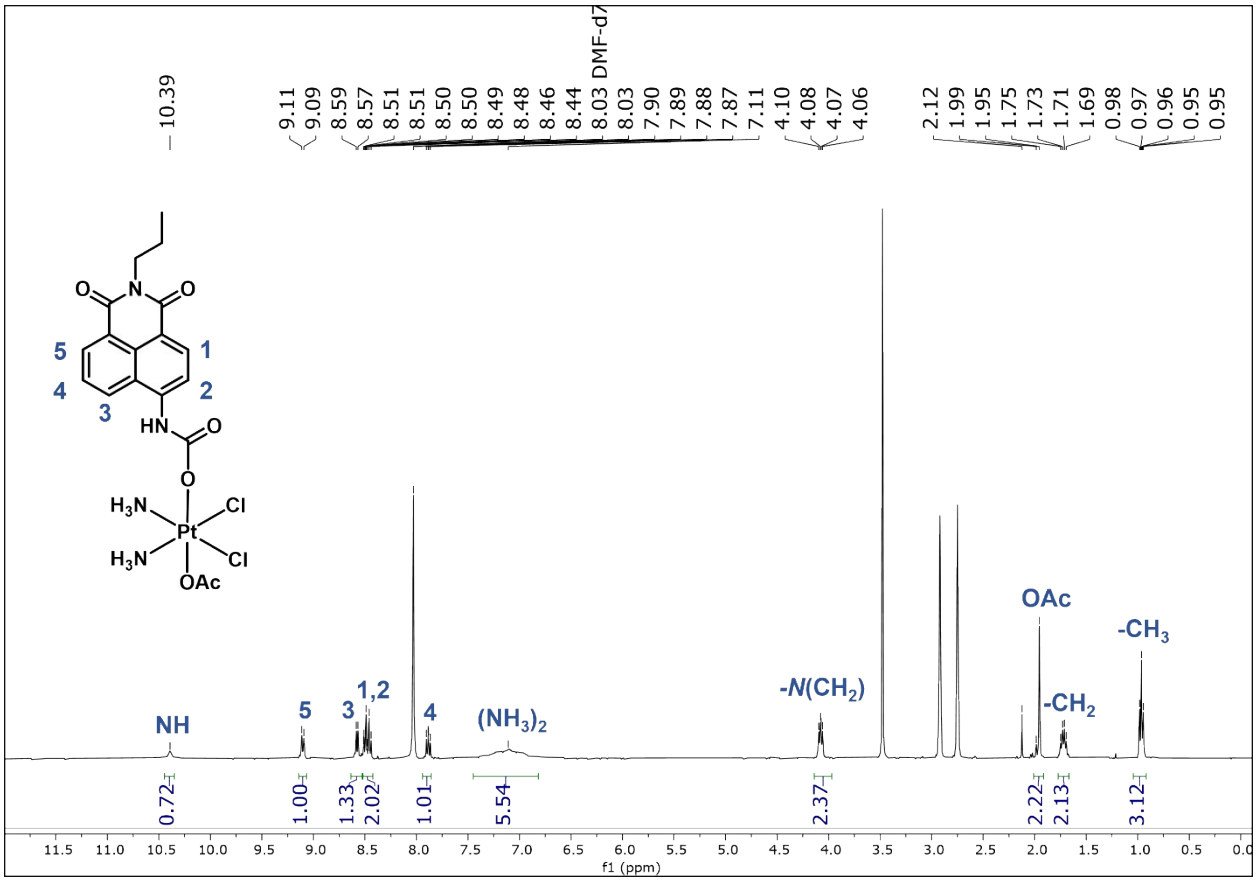

Figure S35. ^{1}H NMR spectrum (400 MHz, 25 °C, DMF-d_7) of **CisNap**.

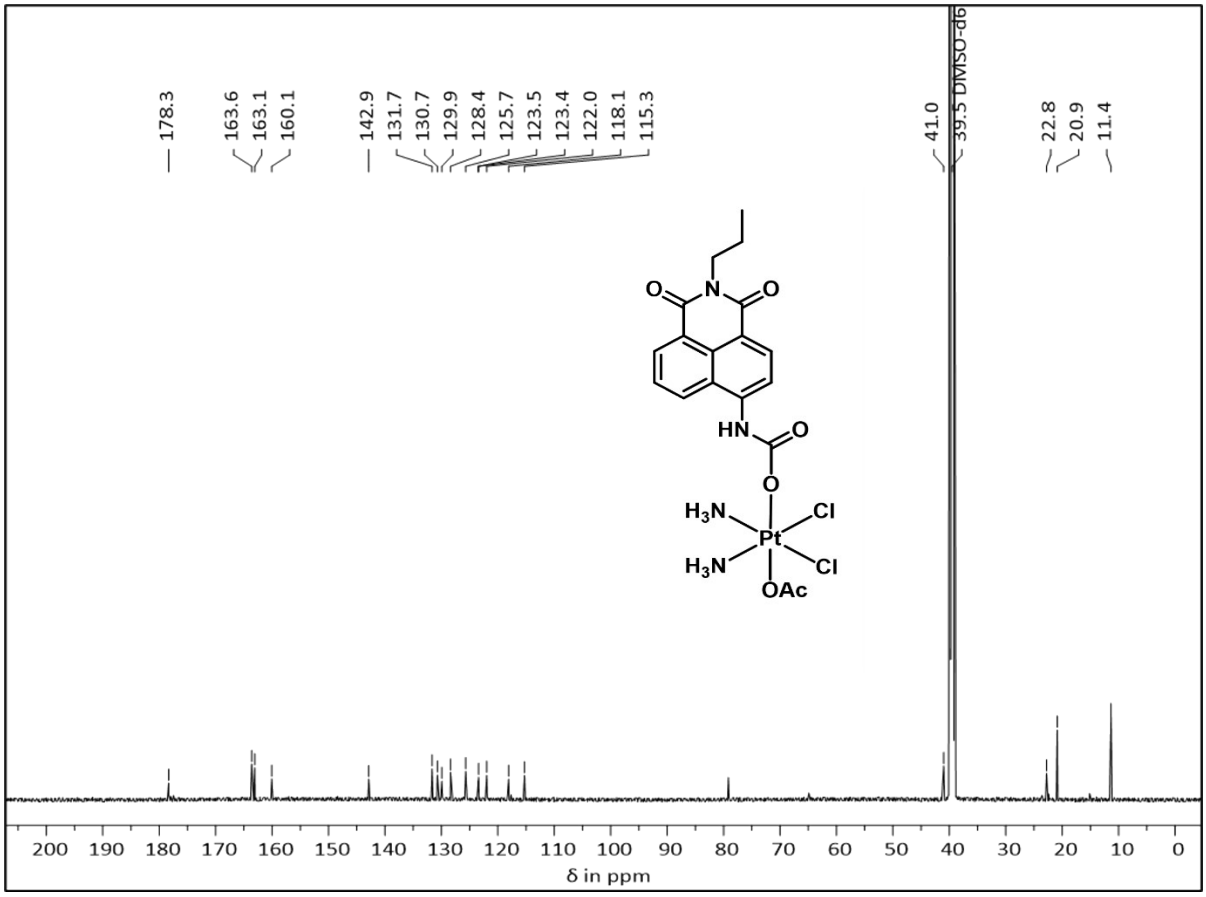

Figure S36. ^{13}C NMR spectrum (101 MHz, 25 °C, DMSO-d_6) of **CisNap**.

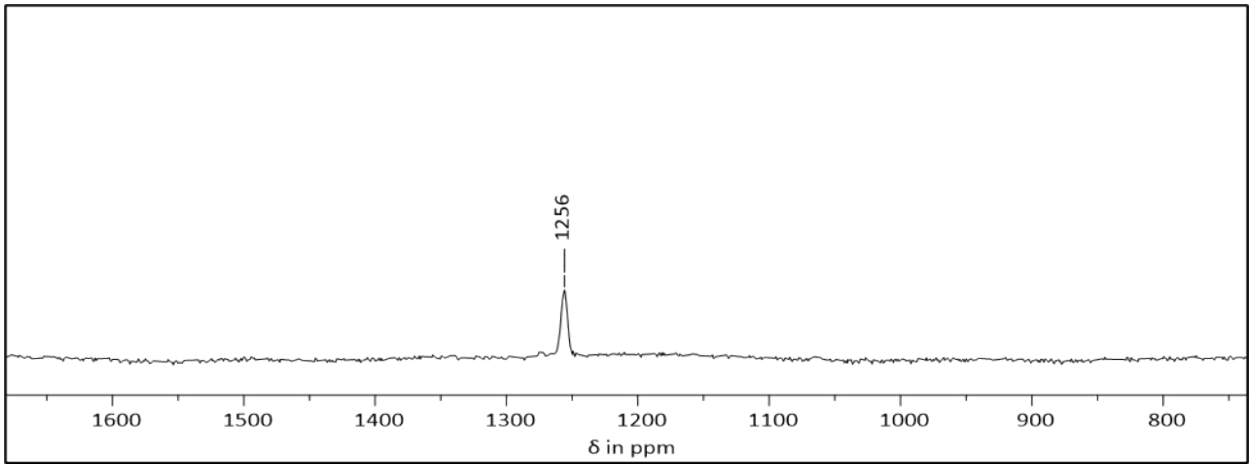

Figure S37. ^{195}Pt NMR spectrum (107 MHz, 25 °C, DMSO-d_6) of **CisNap**.

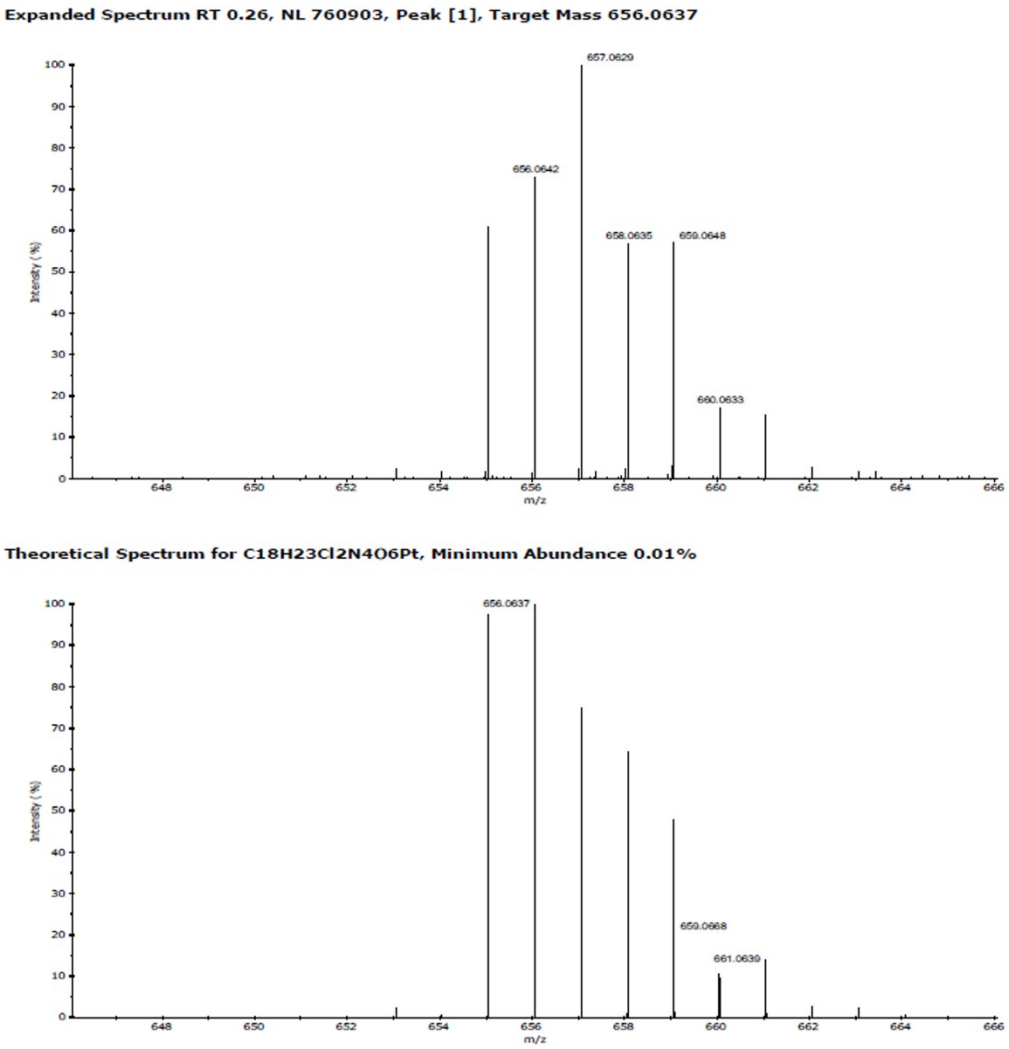

Measured Mass	Calculated Mass	Error (mDa)	Error (ppm)	Formula $[M+H]^+$	Response
656.0642	656.0637	0.49	0.75	$C_{18}H_{23}Cl_2N_4O_6Pt$	736380

The measured m/z value is consistent with your proposed formula for this sample.

Figure S38. HRMS spectrum (+ ion) of **CisNap** in 1 % DMF in CH_2Cl_2/MeOH.

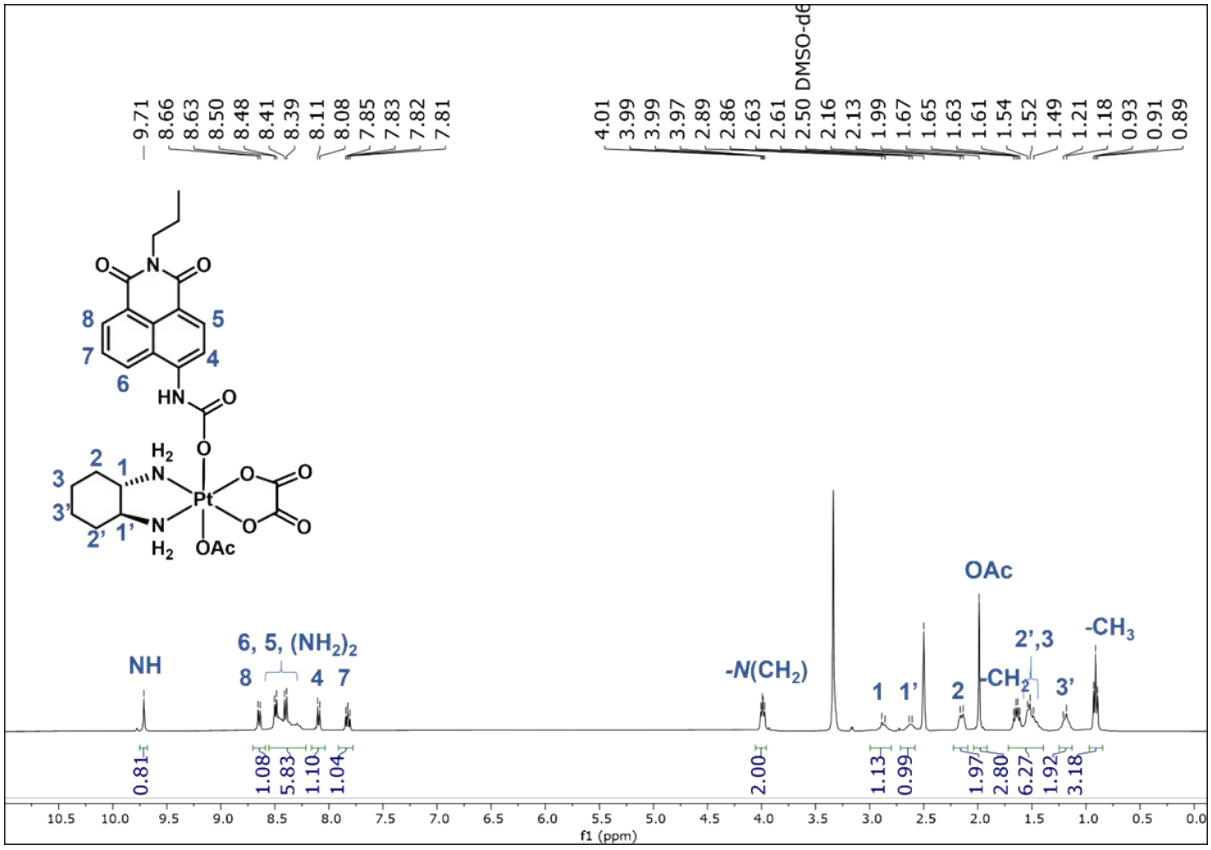

Figure S39. ^{1}H NMR spectrum (400 MHz, 25 °C, DMSO-d_6) of **OxaliNap**.

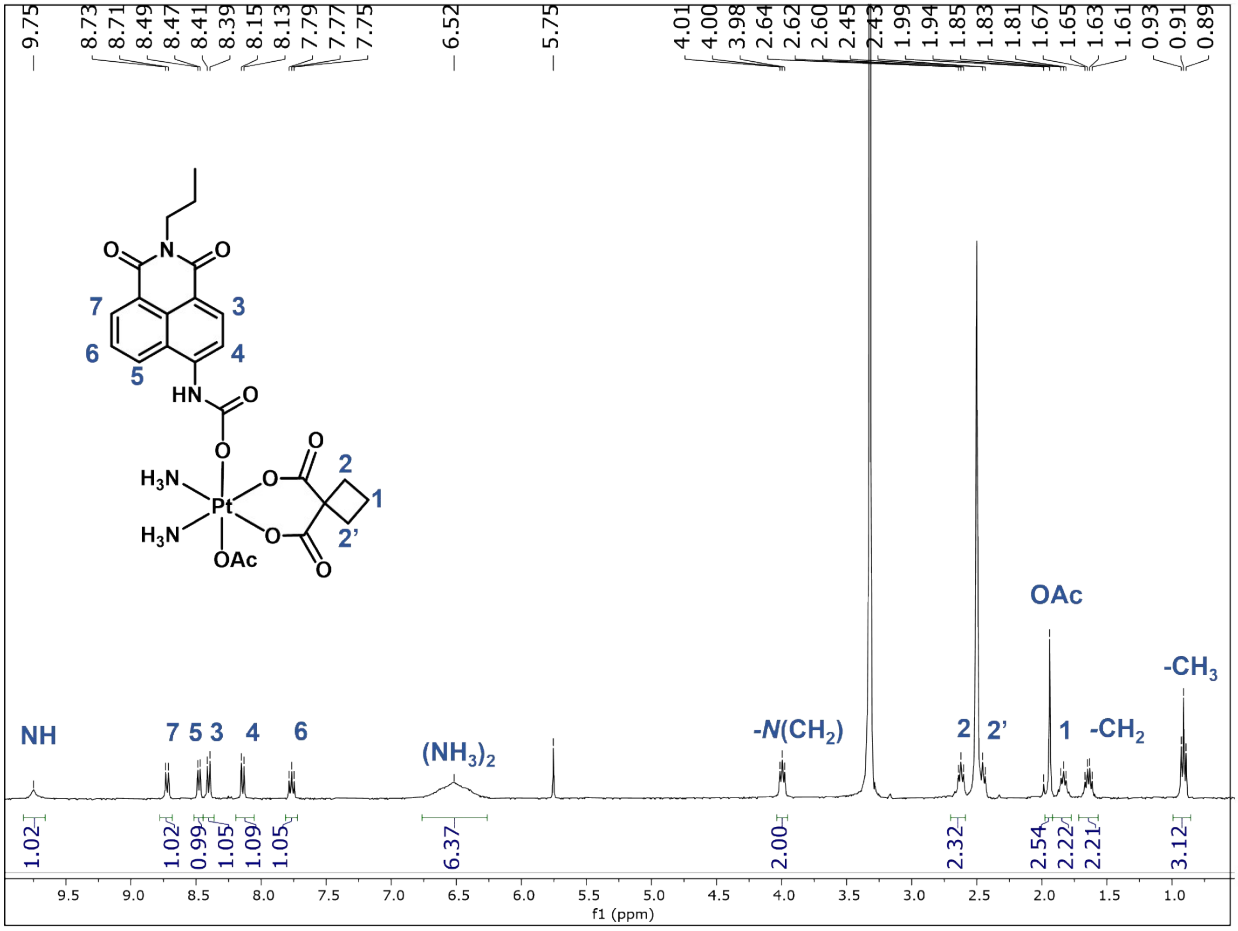

Figure S40. ^{1}H NMR spectrum (400 MHz, 25 °C, DMSO-d_6) of **CarboNap**.

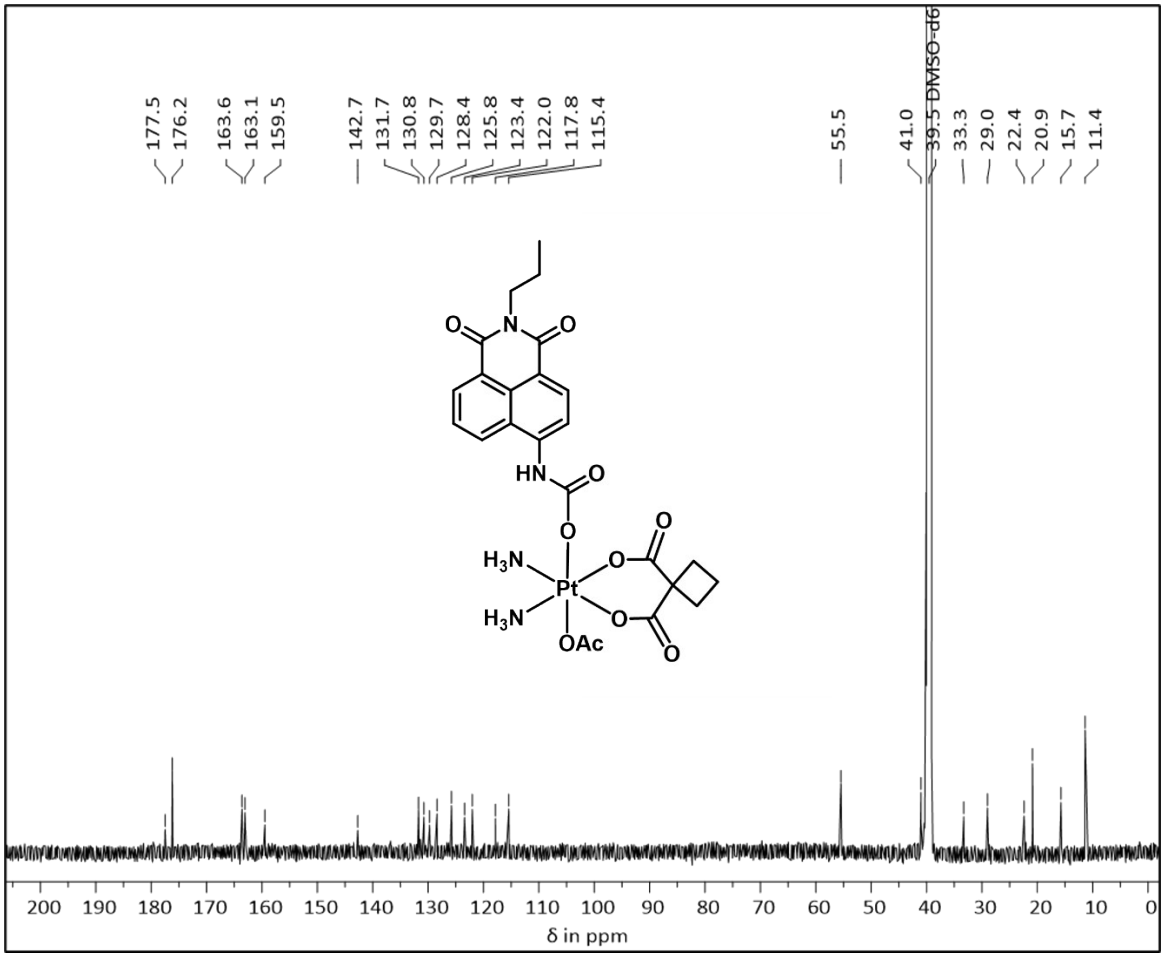

Figure S41. ^{13}C NMR spectrum (101 MHz, 25 °C, DMSO-d_6) of **CarboNap**.

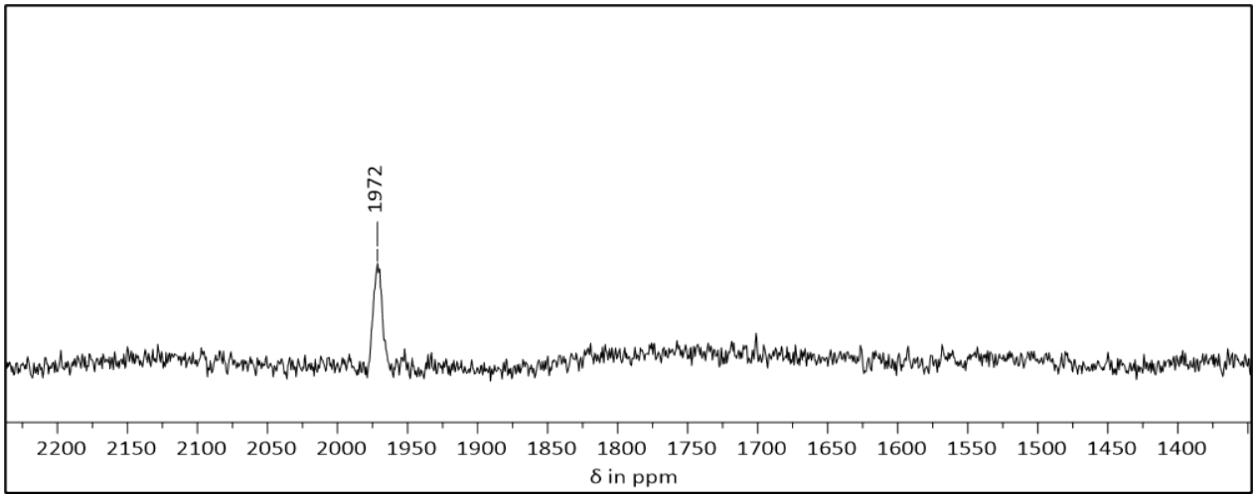

Figure S42. ^{195}Pt NMR spectrum (107 MHz, 25 °C, DMSO-d_6) of **CarboNap.**

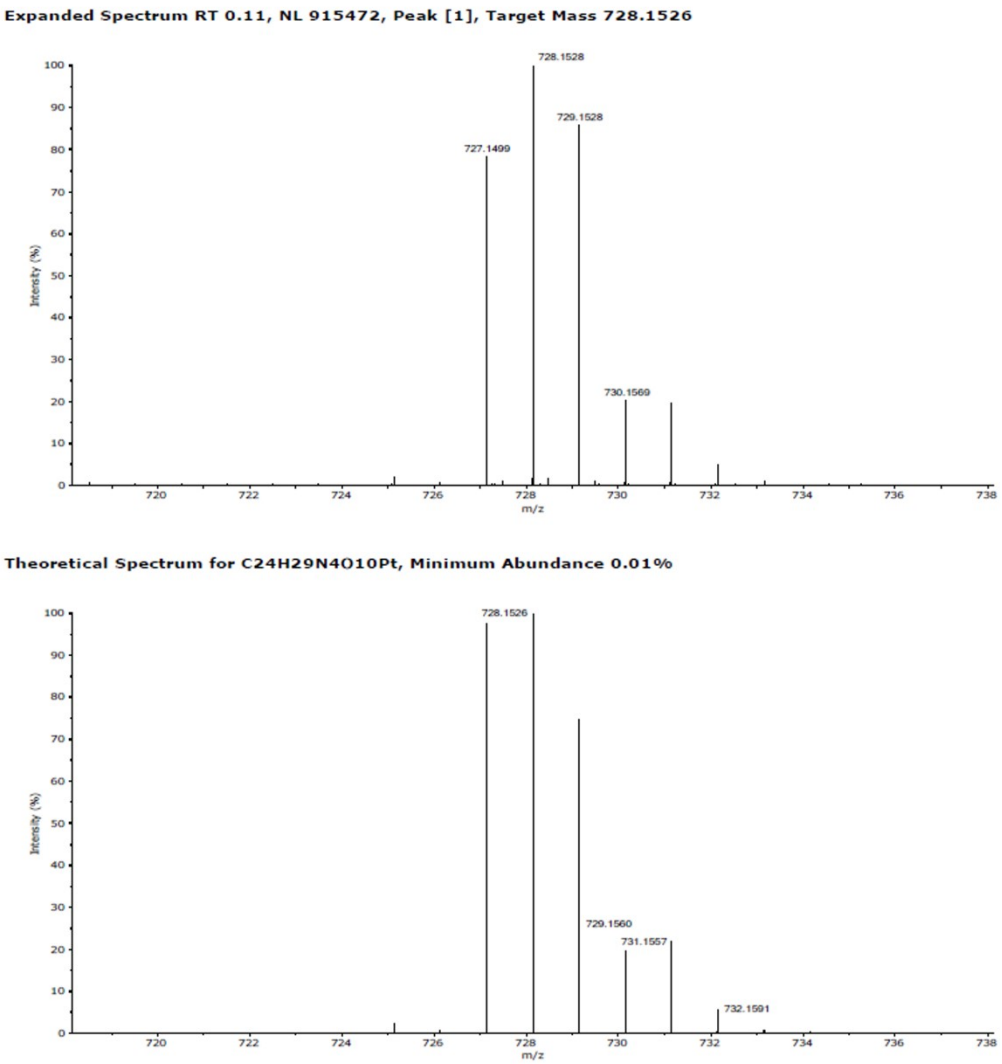

Measured Mass	Calculated Mass	Error (mDa)	Error (ppm)	Formula $[M+H]^+$	Response
728.1528	728.1526	0.19	0.26	$C_{24}H_{29}N_4O_{10}Pt$	4061866

The measured m/z value is consistent with your proposed formula for this sample.

Figure S43. HRMS spectrum (+ ion) of **CarboNap** in 1 % DMF in CH_2Cl_2/MeOH.

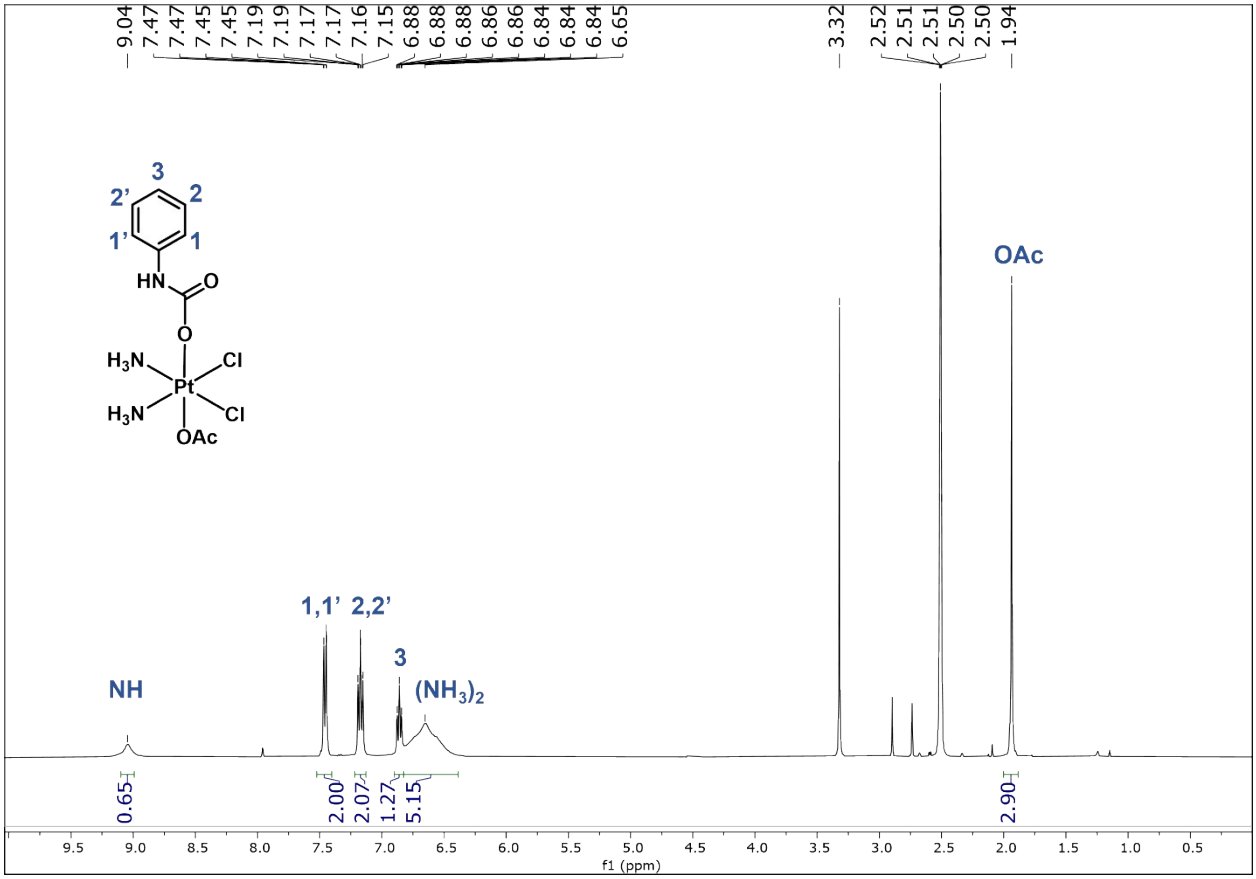

Figure S44. ^{1}H NMR spectrum (400 MHz, 25 °C, DMSO-d_6) of **CisPhen**.

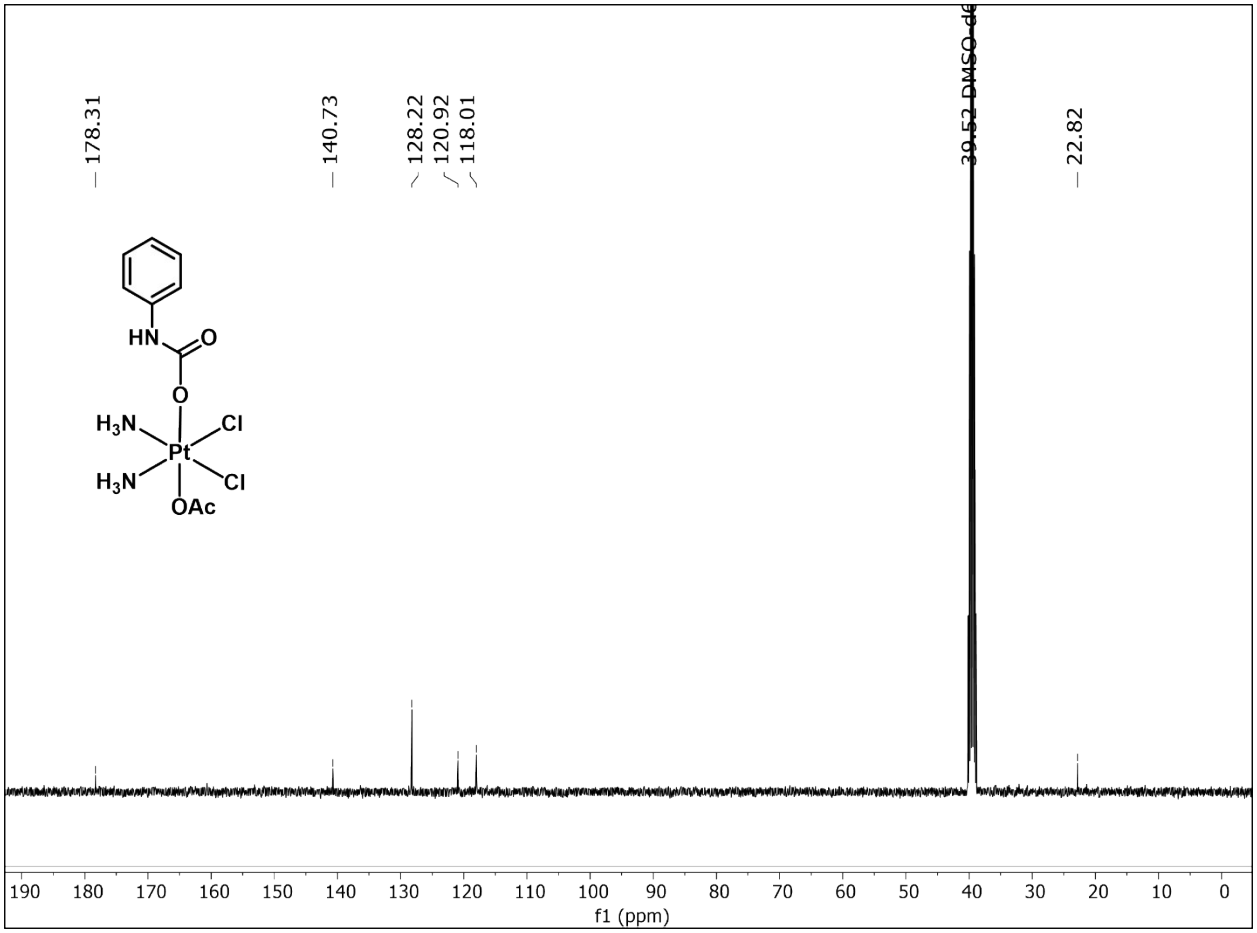

Figure S45. ^{13}C NMR spectrum (101 MHz, 25 °C, DMSO-d_6) of **CisPhen**.

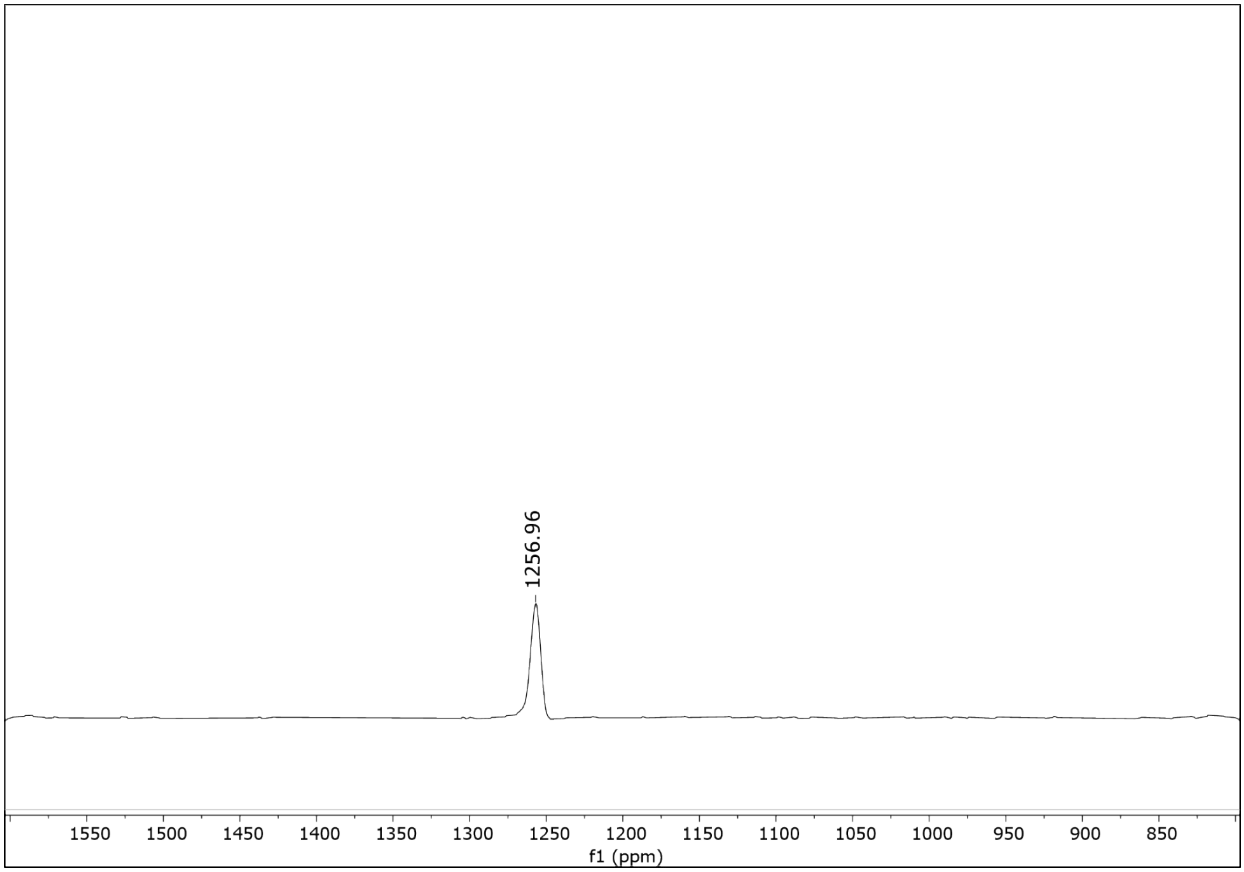

Figure S46. ^{195}Pt NMR spectrum (107 MHz, 25 °C, DMSO-d_6) of **CisPhen.**

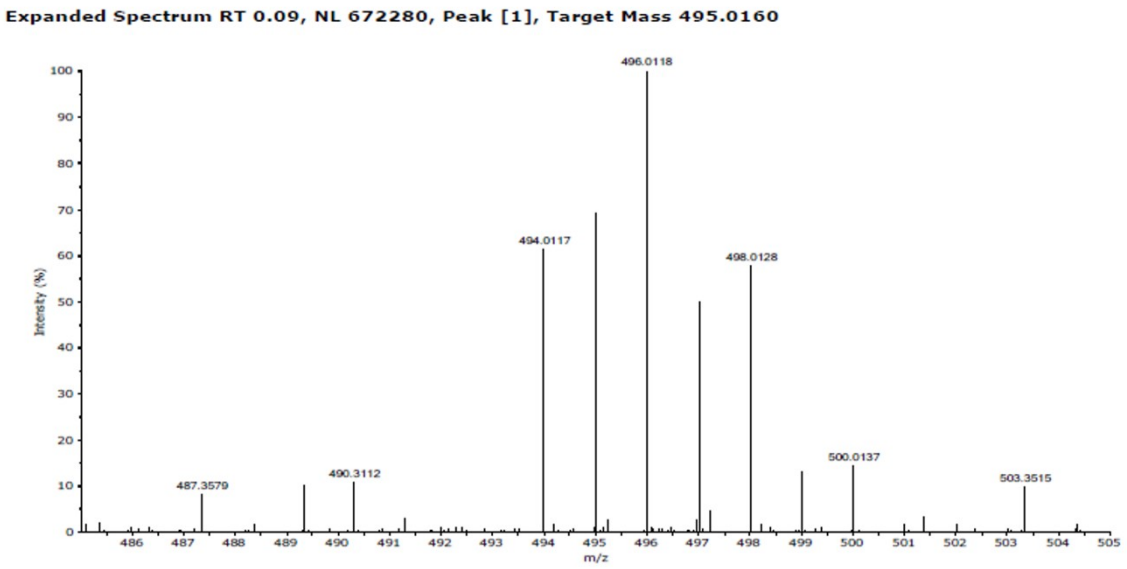

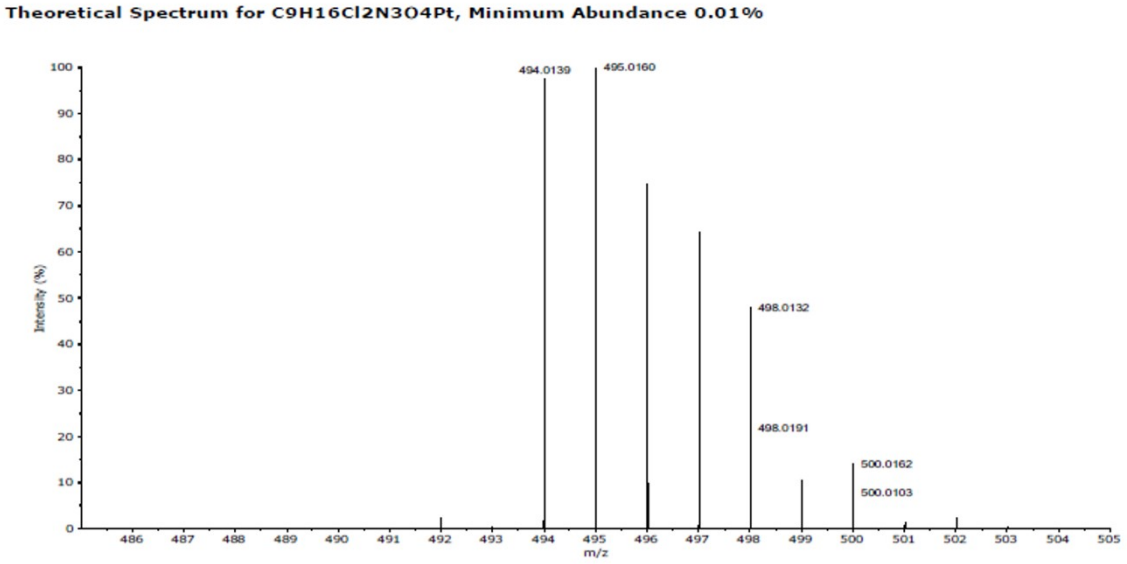

Measured Mass	Calculated Mass	Error (mDa)	Error (ppm)	Formula $[M+H]^+$	Response
495.0152	495.0160	-0.83	-1.67	$C_9H_{16}Cl_2N_3O_4Pt$	124974

The measured m/z value is consistent with your proposed formula for this sample.

Figure S47. HRMS spectrum (+ ion) of **CisPhen** in 1 % DMF in CH_2Cl_2/MeOH.

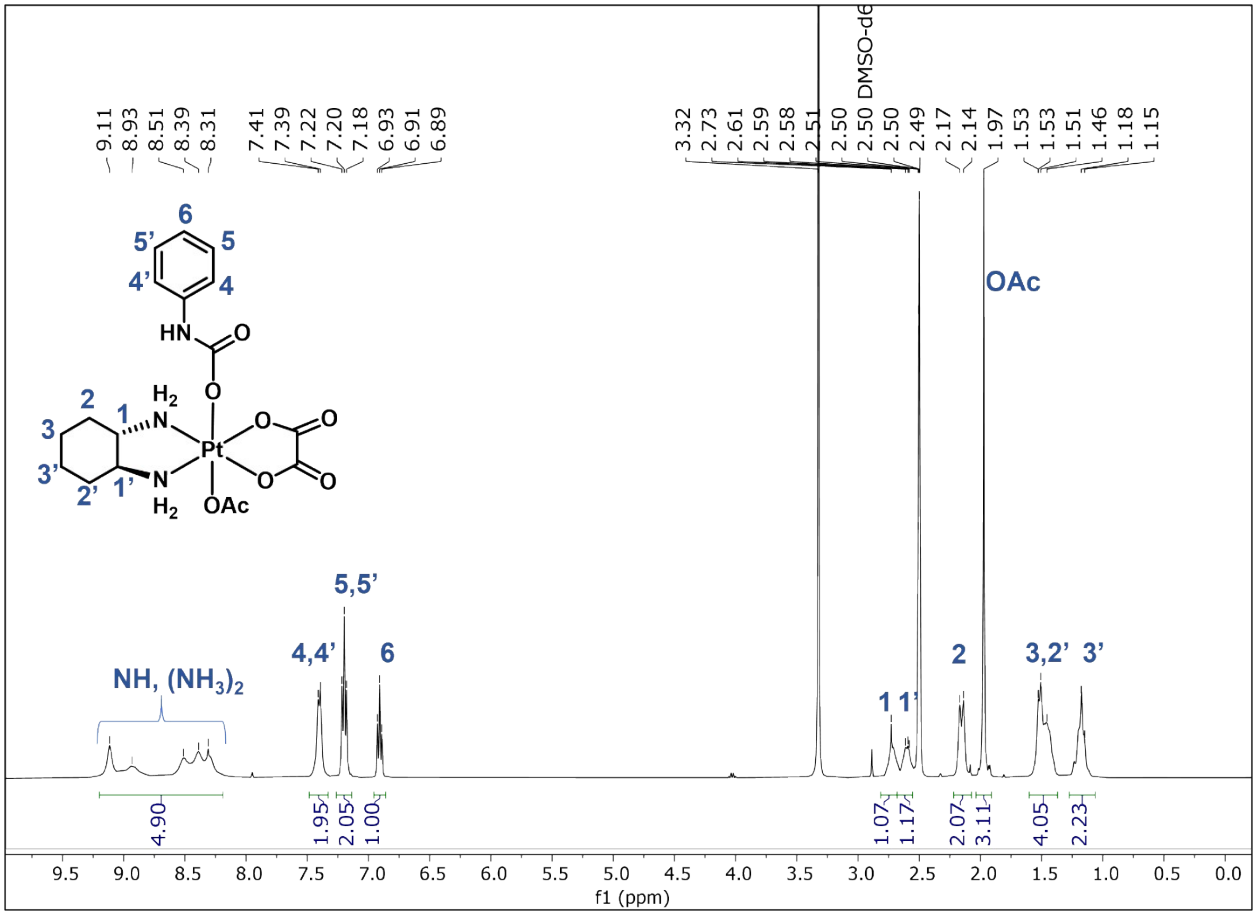

Figure S48. ^{1}H NMR spectrum (400 MHz, 25 °C, DMSO-d_6) of **OxaliPhen**.

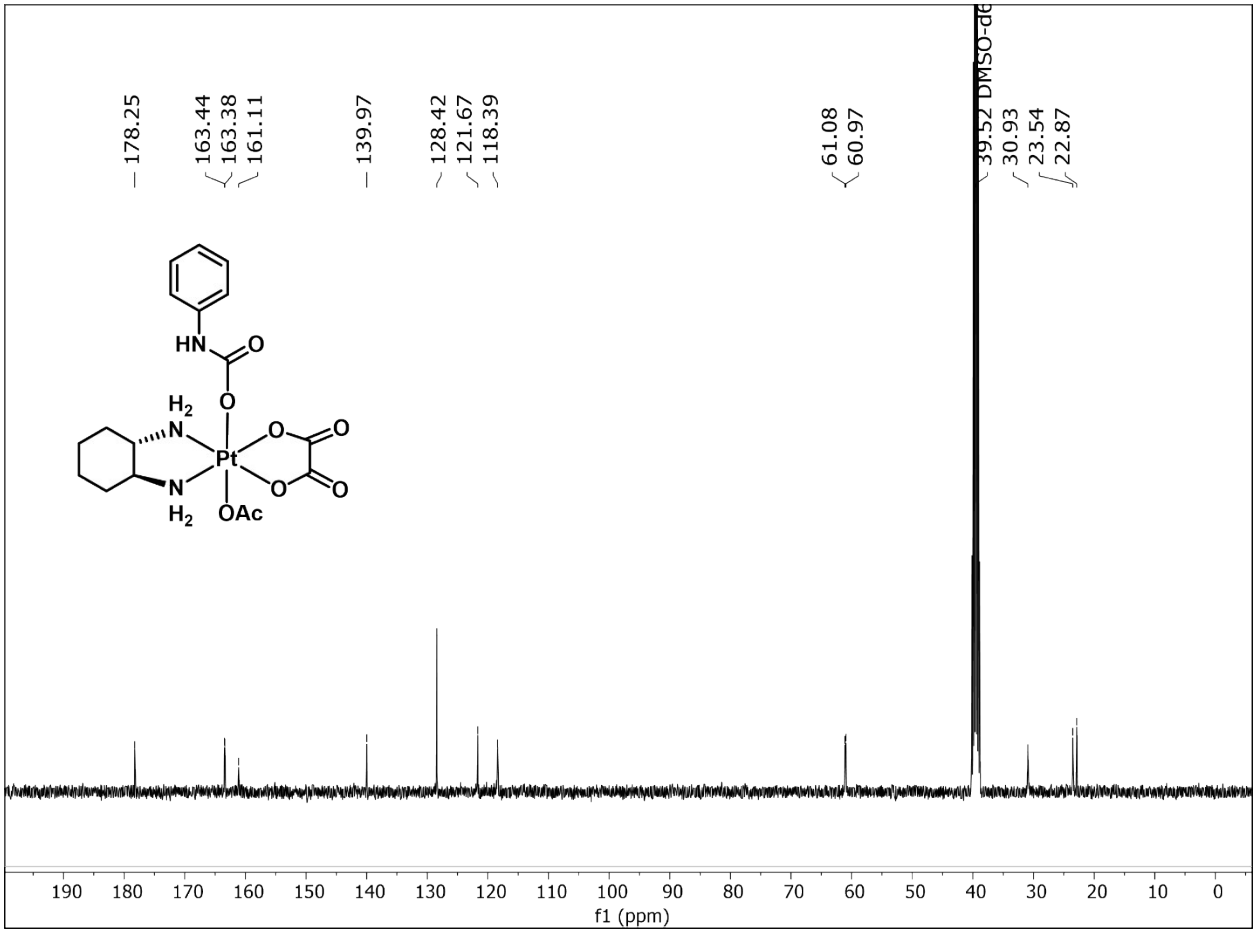

Figure S49. ^{13}C NMR spectrum (101 MHz, 25 °C, DMSO-d_6) of **OxaliPhen**.

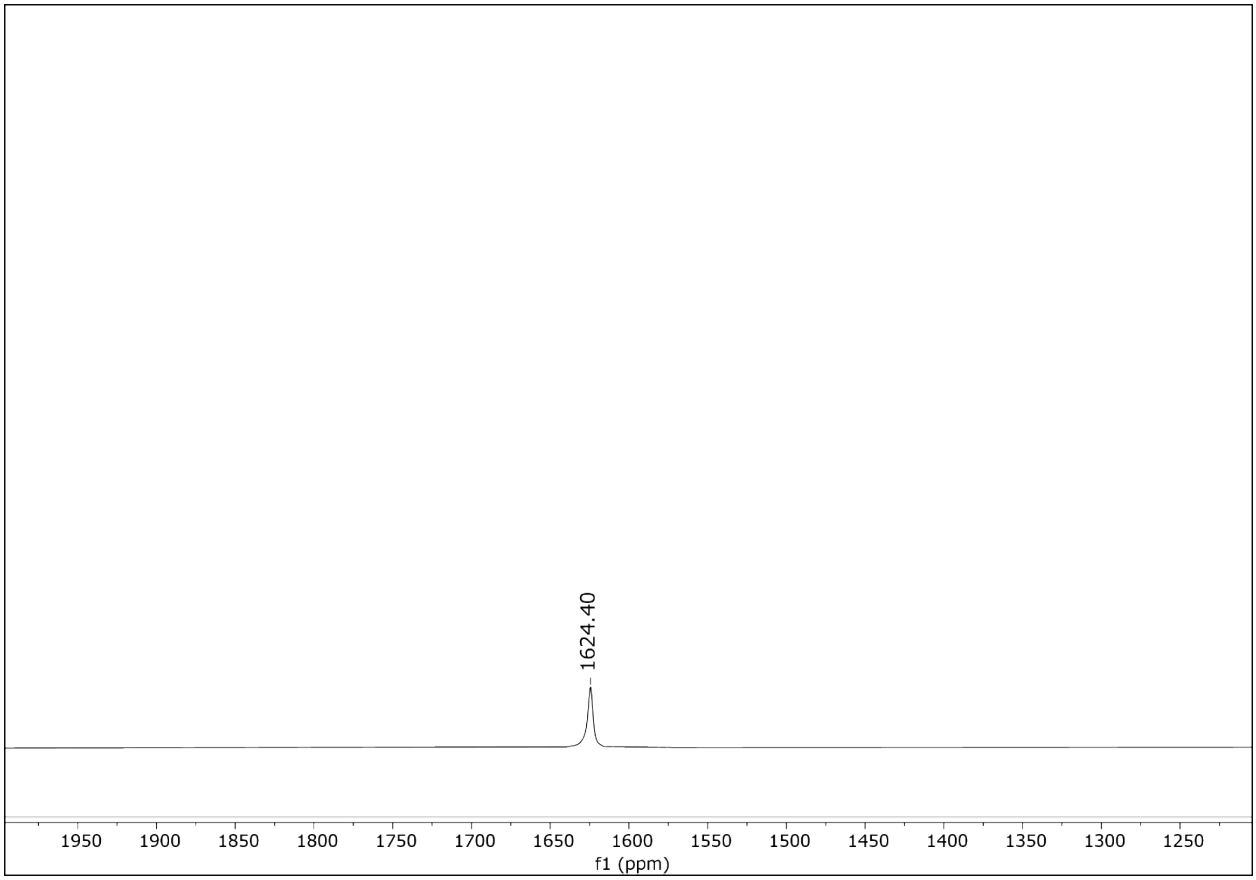

Figure S50. ^{195}Pt NMR spectrum (107 MHz, 25 °C, DMSO-d_6) of **OxaliPhen.**

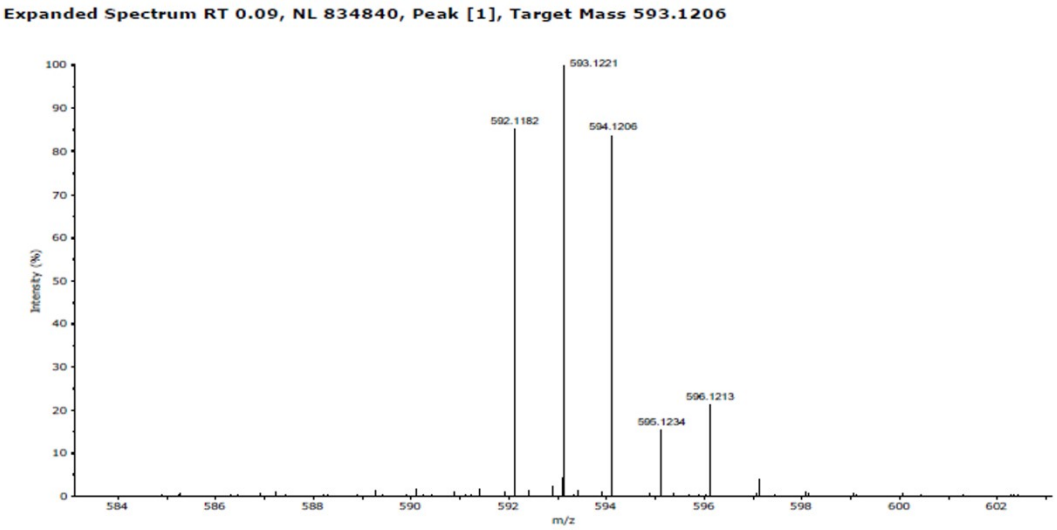

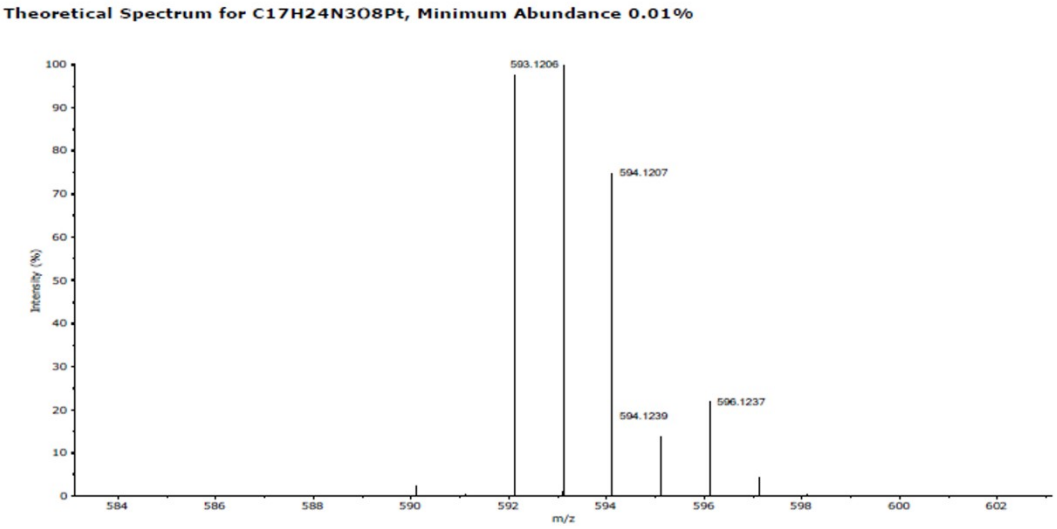

Measured Mass	Calculated Mass	Error (mDa)	Error (ppm)	Formula $[M+H]^+$	Response
593.1221	593.1206	1.52	2.56	$C_{17}H_{24}N_3O_8Pt$	902930

The measured m/z value is consistent with your proposed formula for this sample.

Figure S51. HRMS spectra (+ ion) of **OxaliPhen** in 1 % DMF in CH_2Cl_2/MeOH.

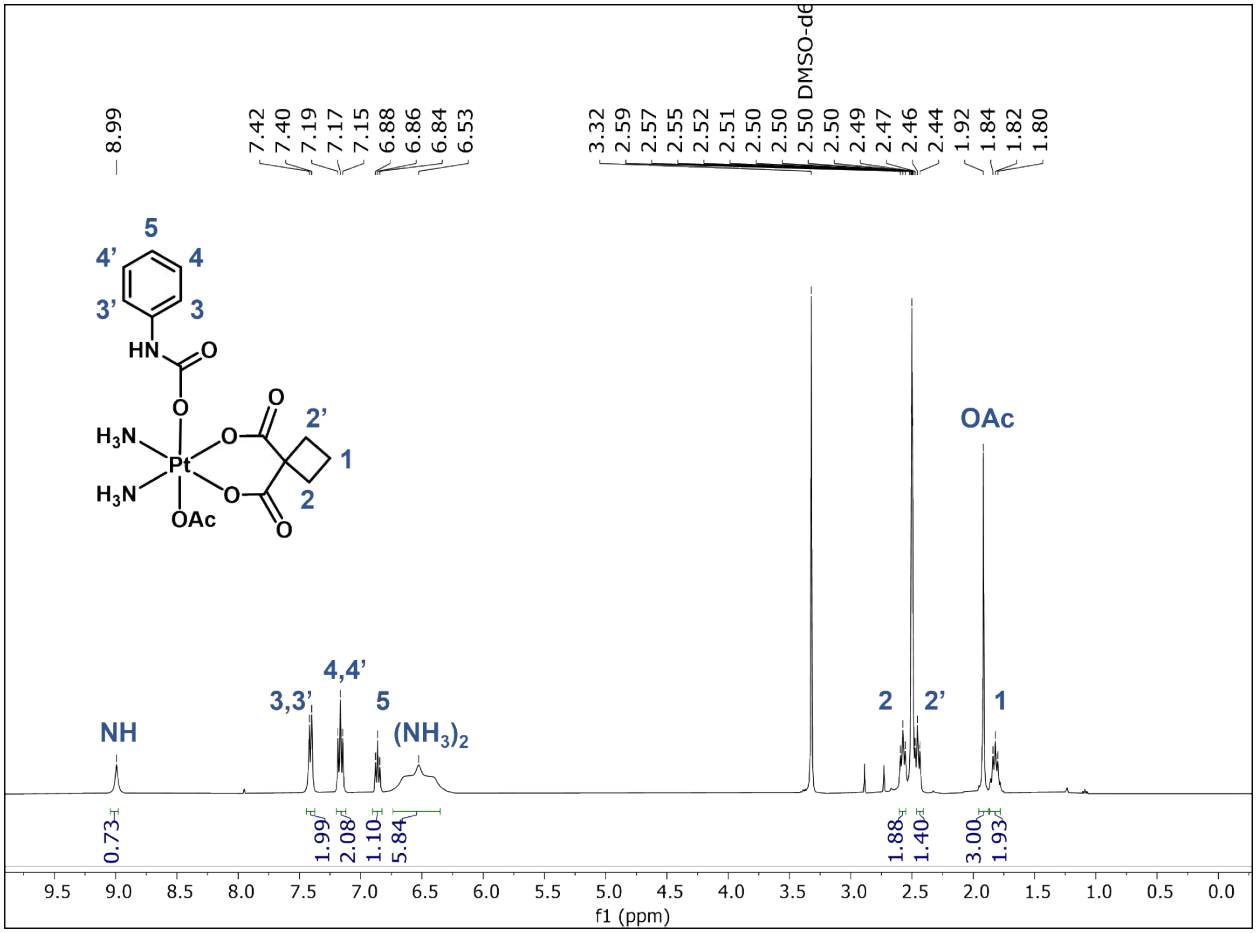

Figure S52. ^{1}H NMR spectrum (400 MHz, 25 °C, DMSO-d_6) of **CarboPhen**.

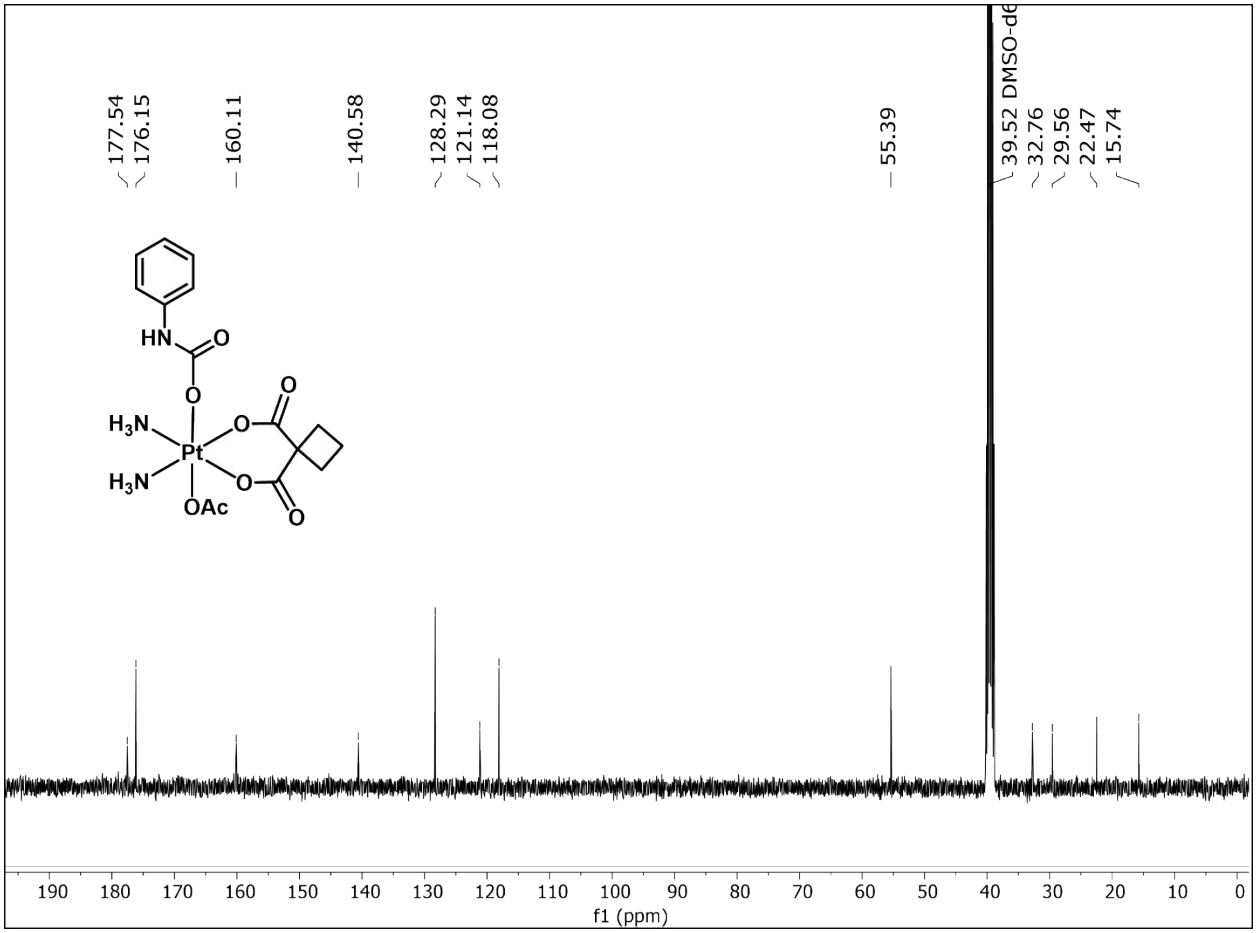

Figure S53. ^{13}C NMR spectrum (101 MHz, 25 °C, DMSO-d_6) of **CarboPhen**.

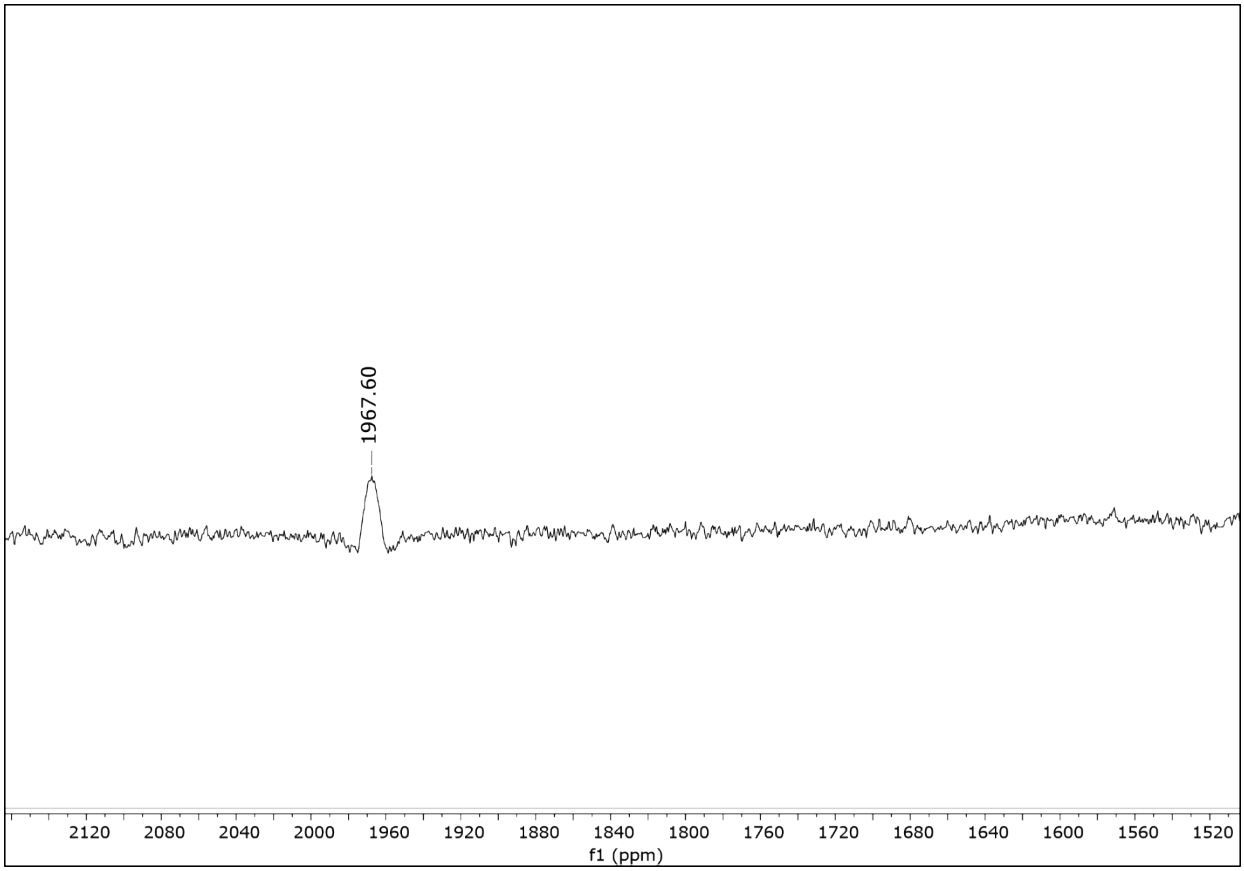

Figure S54. ^{195}Pt NMR spectrum (107 MHz, 25 °C, DMSO-d_6) of **CarboPhen.**

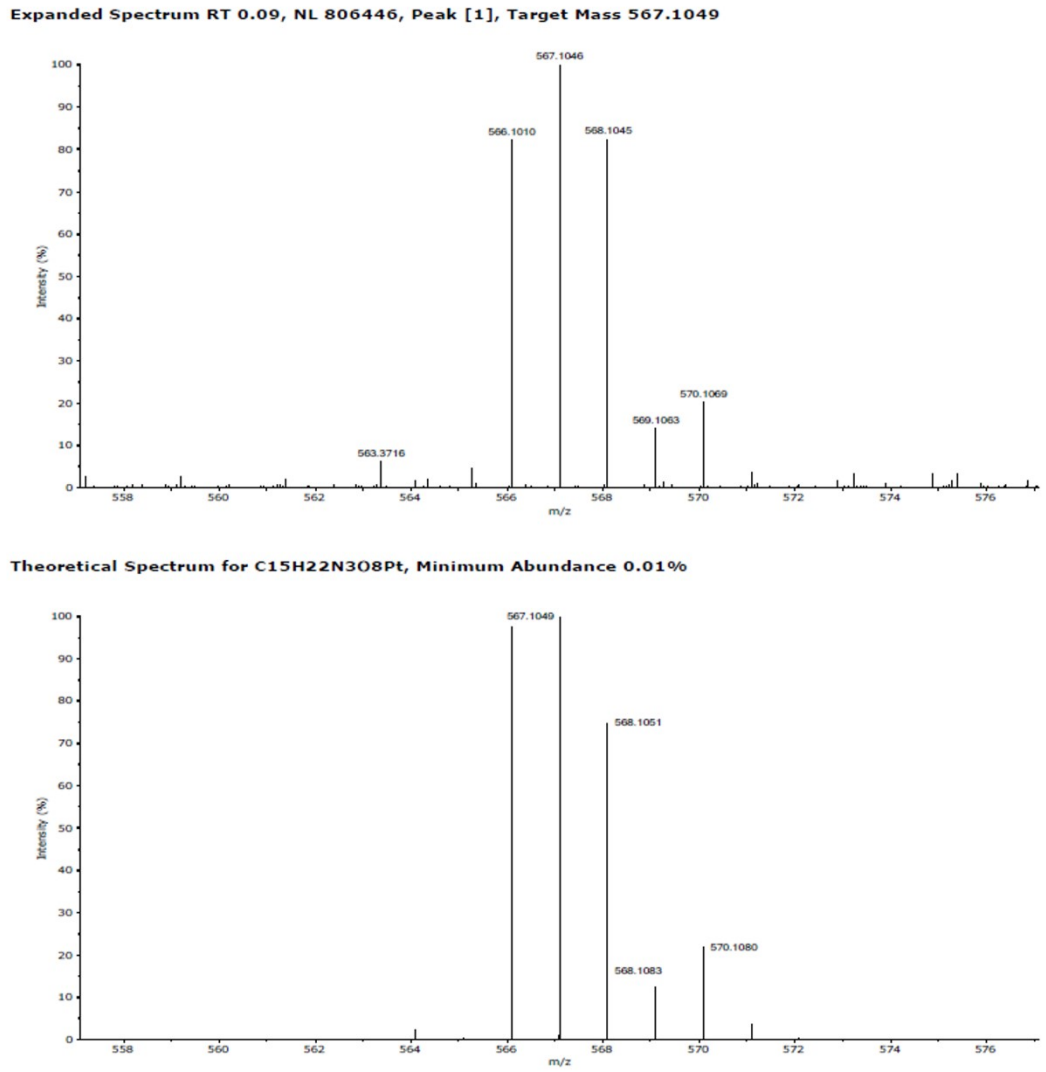

Measured Mass	Calculated Mass	Error (mDa)	Error (ppm)	Formula $[M+H]^+$	Response
567.1046	567.1049	-0.33	-0.59	$C_{15}H_{22}N_3O_8Pt$	298071

The measured m/z value is consistent with your proposed formula for this sample.

Figure S55. HRMS spectra (+ ion) of **CarboPhen** in 1 % DMF in CH_2Cl_2/MeOH.

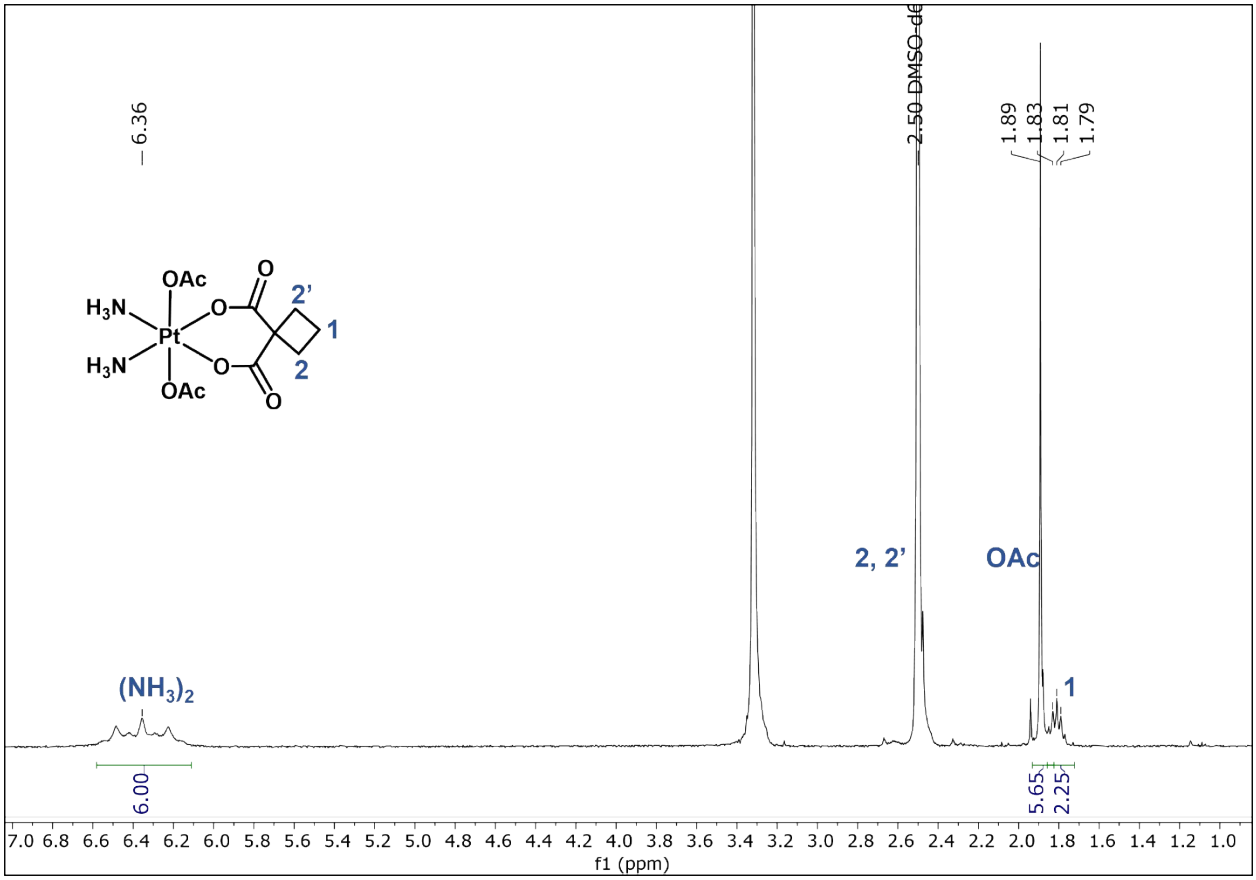

Figure S56. ^{1}H NMR spectrum (400 MHz, 25 °C, DMSO-d_6) of **CarboBisOAc.**

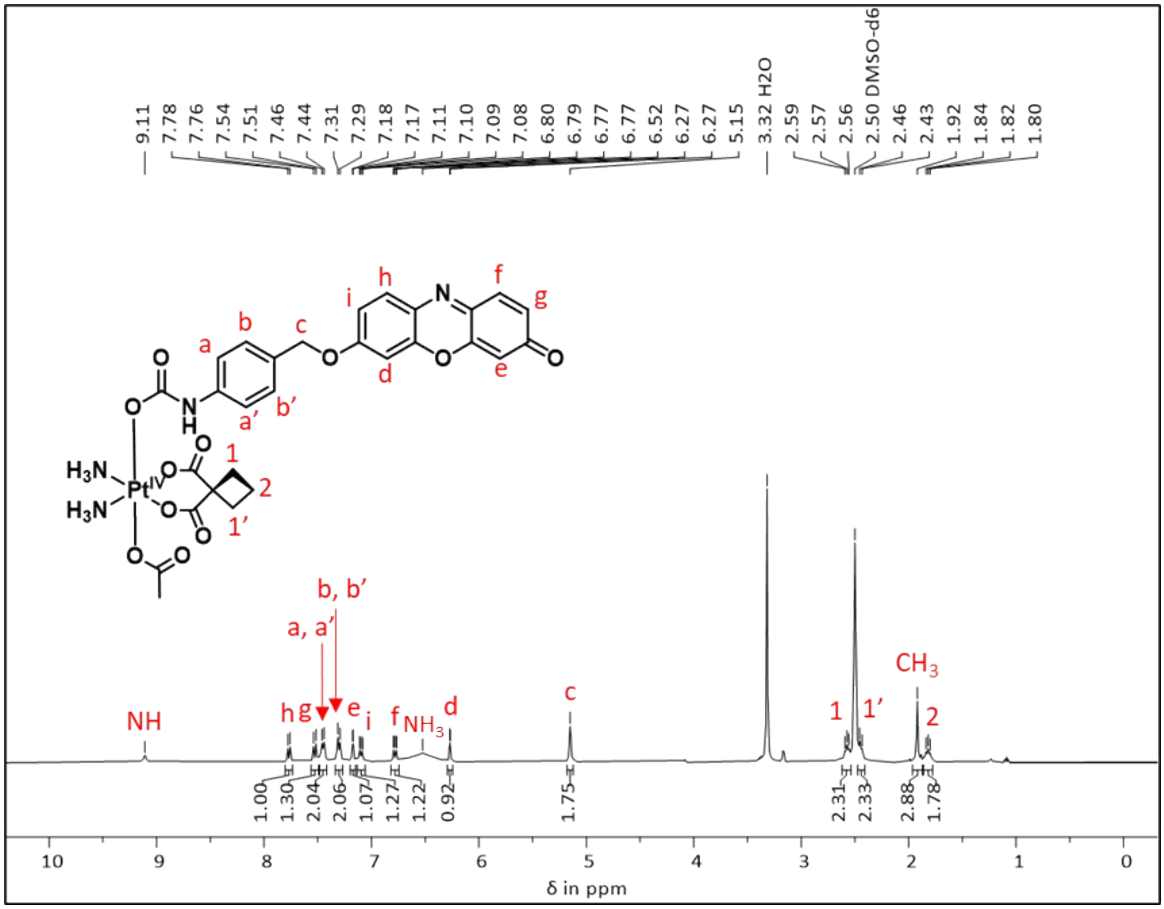

Figure S57. ^{1}H NMR (400 MHz, DMSO-d_6) of **CarboRes.**

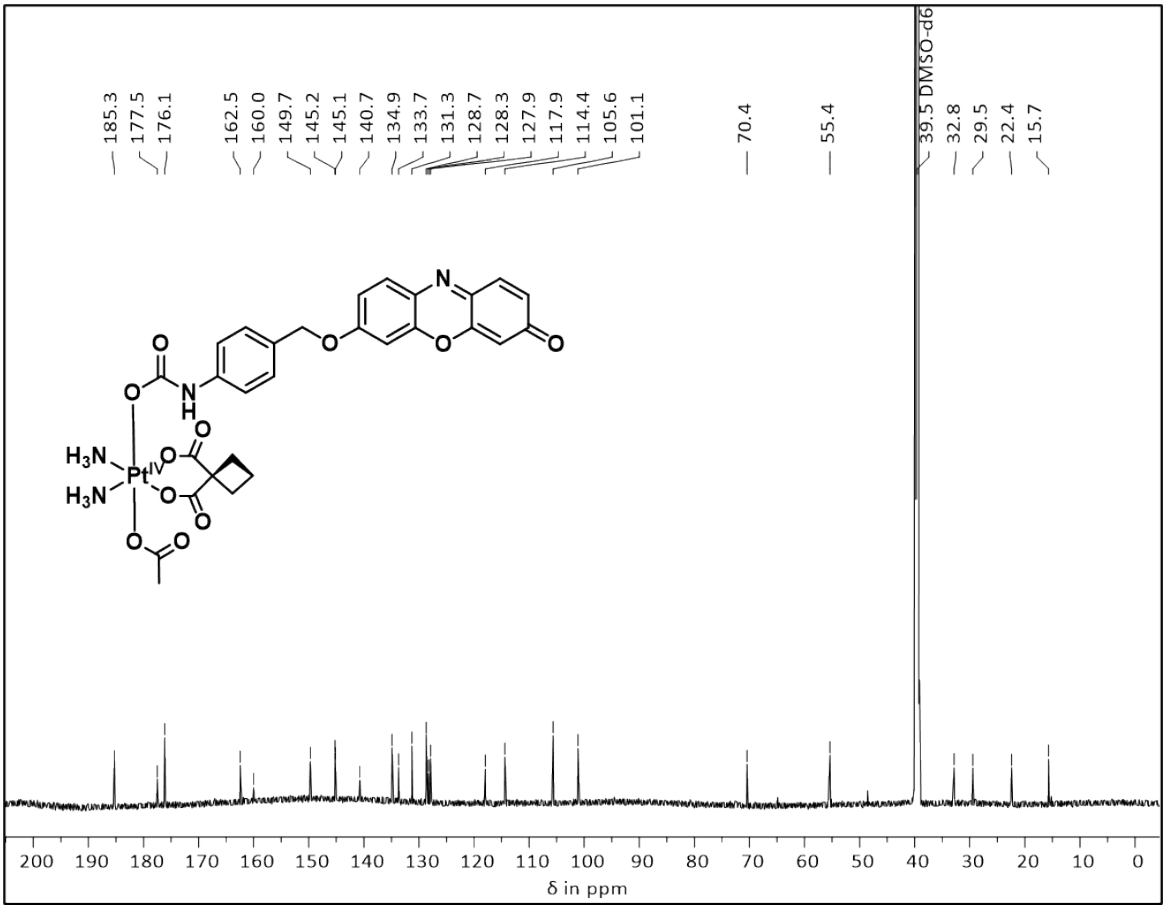

Figure S58. ^{13}C NMR (176 MHz, DMSO-d_6) of **CarboRes.**

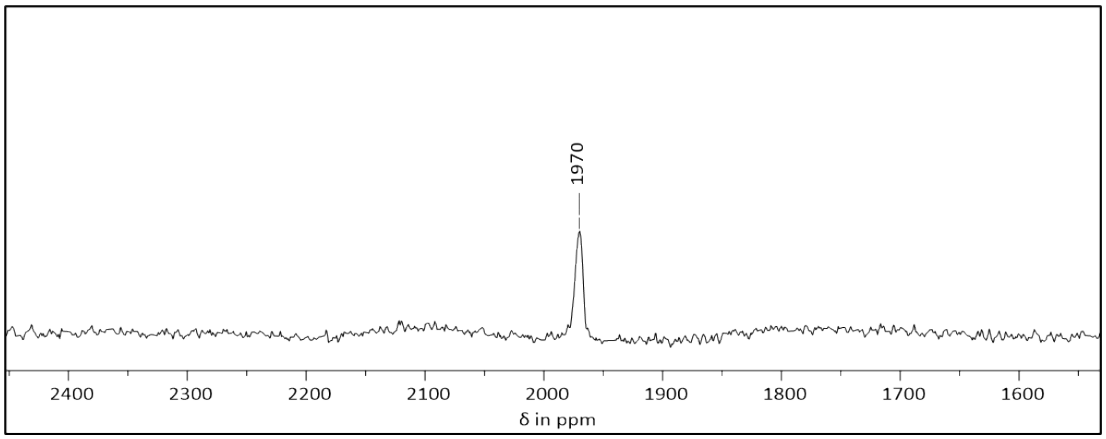

Figure S59. ^{195}Pt NMR spectrum (107 MHz, DMSO-d_6) of **CarboRes.**

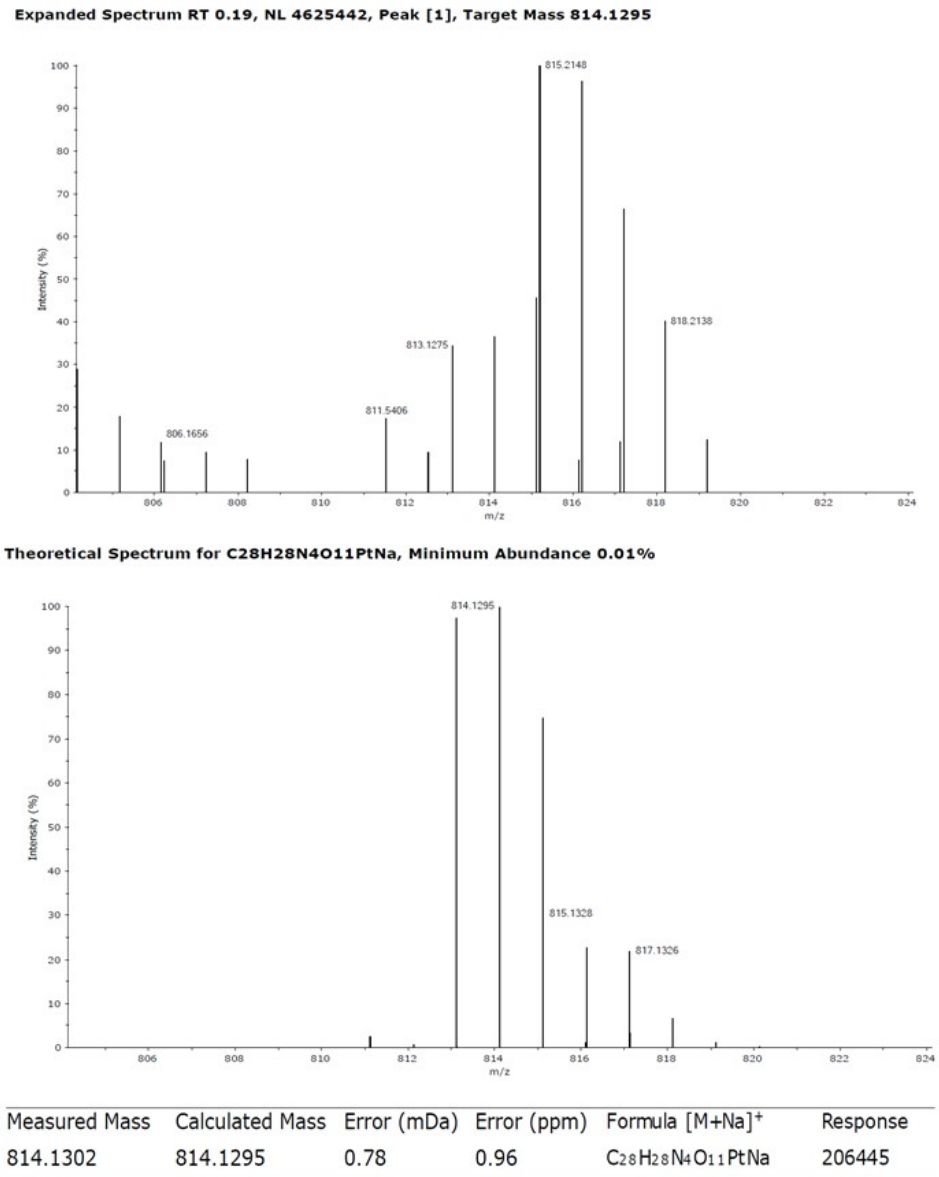

Measured Mass	Calculated Mass	Error (mDa)	Error (ppm)	Formula $[M+Na]^+$	Response
814.1302	814.1295	0.78	0.96	$C_{28}H_{28}N_4O_{11}PtNa$	206445

Figure S60. HRMS spectra (+ ion) of **CarboRes** in 1 % DMF in CH_2Cl_2/MeOH.

6. Computational Details

All calculations were carried out using Gaussian 16.[6] Computational methodology was evaluated against the bond metrics taken from single crystal X-ray data for a related Pt(IV) octahedral complex *trans*-[$Pt^{IV}(O_2CCH_3)_2$(cbdc)(dpda)] reported by Jung et al. (Figure S59).[7]

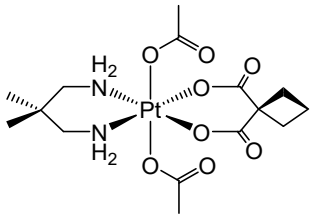

trans-$Pt^{IV}(O_2CCH_3)_2$(cbdc)(dpda)

Figure S61. Structure of *trans*-[$Pt^{IV}(O_2CCH_3)_2$(cbdc)(dpda)] reported by Jung et al.[7]

The functional and basis sets are outlined in Table S1, along with their replication of X-ray structure bonding parameters with a particular focus on Pt–X bond distance (the two Pt–N and four Pt–O bonds in each optimised structures were compared to the crystallographic experimental data, and these differences were averaged to give an 'Average Δcalc–exp' for each method tested). The best replication of bonding parameters was found using the PBE1PBE functional and the –D3 dispersion correction of Grimme et al.[8] in combination with the basis sets 3-21G(H,C,N,O)/LANL2DZ(Pt)[9-13] and an integral equation formalism SCRF continuum solvent method with continuum parameters designed to describe aqueous solvent.[14] The calculated structures of *trans*-[$Pt^{IV}(O_2CCH_3)_2$(cbdc)(dpda)] were confirmed to be minima based on the absence of imaginary frequencies from frequency calculations on the optimised geometries.

Table S1: Methodology development summary. [a]–D3 dispersion correction used throughout. [b]Pt–X bonds = two Pt–N bonds and four Pt–O bonds.

Functional	Basis set			Modifier[a]	Average Δcalc–exp (Pt–X bonds)[b]
	H, C	N, O	Pt		
B3LYP	Def2SVPP	Def2TZVP	Def2TZVPP		0.0341
PBE1PBE	Def2SVPP	Def2TZVP	Def2TZVPP		0.0245
PBE1PBE	3-21G	3-21G	LANL2DZ		0.0208
PBE1PBE	**3-21G**	**3-21G**	**LANL2DZ**	**scrf (water)**	**0.0142**
B3LYP	3-21G	3-21G	LANL2DZ		0.0358
B3LYP	Def2SVPP	Def2SVPP	LANL2DZ		0.0472
M06	Def2SVPP	Def2TZVP	Def2TZVPP		0.0305
PBE1PBE	6-31G	6-311G	LANL2DZ		0.0279
M062X	Def2SVPP	Def2TZVP	Def2TZVPP		0.0262
PBE1PBE	6-31G(d)	6-31G(d)	LANL2DZ		0.0309
PBE1PBE	6-31G(d)	6-311G(d)	LANL2DZ		0.0299
B3LYP	6-31G(d)	6-311G(d)	LANL2DZ		0.0476

Multiple conformers of the Pt(IV)L_6 complexes **CarboBisOAc**, **CarboPhen**, and **CarboNap** were optimised in Gaussian to confirm the lowest energy structures. To the model the reduction of these Pt(IV) complexes, each Pt(IV)L_6 complex (**CarboBisOAc**, **CarboPhen**, and **CarboNap**) (charge = 0, multiplicity = 1) were optimised (and confirmed to be energetic minima via frequency calculations). Single point calculations were then performed using this geometry with addition of two electrons; i.e. $[Pt(IV)L_6]^{2-}$ (charge –2, multiplicity 3) (geometry optimisation of these reduced molecules was deemed not appropriate due to the dissociation of axial ligands upon reduction). The difference in energy between Pt(IV)L_6 and $[Pt(II)L_6]^{2-}$ was then extracted (Table S2), to give an estimate of the first and second electron affinity for each Pt(IV) complex: E(Pt(IV)L_6) – E($[Pt(II)L_6]^{2-}$). These values increase from **CarboBisOAc** to **CarboPhen** to **CarboNap**, in line as expected with the trend in reduction potential.

Table S2: Calculated LUMO energy (E_{LUMO}) and experimental reductional potential (cathodic peak) of Pt(IV)L_6 complexes, calculated values of E(Pt(IV)L_6) – E([Pt(II)L_6]$^{2-}$) for **CarboBisOAc**, **CarboPhen**, and **CarboNap**.

	Pt(IV)L_6 E_{LUMO}	**Reduction potential** (cathodic peak) **(V vs Ag/AgCl)**	**E(Pt(IV)L_6) – E([Pt(II)L_6]$^{2-}$)** (calculated) **(eV)**
CarboBisOAc	–0.0757	–0.77	1.990
CarboPhen	–0.07862	–0.63	2.276
CarboNap	–0.09064	–0.32	4.703

The LUMO energies, E_{LUMO}, were obtained directly from each Pt(IV)L_6 geometry optimised structure, and correlated with experimental reduction potential values (cathodic peak), with excellent agreement ($R^2 > 0.98$) shown in Figure S60.[15] This linear relationship between E_{LUMO} and reduction potential for the Pt(IV)L_6 complexes studied (where the identity of one axial ligand is varied) may allow us to predict the redox characteristics of modified Pt(IV) candidates going forward via simple geometry optimisation calculations.

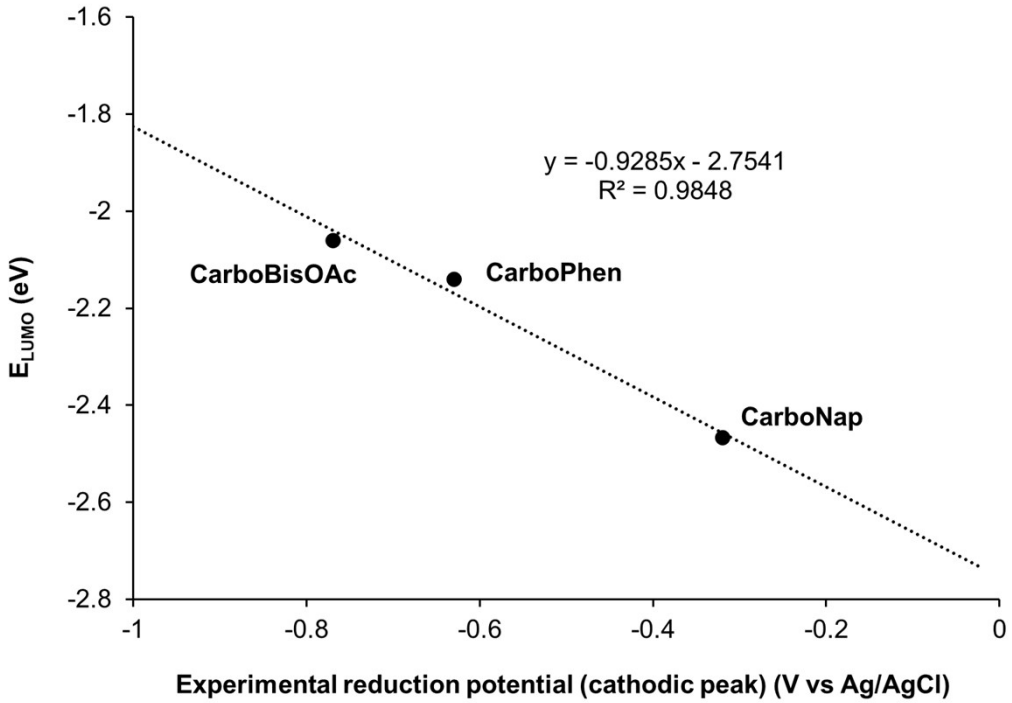

Figure S62. Linear correlation graph of the experimental reduction potentials (cathodic peak) and calculated LUMO energy (E_{LUMO}) for the Pt(IV)L_6 complexes **CarboBisOAc**, **CarboPhen** and **CarboNap**.

CarboBisOAc

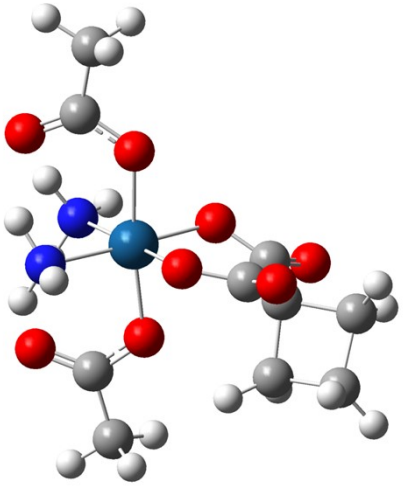

Pt	-0.63502800	0.11204300	0.00126700
N	-1.84762300	1.16055400	1.29853300
H	-1.56206300	0.98377000	2.26937600
H	-1.74714100	2.15951900	1.04389700
N	-1.75358900	0.92513900	-1.52665300
H	-1.41942600	0.58471600	-2.43634900
H	-2.73212600	0.63568500	-1.33719000
O	0.43410100	-0.89467800	-1.33883300
O	2.10840300	-2.27569100	-1.83107700
O	0.37076500	-0.61414200	1.55788100
O	2.36899600	-0.74527900	2.53976500
O	-1.81845700	-1.52082800	0.09077100
O	-3.75901400	-0.32819500	-0.05697400
O	0.71814100	1.59880800	-0.03884800
O	-0.83679000	3.24865500	-0.29496500
C	1.62658500	-1.45388400	-1.04462500
C	2.39726500	-0.96868100	0.16307100
C	1.70994700	-0.76434500	1.49610200
C	3.25633700	0.28787400	-0.30730600
H	2.81977200	0.88449000	-1.10609000
H	3.47094400	0.90692200	0.56784900
C	4.42961800	-0.68360200	-0.63243300
H	4.39306000	-0.99958300	-1.67771000
H	5.43389000	-0.35756400	-0.35617700
C	3.74366100	-1.74921400	0.27579200
H	4.09012500	-1.68411000	1.30880000
H	3.71277300	-2.77460500	-0.09147400
C	-3.14576800	-1.42155300	0.04185200
C	-3.82723900	-2.76092300	0.11583300
H	-3.53734500	-3.26533700	1.04326800
H	-3.49548000	-3.38285000	-0.72211100
H	-4.90810700	-2.62508300	0.08057900
C	0.35452800	2.87691300	-0.17143700
C	1.53707300	3.80592000	-0.15686400
H	2.18832200	3.57275200	-1.00613900
H	2.11357600	3.64449800	0.75934900
H	1.19457900	4.83879100	-0.21701000
H	-2.81137100	0.82579000	1.10501300
H	-1.64449300	1.95278800	-1.43155100

CarboPhen

Pt	0.75744700	-0.67042100	0.08702200
N	0.59160800	-2.12645400	-1.36293700
H	-0.07672900	-2.83313300	-1.00225700
H	0.26794000	-1.71005400	-2.24503500
N	1.31775200	-2.17314000	1.37003300
H	1.49866600	-1.79272700	2.30692000
H	0.48868800	-2.81344100	1.35506900
O	0.94497900	0.60980600	1.59990900
O	0.78514700	2.63916200	2.50307200
O	0.04467500	0.63257200	-1.25464600
O	-1.07056800	2.55628800	-1.52541100
O	-1.15447500	-0.87648500	0.66361400
O	-1.13807100	-3.17020900	0.58695300
O	2.64814900	-0.25107400	-0.45524700
O	3.24966300	-2.44143900	-0.68478600
C	0.78225100	1.94223100	1.48541900
C	0.70578000	2.55620200	0.09798000
C	-0.19761100	1.92257400	-0.92521400
C	2.20220000	2.75602100	-0.40379300
H	2.92668500	2.03747300	-0.02603200
H	2.22071100	2.77588100	-1.49778000
C	2.14557900	4.19470800	0.19947100
H	2.53195500	4.20060600	1.22168400
H	2.59270100	4.99500300	-0.39241900
C	0.58579300	4.09683300	0.21404300
H	0.13617100	4.49287300	-0.69869000
H	0.07463700	4.45517100	1.10700000
C	-1.75686200	-2.06547100	0.53768800
C	3.53194900	-1.21971300	-0.71121100
C	4.89572600	-0.67042300	-1.02830900
H	5.27196300	-0.11859500	-0.16020300
H	4.81862800	0.03230600	-1.86385500
H	5.57266100	-1.48731200	-1.27787600
H	1.54424700	-2.53426100	-1.44541800
H	2.15625900	-2.62406400	0.96650200
N	-3.09959300	-1.99051900	0.34861100
H	-3.60434500	-2.87045400	0.42522600
C	-3.84315000	-0.83122400	0.01399300
C	-3.27925200	0.23729400	-0.69433400
C	-4.05407300	1.34588200	-1.01837300
H	-2.23989900	0.21247600	-0.98286600
H	-3.56661000	2.16476500	-1.53564900
C	-5.19899000	-0.78561600	0.35586400
H	-5.64313200	-1.61180900	0.90148300
C	-5.97484100	0.31879100	0.00723900
H	-7.02452300	0.33822500	0.27986400
C	-5.40526700	1.39606300	-0.67251100
H	-6.00732900	2.26079800	-0.92869800

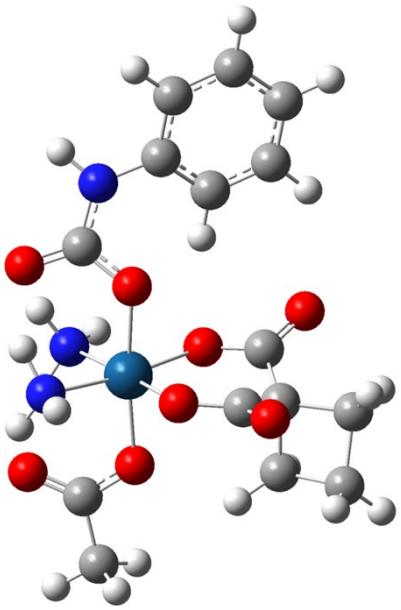

CarboNap

Pt	-2.97073400	-0.48746600	-0.00726300
N	-4.37571100	-0.70294700	1.48139300
H	-4.49597300	-1.69559200	1.72266400
H	-4.02931200	-0.19021200	2.30490400
N	-4.22687500	-1.27497300	-1.41936200
H	-3.80244300	-1.12036200	-2.34494300
H	-4.33452100	-2.28569700	-1.25832000
O	-1.60350500	-0.36160000	-1.44016300
O	0.47493200	0.20753400	-2.00836400
O	-1.75172100	0.27632100	1.38869400
O	-1.04789400	2.36054200	1.87207700
O	-2.39869600	-2.38059000	0.34917900
O	-0.79265800	-3.78444600	-0.42206600
O	-3.55403600	1.40685400	-0.36088500
O	-5.75911100	0.82917900	-0.43298500
C	-0.49955200	0.41260100	-1.28350800
C	-0.55173000	1.59221700	-0.33652000
C	-1.14646200	1.46579100	1.04026400
C	-1.13768300	2.81813300	-1.15930100
H	-1.85306300	2.56252400	-1.94018500
H	-1.57115100	3.52363800	-0.44571300
C	0.31978900	3.21126000	-1.54534600
H	0.60939100	2.75407600	-2.49421100
H	0.56570600	4.27416000	-1.53003100
C	0.82286200	2.34106900	-0.35252700
H	0.90957200	2.92570800	0.56496300
H	1.68837900	1.69924900	-0.51358600
C	-1.09799500	-2.75148900	0.17790700
C	-4.85537400	1.69442400	-0.49588800
C	-5.08556500	3.16124100	-0.72557900
H	-4.57289600	3.46647900	-1.64390800
H	-4.64940000	3.72811700	0.10327100
H	-6.15409900	3.36053300	-0.80391700
H	-5.25638400	-0.28630600	1.13081000
H	-5.12417100	-0.76200300	-1.32983100
N	-0.19717200	-1.88010700	0.77440800
H	-0.63718400	-1.08006400	1.25223000
C	1.16752000	-1.83763000	0.56020900
C	1.91478300	-0.78454300	1.20047600
C	1.83354600	-2.71958300	-0.28858700
C	3.27563500	-0.59205700	0.82872500
C	1.36258000	0.07857900	2.17764100
C	3.18176900	-2.53314700	-0.60006700
H	1.26919700	-3.53007900	-0.72315200
C	4.00291800	0.48843300	1.37680600
C	3.89886500	-1.47175300	-0.08164400
C	2.09281900	1.12833600	2.69969700
H	0.35903800	-0.08434200	2.55088600
H	3.68398100	-3.21053600	-1.28191100
C	5.29194800	-1.27899500	-0.48080800
H	1.63696500	1.78555200	3.43007600
C	5.40307300	0.72711100	0.98154800
C	3.41630800	1.34568400	2.28549900
H	4.00286300	2.16938400	2.67534700
N	5.95479200	-0.18171900	0.08021900
O	5.88549700	-2.02610200	-1.27780000
O	6.06433100	1.68315000	1.42081000
C	7.34358800	0.05102800	-0.36621800
H	7.78966800	0.72614300	0.36589100
H	7.85896400	-0.91248600	-0.36345800
C	7.37235000	0.67544100	-1.76739600
H	8.42026400	0.88470900	-2.01867900
H	6.99250500	-0.06371800	-2.48140200
C	6.54162500	1.96473000	-1.83522700
H	5.47562700	1.73647100	-1.71839600
H	6.82926500	2.64948000	-1.02954900
H	6.67843400	2.46769600	-2.79883500

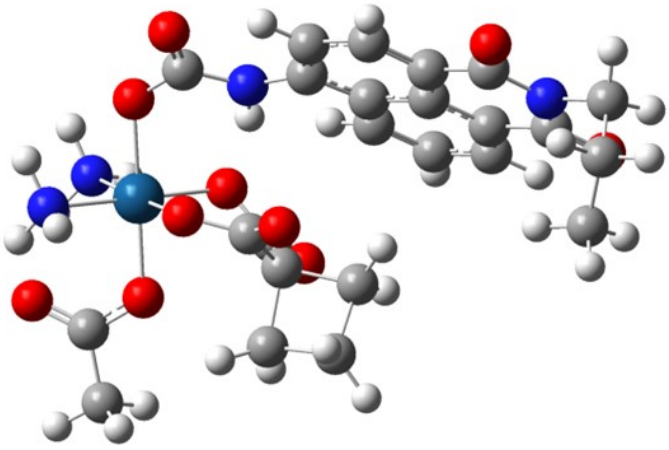

References

1. Z. Deng, C. Li, S. Chen, Q. Zhou, Z. Xu, Z. Wang, H. Yao, H. Hirao, and G. Zhu, *Chem. Sci.*, 2021, **12**, 6536-6542.
2. S. Huang, J. W. Marsh, J. R. G. White, T. Q. Ha, S. A. Twigger, I. Diez-Perez, and A. C. Sedgwick, *New. J. Chem.*, 2024, ***48***, 7548–7551.
3. M. H. C. Boulet, H. R. Bolland, E. M. Hammond and A. C. Sedgwick, *J. Am. Chem. Soc.*, 2023, **145**, 12998-13002.
4. W. Xuan, R. Pan, Y. Cao, K. Liu and W. Wang, *Chem. Commun*., 2012, **48**, 10669-10671.
5. A. Kastner, I. Poetsch, J. Mayr, J. V. Burda, A. Roller, P. Heffeter, B. K. Keppler, C. R. Kowol, *Angew. Chem. Int. Ed.* 2019, **58**, 7464.
6. Gaussian 16, Revision C.01, M. J. Frisch, G. W. Trucks, H. B. Schlegel, G. E. Scuseria, M. A. Robb, J. R. Cheeseman, G. Scalmani, V. Barone, G. A. Petersson, H. Nakatsuji, X. Li, M. Caricato, A. V. Marenich, J. Bloino, B. G. Janesko, R. Gomperts, B. Mennucci, H. P. Hratchian, J. V. Ortiz, A. F. Izmaylov, J. L. Sonnenberg, Williams, F. Ding, F. Lipparini, F. Egidi, J. Goings, B. Peng, A. Petrone, T. Henderson, D. Ranasinghe, V. G. Zakrzewski, J. Gao, N. Rega, G. Zheng, W. Liang, M. Hada, M. Ehara, K. Toyota, R. Fukuda, J. Hasegawa, M. Ishida, T. Nakajima, Y. Honda, O. Kitao, H. Nakai, T. Vreven, K. Throssell, J. A. Montgomery Jr., J. E. Peralta, F. Ogliaro, M. J. Bearpark, J. J. Heyd, E. N. Brothers, K. N. Kudin, V. N. Staroverov, T. A. Keith, R. Kobayashi, J. Normand, K. Raghavachari, A. P. Rendell, J. C. Burant, S. S. Iyengar, J. Tomasi, M. Cossi, J. M. Millam, M. Klene, C. Adamo, R. Cammi, J. W. Ochterski, R. L. Martin, K. Morokuma, O. Farkas, J. B. Foresman and D. J. Fox, Gaussian, Inc., Wallingford CT, 2016.
7. Y.-A. Lee, K. H. Yoo and O.-S. Jung, *Bull. Chem. Soc. Jpn.*, 2003, **76**, 107-110.
8. S. Grimme, J. Antony, S. Ehrlich and H. Krieg, *J. Chem. Phys.*, 2010, **132**, 154104.
9. P. J. Hay and W. R. Wadt, *J. Chem. Phys.*, 1985, **82**, 270-283.
10. P. J. Hay and W. R. Wadt, *J. Chem. Phys.*, 1985, **82**, 299-310.
11. J. S. Binkley, J. A. Pople and W. J. Hehre, *J. Am. Chem. Soc.*, 1980, **102**, 939-947.
12. W. J. Pietro, M. M. Francl, W. J. Hehre, D. J. DeFrees, J. A. Pople and J. S. Binkley, *J. Am. Chem. Soc.*, 1982, **104**, 5039-5048.
13. M. S. Gordon, J. S. Binkley, J. A. Pople, W. J. Pietro and W. J. Hehre, *J. Am. Chem. Soc.*, 1982, **104**, 2797-2803.
14. J. Tomasi, B. Mennucci and R. Cammi, *Chem. Rev.*, 2005, **105**, 2999-3094.
15. K. G. von Eschwege and J. Conradie, *S. Afr. J. Chem.*, 2011, **64**, 203-209.